Towards understanding the mechanism of dimerisation of *Saccharomyces cerevisiae* eukaryotic translation initiation factor 5A

A dissertation submitted in fulfillment of the requirements for the degree of

DOCTOR OF PHILOSOPHY

at

RHODES UNIVERSITY

by

PETRA MONIKA GENTZ

January 2008

Dedicated, in loving memory, to my late father

“Pappi, ich habe es nun endlich geschafft!”

Abstract

Eukaryotic translation initiation factor 5A (eIF5A) is the only known protein to contain hypusine, formed by post-translational modification of a highly conserved lysine residue. Hypusination is essential for eIF5A function, being required for binding of a specific subset of mRNAs necessary for progression of eukaryotic cells through the G_1-S checkpoint. Little structural information is available for eIF5A other than that derived from archaeal homologues. The aim of this study was to conduct structure-function studies on *Saccharomyces cerevisiae* (yeast) eIF5A, encoded by *TIF51A*. Homology models of eIF5A were generated from the *Methanococcus jannaschii* archaeal homologue (aIF5A) and two *Leishmania* eIF5As. The models, along with secondary structure predictions identified an α-helix on the C-terminal domain, unique to eukaryote eIF5A. The *Neurospora crassa* structural analogue, HEX-1, which dimerises in three configurations, was used to generate similar dimeric model configurations of eIF5A.

A biochemical and functional analysis was used to validate the homology models of eIF5A. Since the crystal structures of aIF5A and eIF5A were solved from unhypusinated protein produced in *Escherichia coli*, 6 x His-tagged eIF5A (His-eIF5A) was used for biochemical analysis. This analysis revealed that eIF5A existed as a dimer in solution, dependent on the presence of the highly conserved Cys 39 residue. A yeast *TIF51A*/*TIF51B* null yeast strain, with a chromosomal copy of *TIF51A* under control of P_{GAL1}, was used to confirm that His-eIF5A and selected eIF5A mutants were functional *in vivo*. Biochemical analysis showed that hypusinated His-eIF5A also exists as a dimer, but neither the dimerisation, nor the function of eIF5A are dependent on the presence of Cys 39. Rather they depend on the presence of hypusine (Hpu) 51 and the presence of RNA leading to the conclusion that RNA and hypusine are required for dimerisation and hence function, of native eIF5A *in vivo*. In contrast, a Lys 51 to Arg 51 substitution or RNase treatment of His-eIF5A produced in *E. coli* did not

destabilize the dimeric form, suggesting different folding/dimerisation mechanisms in *E. coli* and yeast cells. The information obtained from the initial homology models, together with the results of the biochemical analysis was used to propose a mechanism for dimerisation of yeast eIF5A involving both hypusine and RNA.

Chapter 1: Literature Review

Chapter 2: *In silico* analysis of eIF5A

Chapter 3: Development of an experimental system for studying the biological activity of eIF5A

Chapter 4: Biochemical characterisation of recombinant eIF5A

Chapter 5: Functional and biochemical analysis of native eIF5A

Chapter 6: General discussion and conclusions

Appendices

List of Figures

List of Tables

List of Abbreviations

eIF5A: eukaryotic translation initiation factor 5A (general)

eIF5A: eukaryotic translation initiation factor 5Aa (aerobic form) referred to as eIF5A hitherto

eIF5Ab: eukaryotic translation initiation factor 5Ab (anaerobic form)

DTT: Dithiothreitol

Yeast: *Saccharomyces cerevisiae*

DHS: Deoxyhypusine synthase

DOHH: Deoxyhypusine hydroxylase

His-eIF5A: N-terminal 6 x His tag on eIF5A

eIF5A-His: C-terminal 6 x His tag on eIF5A

WT: Wild type (commonly eIF5A)

Acknowledgments

I would sincerely like to thank my supervisor, Professor Rosemary Dorrington, for her innovative ideas, without which this project could not have grown. In addition her wise, understanding nature assisted me throughout the last few years, both in a professional and personal manner – Thank you.

Prof Gregory Blatch was invaluable in his assistance with the interpretation of the data, particularly with regards some of the more technical aspects of the structural work and cross-linking studies. The help was greatly appreciated.

Melissa Botha contributed greatly by assisting with the MODELLER and WHAT IF models – you truly will grow into a marvelous scientist – Thanks!

Without the late Lawrence Penckler, we may never have learnt what we did about this interesting little protein.

To the wonderful, unique research group in Lab 417 – thanks for “sharing and caring”.

To my loving husband, Jeremy (MUTZ), “Meine liebe Mammi”, and “Mein Grosser Bruder”, Robbie – Thank you for being so understanding, and for supporting me, especially during the critical moments in the experimental stages and tense writing moments.

Chapter 1: Literature Review

Chapter 1: Literature Review

1.1 The eukaryotic translation initiation factor 5A

The eukaryotic translation initiation factor 5A (eIF5A) is a highly conserved protein that is essential in all eukaryotes and archaebacteria, but not in eubacteria (Schnier *et al*., 1991; Chen & Liu, 1997; Park *et al*., 1997) and is the only protein known to contain the unique amino acid hypusine (Cooper *et al*., 1983). Hypusine was first isolated in its free form in trichloroacetic acid soluble bovine brain tissue (Shiba *et al*., 1971) and was named hypusine as an abbreviation from hydroxyl putrescine and lysine. Originally eIF5A was thought to be involved in translation initiation as it could enhance the synthesis of methionyl-puromycin, which suggested that the protein was involved in the formation of the first peptide bond in translation (Benne & Hershey, 1978). Further experiments conducted by Cooper *et al*. in 1983 showed that not only was eIF5A involved in translation, but it also functioned in cell cycle regulation. eIF5A is an abundant factor, but unlike other initiation factors, it is largely present in the cytoplasm. Only a small amount of the protein is directly associated with the ribosomes (Park *et al*., 1993).

Hypusine is essential for the biological functioning of eIF5A and is formed by the post-translational modification of a highly conserved lysine residue (Park, 1989). This lysine residue is flanked by a stretch of six amino acid residues on either side with a high degree of conservation among different eIF5A species (Park *et al*., 1986). The two-step process of modification (known as hypusination) is dependent on the enzymes deoxyhypusine synthase (DHS) and deoxyhypusine hydroxylase (DOHH) (Murphey & Gerner, 1987). While inhibition of either of these enzymes affects cell growth in mammalian cells (Park *et al*., 1993), only DHS (yDHS or Dys1) is essential in the yeast *Saccharomyces cerevisiae* (referred hitherto as "yeast") (Sasaki *et al*., 1996; Park, 2006). DOHH does not appear to be essential in yeast since a DOHH (yDOHH or Lia1) null strain grows only slightly slower than the parent strain (Park *et al*., 2006).

1.1.1 The yeast eIF5A and eIF5Ab

The yeast genome was the first eukaryotic genome to be completely sequenced (Goffeau *et al*., 1996; Cherry *et al*., 1997). Since there are numerous genes in yeast and humans that encode similar proteins (Botstein & Fink, 1988) and because yeast is amongst the best-studied experimental organisms, the yeast *TIF51A* gene has been the subject of many investigations on eIF5A. This section will deal with eIF5A, specifically in the context of yeast as a model to study higher eukaryotes.

In yeast, eIF5A is encoded by one of two essential genes, namely *HYP2* (*TIF51A*) or *ANB1* (*TIF51B*) mapping to chromosomes V and X, respectively (Wöhl *et al*., 1992; Mehta *et al*., 1990). *TIF51A* encodes eIF5A (isoelectrically more acidic), expressed under aerobic conditions, while *TIF51B* encodes eIF5Ab (isoelectrically more basic), expressed under anaerobic conditions. eIF5A and eIF5Ab, which share 90 % similarity to each other, both carry the hypusine modification and either is sufficient to maintain growth of yeast cells (Schnier *et al*., 1991; Wöhl *et al*., 1993; Schwelberger *et al*., 1993, Magdolen *et al*., 1994). In exponentially-growing cells, eIF5A is more abundant than eIF5Ab, and eIF5A is prone to proteolytic breakdown *in vitro* (Schwelberger *et al*., 1993). Expression of eIF5Ab can, in the presence of oxygen, reverse the lethality of an eIF5A knockout, and eIF5A is able to reverse the lethality of an eIF5Ab knockout under anaerobic growth conditions (Wöhl *et al*., 1993; Schwelberger *et al*., 1993). The human cDNA encoding eIF5A, which is about 60 % identical to the yeast homologue, can substitute for the yeast protein *in vivo* (Schwelberger *et al*., 1993). However, archaeal eIF5A (aIF5A) expressed in yeast is neither hypusinated nor able to rescue growth in eIF5A/b deficient cells (Magdolen *et al*., 1994).

Both *TIF51A* and *TIF51B* encode proteins of 157 residues with predicted molecular weights of between 17 - 20 kDa with similar isoelectric points (pI of between 5.1-5.5) and a mean half-life of about 33 hours (yeast eIF5A: Mehta *et al*., 1990; Schwelberger *et al*., 1993; mammalian eIF5A: Cooper *et al*., 1983; Chung *et al*., 1991; Gerner *et al*., 2002). In individual knockout experiments to determine the role of eIF5A and eIF5Ab, it was determined that *TIF51A*-disrupted strains grew more slowly, while strains lacking *TIF51B* showed no growth phenotype (Schnier *et al*., 1991). Strains lacking both *TIF51A* and *TIF51B* were non viable, showing that eIF5A is essential for cell growth in yeast cells (Schnier *et al*., 1991).

1.1.2 Biosynthesis of active eIF5A

Synthesis of the active eIF5A protein results from the addition of a spermidine moiety (from polyamine synthesis) to the eIF5A precursor, such that a specific lysine residue in eIF5A is modified. The two-step post-translational modification is represented schematically in Figure 1.1A. During polyamine synthesis, spermidine is dehydrogenated in an NAD-dependent manner to form dehydrospermidine. The 4-aminobutyl moiety from spermidine (dehydrospermidine) is transferred to the specific lysine residue of eIF5A precursor by the enzyme DHS. The intermediate formed is a covalent enzyme-imine. Next, hydroxylation of the eIF5A intermediate (deoxyhypusine) is catalyzed by DOHH (Abbruzzese *et al*., 1986) to form the hypusinated protein and thus complete eIF5A activation (Figure 1.1A). DHS is able to equally modify the two forms of precursor eIF5A protein, eIF5A and eIF5Ab (Sasaki *et al*., 1996). The intricate specificity of DHS activity has been examined using spermidine, NAD and putrescine, which can replace the eIF5A precursor as an acceptor of the 4-aminobutyl moiety of spermidine to form homospermidine (Park *et al*., 2003) (Figure 1.1B). The initial conversion of eIF5A precursor to deoxyhypusine is reversible, while the hydroxylation step is irreversible (Park *et al*., 2003). In addition, spermidine, but not spermine is essential for hypusination and consequently growth of yeast cells (Chattopadhyay *et al*., 2003). However, in the presence of the enzyme amine oxidase (coded by *FMS1*), spermine could be oxidised to spermidine.

Site-directed mutagenesis of the lysine residue that is hypusinated, to an arginine residue, resulted in inactive eIF5A (yeast eIF5A: Schnier *et al*., 1991; mammalian eIF5A: Gordon *et al*., 1987; archaeal aIF5A: Bartig *et al*., 1992). Other modifications observed in the yeast eIF5A include the phosphorylation of one serine residue near the N-terminus (Kang *et al*., 1993). Thus there are two post-translational modifications that occur in eIF5A, hypusination and phosphorylation, but the activity of the protein is solely dependent on hypusination (Schnier *et al*., 1991; Kang *et al*., 1993).

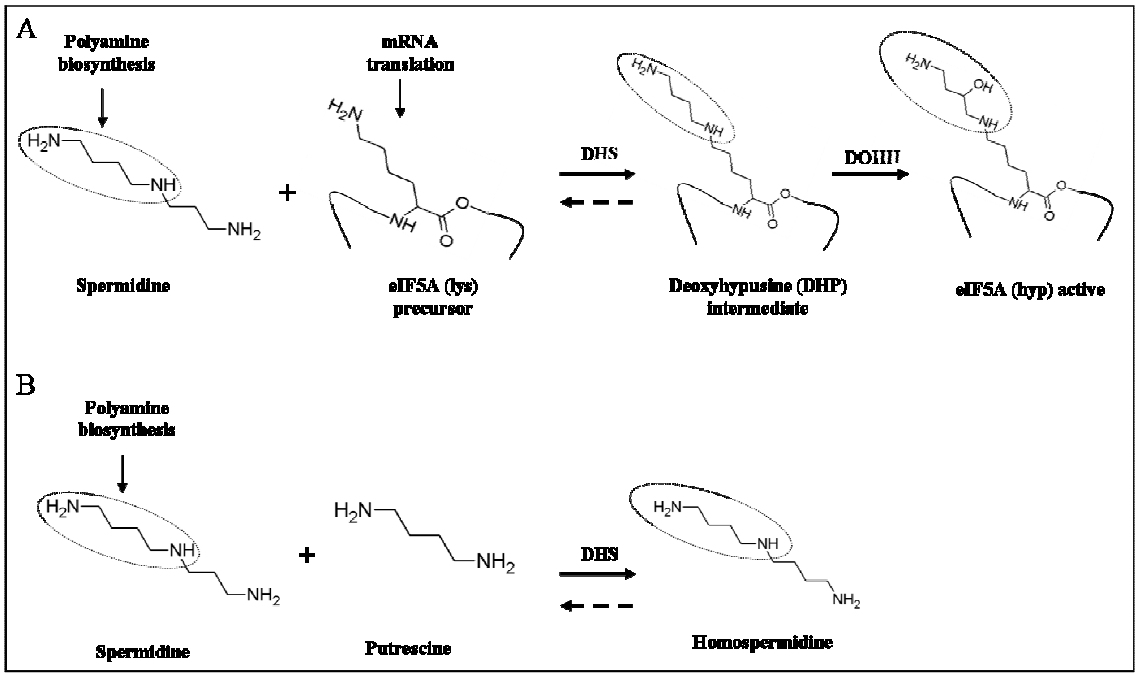

Figure 1.1: The modification of eIF5A. (A) The 4-aminobutyl moiety from spermidine (dotted oval) is transferred to the lysine-containing eIF5A precursor, eIF5A (lys), in the presence of DHS to form the deoxyhypusine (DHP) intermediate. DHP is then hydroxylated by DOHH to form the active, hypusinated eIF5A. The forward reaction resulting in DHP is reversible in the presence of NAD, forming spermidine as the end product (dashed arrow). (B) Spermidine can also be converted by DHS in the presence of NADH + H^+ to homospermidine, in the presence of putrescine as the acceptor. The figure was generated in part using ACD/ChemSketch, 2005 and adapted from information in Murphey & Gerner, 1987; Park *et al.*, 1982, 1993, Park *et al*., 2003; Park, 2006.

1.2 The eIF5A modifying enzymes

1.2.1 Deoxyhypusine synthase (DHS)

In yeast, DHS is a 369 amino acid cytosolic protein encoded by the *YHR068w* (*DYS1*) gene on chromosome VIII existing as a homotetramer (160-170 kDa in size) with a subunit size of 43 kDa and a proposed half-life in the region of 10 hours (Kang *et al*., 1995; Dou & Chen, 1990; Thompson *et al*., 2003). DHS is essential for cell viability (Kang *et al*., 1995; Sasaki *et al*., 1996). Depletion of DHS results in the enlargement of cells followed by a cessation of growth (Park *et al*., 1998). This observation of cessation of growth, accompanied by a marked cell enlargement in cells lacking DHS, is attributed to the role of eIF5A in cell division or on cell cycle progression (Kang *et al*., 1995; Sasaki *et al*., 1996; Park *et al*., 1998).

Structure-function studies have been conducted using recombinant human DHS as well as truncated mutant proteins (Joe *et al*., 1995). The human DHS sequence shows a high degree of identity (58 %) and similarity (73 %) with yeast DHS and both proteins are phosphorylated by protein kinase C (Kang *et al*., 1995; Kang & Chung, 1999; Kang *et al*., 2002). *E. coli* cells expressing recombinant human DHS effectively synthesise deoxyhypusine *in vivo* and regions of DHS critical for enzyme activity have been identified, including a well-conserved internal region of 56 amino acids (Asp 262 – Ser 317), and less conserved regions in the amino terminal and carboxy terminals (Joe *et al*., 1995).

Refinement of the first crystal structure of the human DHS complexed with the NAD co-factor and crystallised in the presence of the known inhibitor, 1,7-diaminoheptane (DAH), showed a ball-and-chain mechanism for the blocking each of the deep active sites (Liao *et al*., 1998). A similar structure for DHS was solved by Umland *et al*. (2004). The crystals were obtained under conditions of high ionic strength and acidic pH. Analysis of the data confirmed that the human DHS protein is a homotetramer, comprising of four potential active sites formed by two tightly-associated dimers with each of the four identical subunits containing a nucleotide-binding (Rossmann) fold (Liao *et al*., 1998; Umland *et al*., 2004). Several conformational changes have been proposed to increase the accessibility of the substrate-binding site. It is likely, however, that the conditions under which the crystals were obtained resulted in an inactive DHS because X-ray diffraction studies on crystals grown at low ionic strength and pH 8.0 (near pH optimum for DHS) have revealed a new configuration of the DHS-NAD complex, more representative of the active form (Murphey & Gerner, 1987; Lee *et al*., 1999; Lee & Park, 2000; Umland *et al*., 2004). This new data showed that the previous ball-and-chain motif was structurally different, allowing accessibility of the previously buried active sites (Umland *et al*., 2004). The dimer configurations of these two structures are represented in Figure 1.2. The structure obtained from crystals soaked in the potent inhibitor, N^1-guanyl-1,7-diaminoheptane (GC_7), resulted in the novel DHS-NAD-inhibitor ternary complex, providing new insights into the mode of substrate binding and reaction mechanism (Figure 1.2B).

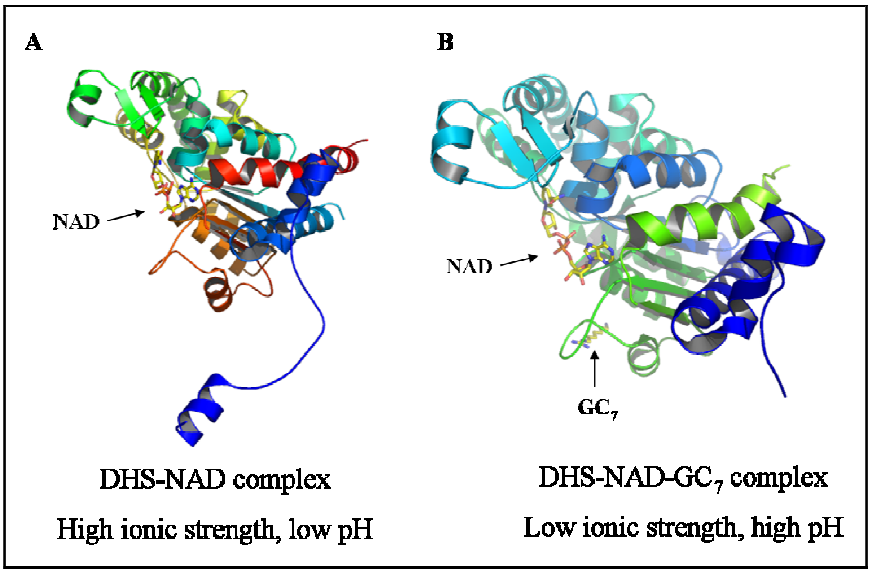

Figure 1.2: Crystal structures of the tightly-associated human DHS dimer. (A): Cartoon model of DHS complexed with NAD, as determined from crystals produced in high ionic strength and low pH conditions. NAD is represented as sticks in the buried active site, forming part of the proposed ball-and-chain mechanism. (B): Cartoon model of DHS complexed with both NAD and GC_7, as determined from crystals produced in low ionic strength and high pH conditions. The complexed NAD and GC_7 are represented as sticks in the more accessible active site, forming part of a unique conformational change upon substrate binding. The models (PDB codes 1RLZ and 1RQD for A and B, respectively) were generated using Pymol (DeLano, 2002). The figure was adapted from information in Liao *et al*., 1998 and Umland *et al*., 2004.

The stoichiometry of the components in the human DHS-eIF5A (precursor) complex has been approximated to be 1 DHS tetramer to 1 eIF5A (precursor) monomer, and confirmed by equilibrium ultracentrifugation data (Lee *et al*., 1999). In addition, the formation of the complex is neither dependent on the presence of NAD^+ nor on spermidine (Lee *et al*., 1999). The human enzyme appears to be different from the *Neurosporra crassa* DHS, in that the latter depends on the presence on NAD^+ for substrate binding (Tao & Chen, 1994, 1995; Dou & Chen, 1990). Further analysis of the structure-function relationship of human DHS has identified critical amino acids involved in the binding of spermidine, NAD^+ and eIF5A precursor (Lee *et al*., 2001). Alanine substitutions of amino acids Asp 243, Trp 327, His 288, Asp 316 and Glu 323 in the predicted spermidine-binding sites, results in a dramatic loss of spermidine binding and enzyme activity, while substitutions of His 288 to Ala also lead to the abolishment of NAD-binding. Similarly, mutation of nearly all the potential NAD-binding site amino acid residues results in a reduction of NAD-binding ability (Lee *et al*., 2001).

1.2.2 Deoxyhypusine hydroxylase (DOHH)

DOHH catalyses the formation of hypusine from deoxyhypusine, the precursor of active eIF5A (Abbruzzese *et al*., 1986). Characterisation of DOHH from partially purified from rat testis suggested the enzyme might have a mode of action similar to propyl and lysyl hydroxylases, members of a group of α-ketoglutarate dioxygenases (Abbruzzese *et al*., 1986). In addition, it seemed likely that the metal ion (Fe^{2+}) required for catalysis was tightly associated with the enzyme, thus eliminating the need for the addition of metal ions during purification procedure (Abbruzzese *et al*., 1986).

Inhibition of DOHH from rat testis has been studied *in vitro* using a variety of polyamines including spermine and its homologue, thermine as well as spermidine and its homologue, caldine. Spermidine and thermine exhibit the strongest inhibition, while spermidine and caldine display less potent inhibitory effects. Spermidine analogues, diamines, including putrescine, free hypusine and deoxyhypusine display little to no inhibition of DOHH activity (Abbruzzese *et al*., 1989). Designed for their ability to anchor in the DOHH active site, catecholpeptides (CCPs) have been found to strongly inhibit hypusine formation *in* vitro (Abbruzzese *et al*., 1991). In addition, their involvement in the utilisation of catechol-mediated chelation provides evidence that a metal ion forms as integral part of the DOHH catalytic centre (Abbruzzese *et al*., 1991). This has been confirmed by Csonga *et al*. (1996), using HeLa cells to determine which metal ion is involved in the action of DOHH. Both Fe(II) and Fe(III) display equal abilities in restoring the hydroxylase activity to control levels following inhibition with ciclopiroxolamine (CPX), a potent metal chelator (Csonga *et al*., 1996).

In yeast, the *YJR070C* (*LIA1*) gene encodes DOHH, while *HLRC1* (*MGC4293*) encodes the human homologue (Thompson *et al*., 2003; Park *et al*., 2006). Highly conserved DOHH gene homologues have also been identified in a variety of eukaryotes from yeast to mammals. Based on sequence profile data, it has been found that DOHH (325 residues in yeast) belongs to a group of HEAT-repeat containing metalloenzymes, typified by eight tandem repeats of an α-helical hairpin superstructure known as a HEAT motif (Andrade *et al*., 2001). DOHH is organised in a symmetrical dyad. HEAT-repeat proteins mediate protein-protein interactions and are involved in cytoskeletal organisation, nucleocytoplasmic and vasuolar transport (Andrade *et al*., 2001). The DOHH structure is dissimilar to the double-stranded β-jelly roll type structures of the dioxygenases, lysyl and collagen propyl hydroxylase, which are dependent on Fe(II) and 2-oxoacid but metal co-ordination site sequences are conserved. This

suggests that the iron-dependent DOHH is a structurally distinct protein hydroxylase (Park *et al*., 2006). Two potential iron co-ordination sites, comprising of two strictly-conserved His-Glu motifs are present in DOHH (Kim *et al*., 2006). Mutation of any of these conserved His-Glu residues abolishes DOHH activity, providing evidence that Fe(II) binding to each of the sites is required for DOHH catalysis (Kim *et al*., 2006). A binuclear iron binding reaction mechanism, distinct from that of other Fe(II)-dependent protein hydroxylases has been proposed (Kim *et al*., 2006).

Critical amino acids required for the binding of substrate to the human DOHH have been identified using alanine substitution. Of the 36 conserved residues within the His-Glu motifs, Glu 57 and Glu 208 were identified as being required for substrate binding, although they are not involved in iron co-ordination. DOHH also specifically recognises only the deoxyhypusinated form of eIF5A, but not the lysine form, and a large portion (20-99 amino acids) of this substrate is required for hydroxylation by DOHH (Kang *et al*., 2007). A model of the deoxyhypusine-DOHH complex has been proposed, whereby the Glu 57 and Glu 208 residues form ionic bridges, anchoring the amino groups of the deoxyhypusine side chains to the active site (Kang *et al*., 2007). Ultimately, a crystal structure for DOHH, may clarify the structure-function relationship of this unique hydroxylase.

1.3 Functions of eIF5A

1.3.1 Role in the cell cycle

Eukaryotic ribosomes are comprised of a 60S large subunit and a 40S small subunit, which together form the 80S particle. Translation occurs by a sophisticated mechanism of recruitment of the ribosome to the mRNA and relies on protein-RNA and protein-protein interactions. While at least eleven translation initiation factors have been identified in the translation machinery, eIF5A is not one of them (Benne & Hershey,1978; Unbehaun *et al*., 2004). Hypusinated eIF5A has, however, been implicated in playing a role in the expression of proteins regulating the transition of the G_1-S phase of the cell cycle in eukaryotic cells (Kang & Hershey, 1994; Hanauske-Abel *et al*., 1994; Jin *et al*., 2003). A schematic representation of the eukaryotic cell cycle is shown in Figure 1.3.

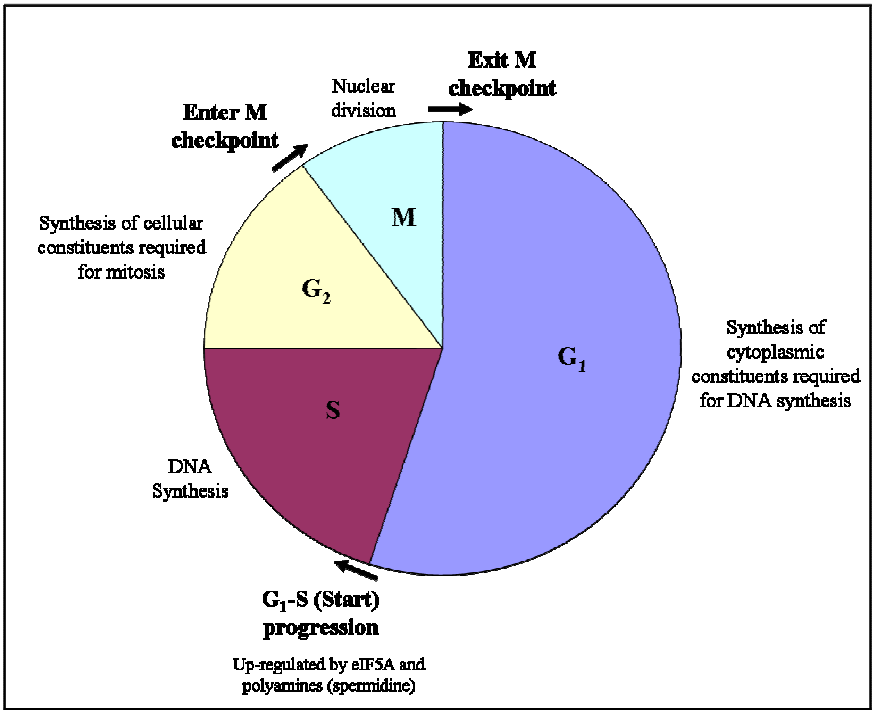

Figure 1.3: Schematic representation of the eukaryotic cell cycle, with its major checkpoints. The G_1 (Gap 1), S (Synthesis) and G_2 (Gap 2) phases together are called interphase and cells occupy between 90-95 % of their time in these phases. Cells spend a short time in the M (Mitosis) phase, where nuclear and cytoplasmic divisions occur. The G_1 and G_2 phases are typified by time delays to allow the cell to monitor the internal and external environments before committing to the next stage. eIF5A, its precursor enzymes, and the substrate spermidine have been shown to be especially important at the G_1-S transition (Start) (Adapted from Alberts *et al.*, 2002).

Modified (hypusinated) eIF5A plays a role in cell growth and differentiation, specifically in cell proliferation (Abbruzzese, 1988; Beninati *et al.*, 1990; Caraglia *et al.*, 1997) and growth of yeast (Schnier *et al.*, 1991). Inhibition of hypusination results in reduced growth of mammalian cells (Park *et al.*, 1984, Abbruzzese, 1989, 1991; Jakus *et al.*, 1993; Park *et al.*, 1993) and induces the reversible arrest in the G_1-S phase of the cell cycle (Figure 1.3) (Park *et al.*, 1981; Park, 1987). Polyamines in general, but specifically spermidine, have been implicated in cellular proliferation, differentiation and embryonic development (Tabor & Tabor, 1985; Pegg 1988) and because spermidine is the direct precursor of hypusine, it has been proposed to be one of the fundamental endogenous components in cellular regulation. Furthermore, active eIF5A has been implicated in determination of cell integrity and cell polarity (Valentini *et al.*, 2002; Zanelli & Valentini, 2005).

The establishment of actin polarity involves cytoskeletal reorganisation, secretion and cell wall deposition. All these activities are essential for bud formation and the G_1-S transition in yeast (Zanelli & Valentini, 2005) and rely on the presence of hypusinated eIF5A. It has also been suggested that eIF5A works in tandem with yeast protein transport-GTPase (Ypt-GTPase) to enhance protein synthesis and secretion required in bud formation during the S-phase transition (Frigieri *et al*., 2007). The small Ypt-GTPase, a member of the rab family and encoded by the essential gene *YPT1*, is involved in vesicular trafficking between the endoplasmic reticulum and the Golgi (Martinez & Goud, 1998; Clague, 1998).

A role of eIF5A in the establishment of cell polarity in a temperature-sensitive mutant strain of *TIF51A* (*tif51A-1*) has also been proposed. The *PKC1* gene, encoding the only yeast protein kinase C (Pkc1), controls a number of cellular processes including as cell-cycle progression and structural organisation of the cytoskeleton (Heinisch *et al*., 1999). At a high copy number, *PKC1* suppresses growth defects and cell polarity defects of the *tif51A-1* strain (Zanelli & Valentini, 2005), which has led to the suggestion that eIF5A plays a role in the Pkc1 pathway essential for bud formation and the G_1/S transition (Zanelli & Valentini, 2005).

The reversible metal chelating inhibitor of DOHH, mimosine, suppresses DOHH activity and thus inhibits hypusine formation and activation of eIF5A, resulting in inhibition of S-phase entry (Watson, *et al*., 1991; Hanauske-Abel *et al*., 1995). Upon removal of the inhibitor, DOHH and thus DNA synthesis resume, and once cells enter the S-phase, re-addition of the inhibitor fails to suppress further progression through the cell cycle. This led to the hypothesis that the highly conserved domain bearing the hypusination site, could act as a selector for a class of specific mRNA substrates (Hanauske-Abel *et al*., 1994). These substrates would be utilised by polysomes allowing for synthesis of DNA to commence. In this case, the mRNA species should disappear and reappear at polysomes upon inhibition and removal of inhibition, respectively of cellular hypusine formation. This was found to be the case, and as a result a subset of polysomal mRNAs were detected and classified, that were associated with the mimosine-mediated modulation of hypusine formation, and subsequent transition of the G_1-S phase (Hanauske-Abel *et al*., 1995).

1.3.2 Role of eIF5A in HIV-1 replication as a potential antiretroviral target

Both the human T-cell leukemia virus type 1(HTLV-1) and human immunodeficiency virus type 1 (HIV-1) encode a *trans*-acting protein that regulates viral gene expression (Feinberg *et al*., 1986; Sodroski *et al*., 1986; Terwilliger *et al*., 1988). Theses nuclear phosphoproteins (Rev in HIV-1 and Rex in HTLV-1) are essential for viral replication and affect the transport, stability, splicing and translation of viral mRNA and accumulate in the nucleoli of infected cells (Sadaie *et al*., 1988; Malim *et al*., 1989; Arrigo & Chen, 1991; Cochrane *et al*., 1990). Rex is functionally interchangeable with Rev in the HIV-1 replication cycle, despite Rex belonging to a different subviral family (Rimsky *et al*., 1989; Sakai *et al*., 1990). Rex binds specifically to the Rev response element (RRE) or Rex response element (RXRE) sequence in viral RNA (Cochrane *et al*., 1990; Malim *et al*., 1990).

Cross-linking experiments and Bio-specific Interaction Analysis (BIA) have shown that eIF5A binds to the HIV-1 Rev activation domain (Ruhl *et al*., 1993). The HIV-1 Rev RNA transport factor requires eIF5A as an essential cofactor, suggesting that eIF5A may play a role in a specific nuclear export pathway. However, Rev in yeast cells does not appear to be exported in an eIF5A-dependent manner, but is rather dependent on the presence of Crm1 (Valentini *et al*., 2002). Immunofluorescence studies show that while eIF5A exists predominantly in the cytoplasm, a significant proportion of eIF5A localises to the nucleus in mammalian cells (Rosorius *et al*., 1999). Microinjection studies of somatic cells have demonstrated that eIF5A acts as a nucleocytoplasmic shuttle protein, the action of which can be inhibited by the addition of the cytotoxin Leptomycin B that blocks the nucleocytoplasmic translocation of HIV-1 Rev (Wolff *et al*., 1997; Wolff & Park, 1999). In addition, binding studies using recombinant GST-eIF5A and nuclear envelope proteins from *Xenopus* oocytes have shown that eIF5A interacts with nucleoporins and nuclear actin (Hoffmann *et al*., 2001). eIF5A has also been indicated as being an indispensable cofactor for Rex function and associates with Rex to form an oligomer (Katahira *et al*., 1995). Taken together, these results support the suggestion that eIF5A plays a role as a nucleocytoplasmic shuttle protein that is utilised by HIV-1 in its replication cycle. However, the archaeal homologue aIF5A has no nucleoocytoplasmic shuffling function, and so this cannot by inference be eIF5A's primary and conserved function (Zanelli & Valentini, 2007).

Inhibition of DOHH activity in mammalian cells results in the suppression of HIV-1 Rev replication (Andrus *et al*., 1998). Treatment of HIV-1-infected cell lines with mimosine, a natural compound and deferiprone, an experimental drug, results in the inhibition of DOHH

and suppresses virus replication by restricting HIV-1 to the early, non-degenerative phase of its reproductive cycle (Andrus *et al*., 1998). In addition, in the HIV-1 infected T-cell line, ACH2, extensive apopototic activity, particularly in cells actively producing HIV-1 following treatment with these drugs has been observed (Andrus *et al*., 1998). Similarly, inhibition of DHS by the novel inhibitor guanylhydrazone CNI-1493 or by RNA interference, results in the suppression of retroviral replication cycle in cell culture and primary cells (Hauber *et al*., 2005). The absence of measurable adverse effects on the general cytotoxicity, cell cycle transition and apoptosis of the inhibited cell lines suggest that the DHS and DOHH enzymes could be suitable targets for antiretroviral therapies (Andrus *et al*., 1998; Hauber *et al*., 2005).

Polyamine biosynthesis in most mammalian cells is regulated by four enzymes, predominantly ornithine decarboxylase (ODC) and S-adenosylmethionine decarboxylase (SAMDC) (Tabor & Tabor, 1984, 1985; McCann & Pegg., 1992; Pegg & McCann., 1992; Schafer *et al*., 2006). The well-established, potent low-molecular weight inhibitor of SAMDC, SAM486A, was used to efficiently suppress HIV-1 replication, including the replication of viruses previously resistant to multiple protease inhibitors and reverse transcriptase inhibitors (Regenass *et al*., 1994; Schafer *et al*., 2006). These studies provide a novel drug-design approach in the suppression of multiple-drug resistant viruses by inhibiting enzymes in the hypusine pathway.

1.3.3 eIF5A as an anti-cancer target

Most anti-cancer therapies are designed to induce cell death or inhibit cellular proliferation (Caraglia *et al*., 2001; Marra *et al*., 2007). Since eIF5A is involved in regulating the cell cycle, the protein has become a target for the development of novel anti-neoplastic agents. The polyamines, spermine and spermidine and putrescine (the diamine precursor for spermidine synthesis) are thought to be responsible for a number of cellular processes including cell growth, cell-cycle regulation, apopotosis and carcinogenesis. Polyamine synthesis results in the formation of hypusine and hence the hypusination process has also been targeted in the development of anti-cancer drugs. The following discussion focuses on the development of inhibitors of the active eIF5A modifying enzymes, DHS and DOHH and other tumour-suppressing agents that involve hypusinated eIF5A The anti-neoplastic agents, with their observed effects on cellular proliferation, are also discussed in this section and are summarised in Table 1.1.

Suppression of spermidine synthesis by D, L-α-difluoromethylornithine (DFMO) and subsequent inhibition of hypusine synthesis results in the thwarting of the G_1-S boundary in Chinese hamster ovary cells. Arrest in late G_1 and inhibition of DOHH activity occurs simultaneously (Park, 1987). Inhibition of hypusination using another compound, 2-(4-hydroxy-toluene-3-yl)-4,5-dihydro-5-carboxythiazole (Carboxythiazole), results in reversible cell cycle arrest in late G_1, in Human T lymphocyes as well as the suppression of human T lymphocytes *in vitro* at the G_1-S boundary, thus reducing cell proliferation (Lalande & Hanauske-Abel., 1990).

Table 1.1: Potential anti-cancer agents which synergistically affect the modulation of cellular proliferation.

Agent	Abbreviation	Cell line	Effects observed	Reference
Interferon α	IFN-α	human epidermoid cancer KB cells	Reduces hypusine synthesis	Caraglia *et al*., 1999
D,L-α-difluoro-methylornithine	DFMO	Chinese hamster ovary cells	Depresses spermidine levels; Suppresses hypusine formation; Arrests cells at the G_1-S transition	Park, 1987
2-(4-hydroxy-toluene-3-yl)-4,5-dihydro-5-carboxythiazole	Carboxythiazole	Human T lymphocytes	Arrests cells at G_1-S phase, Reduces cellular proliferation	Lalande & Hanauske-Abel, 1990
Diaminoheptane	DAH	DH23A cells	Strong inducer of apopotosis; Blocks hypusine synthesis	Tome & Gerner, 1997
Cytosine arabinoside combined with desferioxamine	Ara-C and DSF	Human acute myeloid leukaemic blasts	Induces apoptosis; Growth inhibition; Iron depletion; Inhibitor of deoxyhypusine hydroxylase	Leardi *et al*., 1998
N^1-guanyl-1,7-diaminoheptane; α-difluoromethylornithine; N^1-(3-aminopropyl)-cyclohexamine	GC_7 DFMO APCHA	Mouse mammary carcinoma FM3A cells	Decrease in eIF5A; Decrease in polyamines; Inhibition of cell growth	Nishimura *et al*., 2005
N^1-guanyl-1,7-diaminoheptane	GC_7	Malan-a-murine melanocytes; Tm5 murine melanomal cells	Inhibitor of DHS; Decrease in cell viability; impaired melanomal growth in mice	Jasiulionis *et al*., 2007
Hypusine inhibitors	HIs	Leukemia K562 cells	Anti-proliferative effect	Balabanov *et al*., 2007

In HeLa cells, the association of eIF5A with transglutaminases (TGases) is promoted by the addition of Ca^{2+}, Mg^{2+} and retinoic acid (Singh *et al*., 1998). TGase activity is found to promote apoptosis (Fesus, 1998) and tumour cell proliferation (Nakaoka *et al*., 1994; Johnson,

1994). Beninati *et al*.,1995, 1998). When Balb C-3T3 cells are transfected with the gene for the human TGase, a 50 % retardation of cell proliferation, accompanied by a 50 % increase in apoptosis is observed, presumably through the inactivation of hypusinated eIF5A (Beninati *et al*. 1998). Similarly, the proapoptotic agent Interferon α (IFNα), induces a strong reduction in hypusine synthesis along with apoptotic events in human epidermoid KB cancer cells (Caraglia *et al*., 1999). However, this reduction in hypusine synthesis can be restored by exposing the IFNα-treated cells to the epidermal growth factor (EGF).

The triggering of apoptosis in tumour cells is enhanced by the excess accumulation of polyamines, specifically spermidine (Tome & Gerner, 1997). This cytostasis or cytoxicity has been attributed to excess putrescine or polyamines in a number of mammalian cell lines (Brunton *et al*., 1991; Mitchell *et al*., 1992; Packham & Cleveland, 1994; McCloskey *et al*., 1995; Tobias & Kahana, 1995). However, in hepatoma DH23A/b cells which express high levels of ornithine decarboxylase, there is an accumulation of putrescence resulting in the inhibition of hypusination and results in the induction of apoptosis (Tome & Gerner, 1997). Diaminoheptane (Table 1.1), a strong inducer of apoptosis, also blocks post-translational modification of eIF5A (Tome *et al*., 1997). The addition of cytosine arabinoside (Ara-C) combined with desferioxamine (DSF), a powerful iron-depleting agent, result in growth inhibition and an increase in the induction of apoptosis (Leardi *et al*., 1998). The precise mechanism by which the accumulation of putrescine and polyamine effect the inhibition of hypusination, and induce apoptosis is yet to be determined.

More recently, three other potential chemotherapeutic agents, namely N^1-guanyl-1,7-diaminoheptane (GC_7), α-difluoromethylornithine (DMFO) and a combination of N^1-(3-aminopropyl)-cyclohexamine (APCHA) with DMFO (Table 1.1), were investigated for their ability to inhibit cell growth by reducing polyamine (and more specifically spermidine) synthesis, and thus decreasing levels of active eIF5A (Nishimura *et al*., 2005). Treatment of mouse mammary carcinoma cells with GC_7 resulted in the inhibition of hypusine synthesis without a decrease in total polyamines, while DFMO resulted in a decrease in both polyamines and hypusine synthesis (Nishimura *et al*., 2005). This suggests that polyamines and eIF5A can independently affect cell proliferation. DMFO plus APCHA-treated cells showed a reduction of total polyamines with little to no reduction of hypusine synthesis (Nishimura *et al*., 2005). GC_7 also has been reported to impair melanomal growth in melanomal mice (Jasiulionis *et al*., 2006).

The expression of hypusinated eIF5A is down-regulated by the tyrosine kinase inhibitor, Imatinib (Table 1.1) (O'Dwyer & Druker, 2001; Balabanov *et al*., 2007). Imatinib treatment has been used extensively in the inhibition of BCR-ABL tyrosine kinase in patients with chronic myeloid leukemia. The use of hypusine inhibitors (HIs) alone has been shown to result in a reduction in cellular proliferation in BCR-ABL-positive and –negative leukemia K562 cell lines. However, when HIs were combined with Imatinib, the anti-proliferative effect was confined to BCR-ABL-positive cells (Balabanov *et al*., 2007*).*

Hypusinated eIF5A partners with syntenin, a protein that binds to the cytoplasmic domains of the syndecans (transmembrane proteoglycans) to collaborately regulate p53 activity (Grootjans *et al*., 1997; Li *et al*., 2004). The transcription factor p53 is a tumour suppressor scaffolding protein understood to be the major component of the DNA damage response pathway (Lane, 1992; Rahman-Roblick *et al*., 2007). In 50 % of human cancers, the p53 gene is mutated (Bourdon, 2007). Li *et al*., (2004) have recently shown that the eIF5A-syntenin complex functions to regulate p53 and p53-dependent apoptosis. While over-expression of eIF5A alone leads to the up-regulation of p53 activity and thus p53-dependent apoptosis, or sensitises cells to apoptotic events by anti-neoplastic agents, administration of eIF5A together with syntenin results in significantly lowered p53 protein levels (Li *et al*., 2004). Furthermore, induction of apoptosis in colon carcinoma cells by the over-expression of either active eIF5A or unmodified mutant eIF5A protein reveals that unhypusinated eIF5A may be sufficient to induce programmed cell death (Taylor *et al*., 2006; Taylor *et al*., 2007).

The expression of p53 relies on the presence of eIF5A following the apoptotic induction by treatment with Actinomycin D (Taylor *et al*., 2006; Taylor *et al*., 2007). Subcellular localisation experiments show that following induction of apoptosis (by either death receptor activation or treatment with Actinomycin D), eIF5A is rapidly translocated from the cytoplasm to the nucleus. These results suggest that eIF5A may have pro-apoptotic functions when translocated to the nucleus and that this function may not be dependent on the presence of the hypusine modification (Taylor *et al*., 2006; Taylor *et al*., 2007).

1.3.4 eIF5A is an mRNA binding protein

eIF5A has been proposed to act as a bimodular protein, interacting with both nucleic acid and protein (Liu *et al*., 1997). Motif analysis showed that eIF5A has a cluster of basic amino acids at the N-terminus, and a region rich in leucine at the C-terminus. This, together with the observation that eIF5A closely resembles the structure of Cold shock protein A (CspA), an

RNA chaperone with a distinct oligonucleotide binding (OB) fold, has led to the hypothesis that eIF5A could itself bind RNA (Jiang *et al*., 1997; Liu *et al*., 1997). This was confirmed by gel mobility shift assays, which demonstrated that eIF5A binds RNA in a hypusine-dependent manner (Liu *et al*., 1997). Another interesting observation is that protein synthesis is reduced by about 30 % when compared with wild-type rate in eIF5A-depleted cells, with a slight change in total polysomal profiles (Kang & Hershey, 1994; Zanelli *et al*., 2006). This suggests that eIF5A is not required for general protein synthesis, but is rather involved in the translation of certain mRNAs (Kang & Hershey, 1994).

GST-pulldown experiments have shown that eIF5A associates with translationally active ribosomal components in a hypusine-dependent manner, specifically the eukaryotic translation elongation factor (eEF2), 60S ribosomal protein P0 and the 40S ribosomal protein S5 (Zanelli *et al*., 2006). Because eIF5A co-fractionates with monosomes in a translation-dependent manner and non-functional mutants of eIF5A are also sensitive to translation inhibitors, a role for this factor in translation elongation, rather than translation initiation was proposed (Zanelli *et al*., 2006). eIF5A is dissociated from ribosomes upon treatment with EDTA or RNase A (Zanelli *et al*., 2006). Since eIF5A associates with EF2, it is proposed that eIF5A associates specifically with translationally active (elongating) ribosomes (Zanelli *et al*., 2006).

Systemic evolution of ligands by exponential enrichment (SELEX) was used to identify the consensus RNA binding sequence recognised by eIF5A. The Post-SELEX RNAs obtained after 16 rounds of enrichment all shared a high sequence homology, typified by the conserved motifs, UAACCA and AAUGUCACAC (Xu & Chen, 2001). Further refinement determined the consensus sequence as being AAAUGUCAC with the RNA bound to eIF5A being sensitive to ribonuclease attack. Most importantly, hypusine was again identified as a critical factor in the sequence-specific binding of eIF5A to the RNA (Xu & Chen, 2001). Additional research demonstrated the direct binding of cloned RNA species to eIF5A by electromobility assays, and the species were identified by affinity co-purification and PCR differential display (Xu *et al*., 2004). Many RNA-binding proteins do not target defined RNA sequences, but rather structural elements such as hairpins, bulges and stem-loops. The cloned RNAs all had the potential to form extensive secondary structural elements, particularly stem-loops (Xu *et al*., 2004).

In a separate study in *S. cerevisiae,* the turnover rates of mRNA were thought to have significant effects on the expression of certain genes and would allow for flexible protein levels in the cell. During experiments to determine factors involved in increased levels of unstable pre mRNAs, a mutant form of *TIF51A* was identified (Zuk & Jacobson, 1998). This mutant *tif51A* was shown to encode a change of Ser 149 to Pro 149 (S149P) at the C-terminus of eIF5A. The substitution resulted in decreased mRNA decay, and a 30 % decrease in overall protein synthesis. An additional observation was that the cells bearing the *tif51A* allele also accumulated uncapped mRNAs (Zuk & Jacobson, 1998). These results implied that eIF5A was involved in the regulation of 5'-> 3' exonucleolytic decay. Another *tif51A* mutant was analysed in a yeast knockout system, this time with a point mutation at Val 81 to Gly (V81G) (Schrader *et al*., 2006). Not only was strong temperature sensitivity observed, but also an accumulation of nonsense-containing RNAs. These RNAs are known to be degraded by the polyadenylation-independent 5'-> 3' mRNA decay pathway, also known as nonsense-mediated decay (NMD). Other effects included reduced telomere silencing and telomere shortening (Schrader *et al*., 2006). Together, these observations reinforced the proposal that eIF5A influences essential cellular functions such as cell viability and senescence through its role in RNA processing, particularly the translation of the suite of mRNAs required for programmed cell death (Wang *et al*., 2001; Schrader *et al*., 2006).

Veress *et al*., (2000) showed that polyamine depletion resulted from the addition of the α-difluoromethylornithine (DFMO) inhibitor in Rat-2 cells. This depletion was coupled with the blocking of cell growth, and also resulted in the stabilisation of mRNAs. It was deduced that the lack of spermidine for the hypusination of eIF5A influenced the mRNA turnover, and provided an efficient means for cells to resume growth after the recovery from polyamine starvation (Veress *et al*., 2000).

The human cancer-promoting gene, cyclooxygenase-2 (COX-2) has been determined to have consensus eIF5A response elements (EREs) in its 3'-untranslated region (3'-UTR) (Parker & Gerner, 2002). The depletion of polyamines by DL-α-difluoromethylornithine (DFMO) treatment results in the induction of COX-2 mRNA steady-state levels in various human cancer cell lines (Parker & Gerner, 2002), suggesting that polyamines negatively regulate COX-2 levels by a post-transcriptional mechanism, mediated by eIF5A.

Tandem affinity purification (TAP) along with mass spectroscopy (MS), has been employed to search for and identify potential eIF5A-interacting proteins (Jao & Chen, 2006). Deoxyhypusine synthase was identified as the sole protein partner of hypusinated eIF5A at high (150 mM) salt concentrations. Upon the lowering of salt concentrations to 125 mM or less, a new set of eIF5A-bound proteins were identified, which were identified as the components of the 80S ribosome complex. Treatment with both RNase and EDTA resulted in the disassociation of the eIF5A-RNA complex into its components and the 40S and 60S ribosomal subunits (Jao & Chen, 2006). Mutation of the hypusine (lysine) to arginine, resulted in the abolishment of the eIF5A-ribosome interaction. These results show that eIF5A requires hypusine to form a molecular complex with actively translating ribosome in order to perform its essential role in the cell (Jao & Chen, 2006).

Finally, an archaeal protein (aIF5A) isolated from *Halobacterium sp*. NRC-1 with strong homology to yeast and human eIF5A showed RNA-degrading activity whether it was hypusinated or not (Wagner & Klug, 2007). However, there is also some evidence that human eIF5A shows hypusinated ribonucleolytic activity (Xu & Chen, 2004; Wagner & Klug, 2007). In addition, RNA binding with aIF5A was observed, but only from protein purified from the native host, i.e. hypusinated protein. These results indicate RNA binding is hypusine-dependent, while RNA cleavage activity is hypusine-independent. Also, both domains of aIF5A, the N-terminal domain with its charged amino acids, and the C-terminal domain are required for RNA cleavage activity. Interestingly, the ribonucleolytic activity of aIF5A also seemed to depend on its oligomeric state (Wagner & Klug, 2007). The human eIF5A protein has also been found to exist in a number of oligomeric states (Chung *et al*., 1991). Using exclusion chromatography and analytical ultracentrifugation, the study demonstrated that hypusinated eIF5A exists as a dimer in solution and is capable of undergoing reversible self-association to form higher oligomers (Chung *et al*., 1991).

1.3.5 Function of eIF5A in protein synthesis

eIF5A was originally identified as a general translation initiation factor as it stimulated the synthesis of methionyl-puromycin *in vitro* (Benne & Hershey,1978; Kang & Hershey, 1994). Following this, eIF5A was thought to be involved in the translation of a specific subset of mRNAs rather than in general protein synthesis (Kang & Hershey, 1994). This was demonstrated by work showing that hypusinatedeIF5A interacts with the structural components of the 80S ribosome and translation elongation factor 2 (Zanelli *et al*., 2006; Jao

& Chen, 2006), suggesting a role for eIF5A in translation elongation. More recently, mutational analysis of eIF5A showed that the region around hypusination site, specifically residues K47D and K50R (human eIF5A) and K56A and Q22H/L93F (in yeast eIF5A) and not only the highly conserved lysine (K51 in yeast), played a role in protein synthesis (Cano *et al*., 2008; Dias *et al*., 2008). Although a specific mechanism for eIF5A in protein synthesis is not available, it is worth reviewing eIF5A's role in translation initiation or elongation based on this new evidence.

1.4 Structure of eIF5A

When eIF5A was first purified from rabbit reticulocytes and the resulting cDNA was cloned and analysed for the product, the prediction was that eIF5A possessed little secondary structure at the amino terminal region of the protein and that the carboxy terminal region was rich in alpha helices (Smit-McBride *et al*., 1989). This has subsequently been shown not to be the case, at least for archaeal homologues of eIF5A. The crystal structures of the eIF5A homologues (aIF5A) from *Methanococcus jannaschii*, *Pyrobaculum aerophilum* and *Pyrococcus horikoshii* have been solved using multiple isomorphous replacement (MIR) or multiwavelength anomalous diffraction (MAD) (Kim *et al*., 1998; Peat *et al*., 1998; Yao *et al*., 2003). MIR and MAD techniques make use of the addition of a reducing agent such as dithiothreotol (DTT) or β-mercaptoethanol to keep the substituting heavy atoms (Hg, Se, Ir) in a reduced form. All the structures to date were derived from purified protein expressed in *E. coli* and were thus not hypusinated (Kim *et al*., 1998; Peat *et al*., 1998; Yao *et al*., 2003). Although the crystal structure is not currently available, attempts have been made to produce homology models of the human eIF5A based on aIF5A and unpublished protozoan eIF5A structures (Facchiano *et al*., 2001; Costa-Neto *et al*., 2006).

The aIF5A protein consists of two distinct anti-parallel β-sheet folding domains separated by a flexible hinge (Figure 1.4). Each of the domains has a well-defined hydrophobic core inside the β-barrels (Peat *et al*., 1998). The conserved lysine residue, that is the site of hypusination, is in all cases, located in the middle of a highly-conserved stretch of residues on a long, protruding hairpin loop of domain I (Figure 1.4). Most of the amino acid residues conserved between the three aIF5A proteins are found to be within domain I (N-terminus) while domain II (C-terminus) is less conserved (Yao *et al*., 2003). Both domains have the capacity to bind nucleic acids. Domain I contains an SH3-like barrel motif that is found in the DNA binding domains of a number of proteins, including HIV-integrase (Lodi *et al*., 1995, Eijkelenboom *et*

al., 1995). Domain II, forming a barrel structure between the sheets and loops, resembles the oligonucleotide-binding fold (OB Fold) of several proteins, but is most similar to the *E. coli* cold shock protein A (CspA), which has a recognised RNA-binding fold (Schindelin *et al*., 1994; Murzin, 1993). There is only a 10 % sequence identity between the *E coli* CspA and the *M. jannaschii* aIF5A, attributed mainly to the differences in size of the proteins.

A comparison of the three currently available archael crystal structures is represented in Figure 1.4, displaying the relative position of the lysine that is hypusinated in each (as sticks). All three models share the same backbone structure of β-sheet arrangement and variations are observed in the presence of partial α-helical turns in the C-terminal domain.

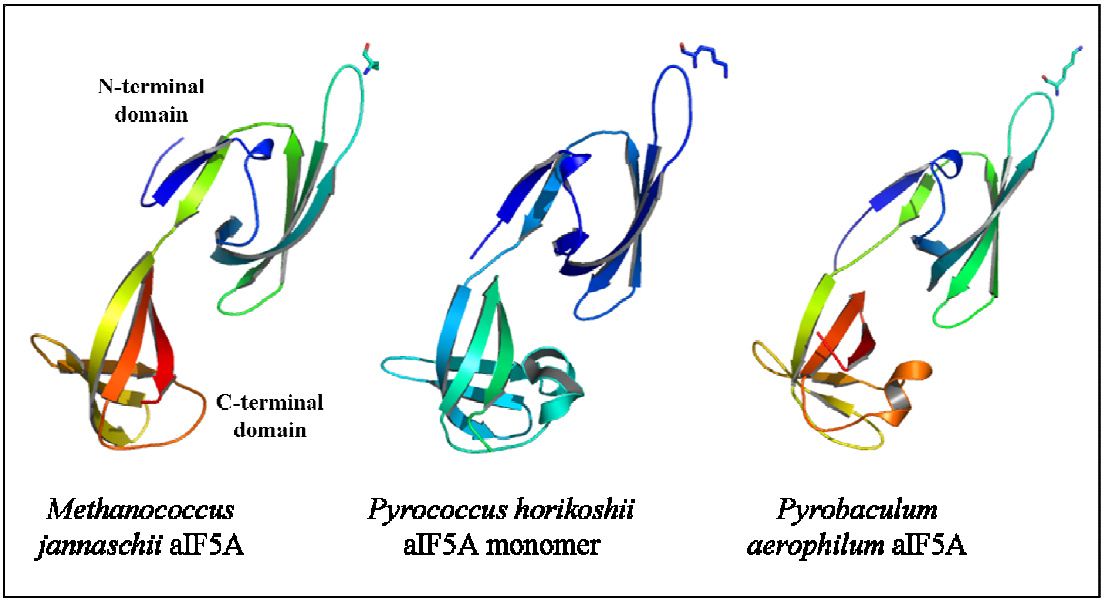

Figure 1.4: Models of the crystal structures of three archaebacterial initiation factor 5As (aIF5As). From left to right: Models of the crystal structures of *Methanococcus jannaschii* (PDB code 2EIF), *Pyrococcus horikoshii* (PDB code 1IZ6; monomeric unit) and *Pyrobaculum aerophilum* (PDB code 1BKB). Marked in sticks on each model is the highly-conserved lysine residue (equivalent to Lys 51 in yeast) on the N-terminal region of the protein. Partial α-helical turns are present on the latter two crystal structures near the C-terminus (Kim *et al*., 1998; Peat *et al*., 1998; Yao *et al*., 2003). The figures were generated using Pymol (DeLano, 2002).

1.5 The evolution and conservation of eIF5A

Yeast contains two clusters of eight genes each on chromosomes V and X, namely ARC and COR regions, which include *TIF51A* and *TIF51B* respectively (Melnick & Sherman, 1993). Comparisons and alignments of the two regions show a possible ancestral relationship, arising due to duplication, transposition and single rearrangement events, followed by extensive

divergence, another explanation for the interchangeability of the two genes under aerobic or anaerobic growth conditions (Melnick & Sherman, 1993).

Although hypusine, its precursor deoxyhypusine, eIF5A, DHS and DOHH occur in all eukaryotes, only eIF5A, hypusine and DHS have been detected in archaeal proteomes (Park 2006). The presence of deoxyhypusine and hypusine has been reported in archaeal species (Bartig *et al*., 1992), but it is unclear how hypusine can be produced without the presence of DOHH. The stretch of amino acids surrounding the highly-conserved lysine residue (Lys 51 in yeast) is highly conserved amongst the eukaryotic and archaeal initiation factor 5As (Park *et al*., 1986, 1993; Bartig *et al*., 1992). The yeast and human eIF5A proteins share 64 % sequence identity while yeast eIF5A shares about 35 % sequence identity with archaebacterial translation initiation factor 5A (aIF5A), (Schnier *et al*., 1991; Magdolen *et al*., 1994).

Although no evidence for the existence of deoxyhypusine in eubacteria, elongation factor P (EF-P), an orthologue of eIF5A has been identified as being essential in bacteria as it stimulates the peptidyl transferase activity of ribosomes (Glick & Ganoza, 1975; Kyrpides & Woese, 1998; Brochier *et al*., 2004). Phylogenetic analysis has resulted in the identification of several bacterial species that contain DHS cognate genes. These are presumed to have been transferred by horizontal gene transfer from the archaea. DHS does not ordinarily occur in bacteria so it is unlikely that EF-P undergoes deoxyhypusine modification (Brochier *et al*., 2004). This suggests that eIF5A and the hypusination machinery (DHS and DOHH) have evolved sequentially, but in an independent manner (Brochier *et al*., 2004). The crystal structure of EFP from *Thermus thermophilus* HB8 shows that EFP consists of three domains, arranged in an "L" shape: domain I sharing topological similarities to the N-terminal portion of eIF5A (Figure 1.5A), and domains II and III sharing a topology with the C-terminal region of eIF5A (Figure 1.5B) (Hanawa-Suetsugu *et al*., 2004). To some extent, eIF5A shares a remarkable functional similarity with EFP, in that both are affected by peptidyl-transferase inhibitors *in vitro* (Aoki *et al*., 1997a; Hanawa-Suetsugu *et al*., 2004); both are essential for cell viability and bind to elongating ribosomes (Aoki *et al*., 1997b; Ganoza *et al*., 2002) and both may affect protein synthesis (Kang & Hershey, 1994).

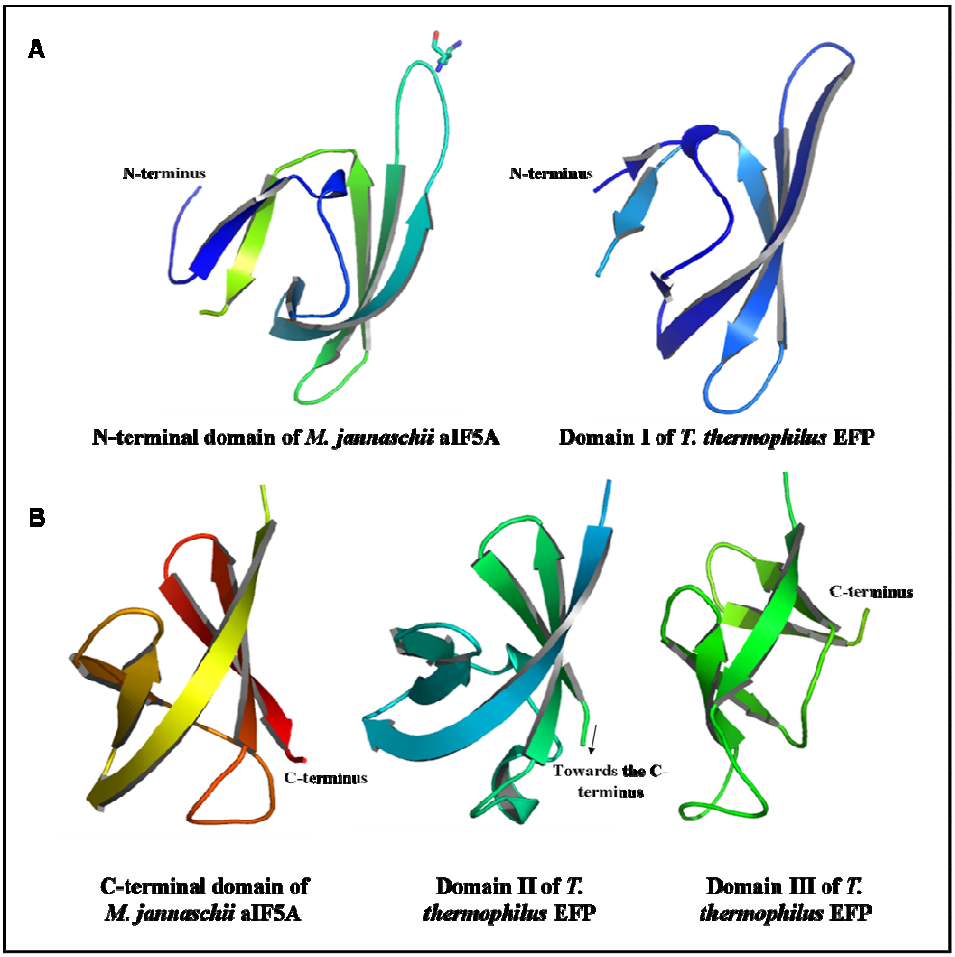

Figure 1.5: Comparison of the crystal structures of aIF5A with EFP. (A): Domain I of *T. thermophilus* EFP (right) structurally resembles the N-terminal region of the *M. jannaschii* aIF5A (left), while the crystal structure of domains II and II of EFP are similar to the C-terminal portion of aIF5A (B). The cartoon representations were generated using Pymol (DeLano, 2002) from *M. jannaschii* aIF5A (PDB code 2EIF) and *T. thermophilus* EFP (PDB code 1UEB) (Kim *et al*., 1998; Hanawa-Suetsugu *et al*., 2004).

Cold shock protein A (CspA), another orthologue of eIF5A, has also been suggested to be evolutionarily linked to eIF5A, mainly because this 7.4 kDa protein structurally resembles the C-terminal portion of eIF5A (Figure 1.6) (Jiang *et al*., 1997; Kim *et al*., 1998). Although no specific RNA targets have been found to bind to CspA, it is thought that it has a broad sequence specificity for binding, reinforcing its role as an RNA chaperone. CspA functions by either destabilizing RNA secondary structures making them more susceptible to ribonuclease attack, or by preventing the formation of secondary structures in RNA molecules at low temperatures (Jiang *et al*., 1997). Thus it can be extrapolated that the observed RNA-binding capacity and mRNA turnover of eIF5A could be mediated by the OB-fold.

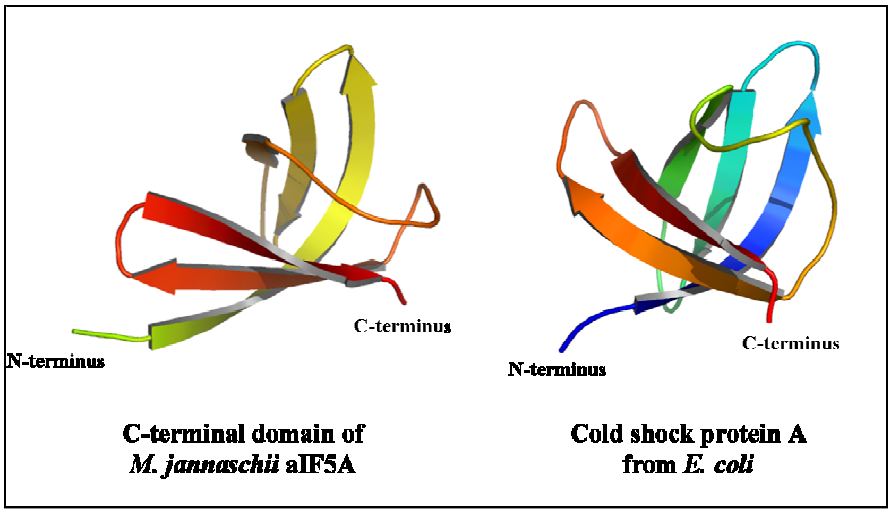

Figure 1.6: Structural comparison of CspA and aIF5A. Cartoon depiction of the *E. coli* RNA-chaperone, CspA (right; PDB code 1MJC) (Schindelin *et al*., 1994; Feng *et al*., 1998), that bears a strong resemblance to the C-terminal domain of *M. jannaschii* aIF5A (left; PDB code 2EIF) (Kim *et al*., 1998; Jiang *et al*., 1997). Models were generated using Pymol (DeLano, 2002).

HEX-1, the major self-assembly protein component of Woronin body function (septal pore sealing) in *Neurospora crassa*, has a potential ancestral link to eIF5A (Yuan *et al*., 2003). HEX-1 fails to complement an eIF5A mutant in yeast, presumably because it lacks the ability to undergo hypusination, so although a structurally-related analogue, it displays a high degree of functional divergence (Holm & Sander, 1999; Jedd & Chua, 2000; Yuan *et al*., 2003). The structural similarities between the HEX-1 monomer and aIF5A are depicted in Figure 1.7.

The structural comparisons of the eIF5A homologue, aIF5A, with the orthologues CspA and EFP and the analogue, HEX-1 are summarised in Table 1.2. All of the above have in common an OB-fold, and with the exception of CspA, all have an SH-3-type β-barrel architecture. These proteins, along with a more detailed eIF5A structural analysis, will be discussed extensively in Chapter 2.

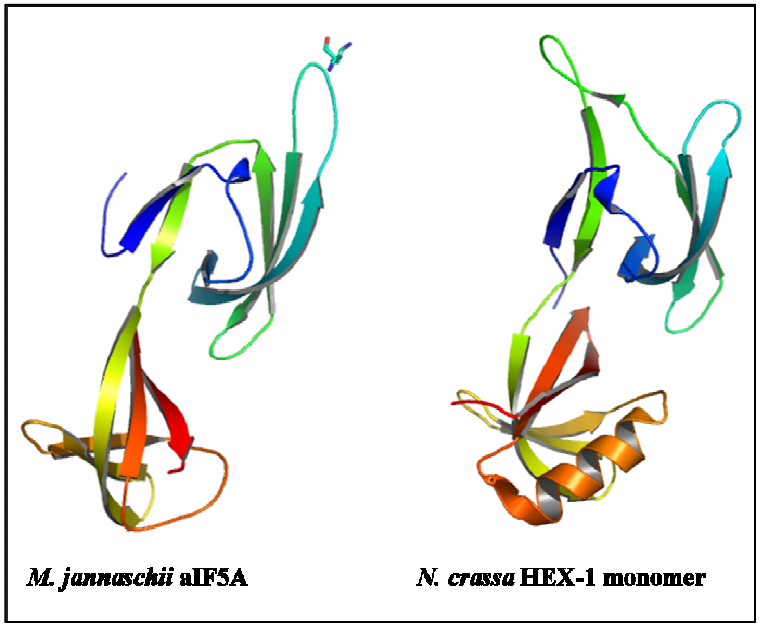

Figure 1.7: Crystal structure comparison of aIF5A and HEX-1. On the left is a cartoon representation of the *M. jannaschii* aIF5A (PDB code 2EIF; Kim *et al*., 1998), depicting the lysine residue that is modified (Lys 51 in yeast) as sticks. On the right is a comparative crystal model of the *N. crassa* HEX-1 protein (PDB code: 1KHI; Yuan *et al*., 2003). Although HEX-1 contains a C-terminal region α-helix, the monomer show remarkable structural similarity. Models were generated using Pymol (DeLano, 2002).

Table 1.2: Structural comparison of the eIF5A homologue, aIF5A, orthologues, CspA and EFP and analogue HEX-1.

Relation to eIF5A	**Homologue**	**Orthologues**		**Analogue**
	aIF5A	**CspA**	**EFP**	**HEX-1**
Host Organism	*M. jannaschii*	*E. coli*	*T. thermophilus*	*N. crassa*
PDB Code	2EIF	1MJC	1UEB	1KHI
Topological features	SH3-type barrels; Lacks OB-Fold	OB-Fold	SH3-type barrels; OB-fold	SH3-type barrels; Predicted OB-Fold
Predicted Functions	Translation initiation; binding of nucleic acid	RNA-Chaperone; Binding of nucleic acid	Translation elongation; binding of nucleic acid	Self-assembly protein; septal pore sealing; nucleic acid binding
Size (monomer)	16 kDa	7.4 kDa	20.2 kDa	19 kDa
Structural similarity to eIF5A	aIF5A similar to both N- and C-terminal regions of eIF5A	CspA similar to the C-terminal domain of eIF5A	Domain I similar to N-terminal region of eIF5A; Domains II and III similar to C-terminal region of eIF5A	N- and C-terminal domains similar to eIF5A
Sequence identity to aIF5A	100 %	24 % to the C-terminal portion of aIF5A	27 %	20 %

1.6 Knowledge Gap

The biological functions of eIF5A are not well understood, although several roles have been proposed, including cell-cycle regulation, HIV-replication, carcinogenesis, apoptosis and nucleocytoplasmic transport of mRNA during the translation process, all of which are dependent on the presence of hypusine. Hypusine is also required for eIF5A to bind specific RNA sequences and to form associations with translationally active ribosomal components.

The biochemical synthesis of hypusine has also been extensively studied, with an emphasis on the structure of the eIF5A modification enzymes DHS and DOHH. Recently, the focus has shifted to developing an understanding of the biological interactions of these enzymes with eIF5A, as well as ligands interacting with eIF5A *in vivo*. Exactly how hypusine relates to the function of eIF5A *in vivo* is as yet not clear, because structural information has been predominantly derived from X-ray crystallographic studies on several aIF5As (Kim *et al*., 1998, Peat *et al*., 1998; Yao *et al*., 2003) and two protozoan (unpublished) eIF5A which were crystallised in their unhypusinated form.

In contrast to eIF5A, there has not been substantial biochemical characterisation of aIF5As. There is now evidence which suggests that there might be significant differences the biological function of the archaeal and eukaryotic homologues. For example, hypusine is required for RNA binding in aIF5A and eIF5A, while RNA cleavage activity is hypusine-dependent only in aIF5A (Wagner & Klug, 2007). This raises the question of how relevant the structural information derived from archaeal homologues of eIF5A are in providing insights into how the protein functions *in vivo*. Finally, there is no structural data available for eIF5A in its modified (hypusinated) form and it remains to be seen whether the presence of hypusine results in conformational changes of the protein which are required for its functions *in vivo*, including the binding of specific RNAs.

1.7 Research Aim

The overall aim of the research described in this thesis is to produce an homology model of the yeast eIF5A and to conduct biochemical and functional analyses to validate the model.

1.8 Research objectives

1. To generate an homology model of yeast eIF5A using available structures of homologues and analogues.
2. To develop an experimental system and to conduct a biochemical and functional characterisation of native yeast eIF5A.
3. To relate the biochemical and functional data to the predicted structure of eIF5A.

Chapter 2: *In silico* analysis of eIF5A

Chapter 2: *In silico* analysis of eIF5A

2.1 Introduction

A number of crystal structures of eIF5A homologues have been published, including the archaeal translation initiation factor (aIF5Aa) from *Methanococcus jannaschii* (Kim *et al*., 1998), *Pyrobaculum aerophilum* (Peat *et al*., 1998) and *Pyrococcus horikoshii* (Yao *et al*., 2003). In addition, human eIF5A has been crystallised, but the structure has not been solved (Sun *et al*., 2005; Facchianao *et al*., 2001). In each case, the crystal structures were derived from recombinant protein produced in *E. coli*. The information derived from this structural data is thus limited to the archaeal homologue of eIF5A, in its monomeric form, and lacks the post-translational modification of hypusine.

Molecular models of the human eIF5A protein have been produced based on the crystal structure of the eIF5A from *Leishmania brasiliensis* (Costa-Neto *et al*., 2006). In addition, circular dichroism (CD) data was obtained with a synthetic peptide of the loop region bearing the hypusination site, which showed that this critical region may adopt an ordered conformation that might contribute to functionality of human eIF5A with Dexoyhypusine synthase (DHS) or with nucleic acids. Since there is no structural data available for yeast eIF5A, an homology model could provide insights into bridging the structure-function relationship gap.

The main objective of the research discussed in this chapter was to make use of *in silico* tools to predict the structure of yeast eIF5A. It is hypothesised that the yeast eIF5A protein is similar enough to the archaeal homologues to produce a homology model. This model could then be used to identify regions important for the structural integrity and/or function of yeast eIF5A. Since it is postulated that human eIF5A exists mainly in a dimeric form in solution, and since aIF5A from *Halobacterium sp*. depends on its oligomeric state to be active, it was not unreasonable to assume that yeast eIF5A may also exist as a dimer or even in higher oligomeric states (Chung *et al*., 1991; Wagner & Klug, 2007). Furthermore, the eIF5A structural analogue, HEX-1 from *Neurospora crassa*, exists as a crystal lattice, formed by three types of dimer interactions (Yuan *et al*., 2003). Thus it is also hypothesised that the yeast eIF5A mimics the dimer configurations employed by the evolutionary-related structural analogue, HEX-1.

2.2 Materials and Methods

2.2.1 Alignment of eIF5A sequences

The non-redundant GenBank nucleotide database (NCBI) and Swiss Prot protein sequence database (SwissProt) were searched using the amino acid sequence of *S. cerevisiae* (yeast) eIF5A (Accession code NP010880) employing the BLASTP algorithm (Altschul *et al*., 1997). The results were then restricted to those with the highest scores for proteins with known three dimensional structures in the Protein Data Bank (PDB). The search results included the identification of the *Methanococcus jannaschii* aIF5A (PDB entry 2EIF), *Pyrococcus horikoshii* aIF5A (PDB entry 1IZ6), *Pyrobaculum aerophilum* aIF5A (PDB entry 1BKB), *Leishmania mexicana* eIF5A (PDB entry 1XTD), *L. brasiliensis* eIF5A (PDB entry 1X6O) and the *Neurosporra crassa* HEX-1 proteins (PDB entry 1KHI). The *S. cerevisiae* (yeast) eIF5A (Accession code NP010880), *Homo sapiens* eIF5A (Accession code NP001961) and *L. mexicana* eIF5A (Accession code 1XTDA) protein sequences were aligned using the CLUSTALW algorithm (Chenna *et al*., 2003). The sequences of *M. jannaschii* aIF5A (Accession code 2EIFA), *P. horikoshii* aIF5A (Accession code 050089) and *P. aerophilum* aIF5A (Accession code P56635) were also aligned using CLUSTALW (Chenna *et al*., 2003).

2.2.2 Structural prediction and homology modeling

Secondary structure prediction of α-helices and β-sheets was performed using JPred (Cuff & Barton, 1999). Three-dimensional molecular models of yeast eIF5A were generated using the Swiss Model first-approach mode tool (Guex & Pietsch, 1997; Schwede *et al*., 2003), using the three-dimensional structure of the eIF5A from *L. mexicana* (Protein Data Bank (PDB) entry 1XTD) or the aIF5A from *M. jannaschii* (PDB entry 2EIF). Yeast eIF5A homology models were also generated using WHAT IF (Vriend, 1990) and MODELLER (Sali *et al*., 1995) and outputs were verified using WHAT_CHECK (Hooft *et al*., 1996) and PROCHECK (Laskowski *et al*., 1993). Pymol was used to view and manipulate monomeric structural representations of eIF5A, its homologues and analogues (DeLano, 2002). Oligomeric structures were derived from the template protein by identifying symmetry mates within a unit cell, within a distance of 4 Angstroms (Å).

2.3 Results and Discussion

Since the structure of eIF5A could be used to derive a possible mechanism by which the protein functions, an *in silico* analysis of the yeast eIF5A was performed. This involved drawing inferences, using homology modeling and secondary structure predictions, from current crystal structure data derived from the well-studied archaeal homologues *M. jannaschii* (Kim *et al*., 1998), *P. horikoshii* (Yao *et al*., 2003) and *P. aerophilum* (Peat *et al*., 1998). Structural information on eukaryotic homologues of yeast eIF5A is limited, but databases such as the Protein Data Bank were useful in retrieving structural information from other homologues and analogues of eIF5A. The homologue of particular interest was the eIF5A from *L. mexicana* because although not published, the three-dimensional structure is available on the database. The analogue of interest was the distantly related, functionally diverse, but structurally related *Neurospora crassa* protein HEX-1 (Yuan *et al*., 2003). HEX-1 is known to dimerise by three distinct configurations to ultimately form a crystal lattice. Although eIF5A is not known to form such a lattice, it was useful to make use of these configurations to predict oligomeric models of eIF5A.

2.3.1 Protein alignments and secondary structure predictions

Firstly, yeast eIF5A was analysed in comparison with other eIF5A proteins for regions of conservation. Yeast eIF5A shares a 60 % and 43 % sequence identity with human eIF5A and *L. mexicana* eIF5A respectively. As expected, alignment of these proteins shows a high degree of conservation of the area flanking the highly conserved (hypusinated) lysine (Figure 2.1A, highlighted in blue). Although only three of the eIF5A proteins are represented, extensive alignments with other eIF5A show similar degrees of conservation in the areas highlighted in Figure 2.1A (and data not shown). In addition either an “RPCK” or a “PCK” motif was observed when aligning the various eIF5A proteins (Figure 2.1A, highlighted in yellow). Also notable was that there were at least 2 cysteine residues in eIF5A proteins (data not shown).

In contrast, when aligning the archaeal translation initiation factor 5Aa (aIF5Aa) proteins (Figure 2.1B), only a "PC" motif was conserved. Moreover, only 1 cysteine residue was observed for each aIF5Aa analysed (data not shown). Three of the aIF5Aa proteins were aligned to represent the areas of conservation obtained in all aIF5Aas analysed (Figure 2.1B and data not shown). These included the *M. jannaschii*, *P. horikoshii* and *P. aerophilum* aIF5Aa proteins. *M. jannaschii* shares a 44 % and 49 % sequence identity with *P. horikoshii* and *P. aerophilum* respectively. The region flanking the hypusinated lysine residue in aIF5Aa was highly conserved, but not to the same extent as in eukaryotes. There were also a greater number of aromatic residues observed in eIF5A proteins when compared with aIF5Aa proteins (Figure 2.1A and B, highlighted in green).

Next, predictions were performed to determine the secondary structure of yeast eIF5A. An α-helical region was predicted near the C-terminus of the protein (sequence ELGDSLQTAF) and eleven anti-parallel beta sheet regions were identified (Figure 2.2). The β-sheet arrangement compared favourably with the current crystal structure data available for archaeal homologues (Kim *et al*., 1998, Peat *et al*., 1998, Yao *et al*., 2003). This α-helical region seems to be exclusive to eukaryotes as was not observed in any of the aIF5Aa crystal structures. Interestingly, the predicted secondary structures appeared to lie within less-conserved regions of the eIF5A proteins.

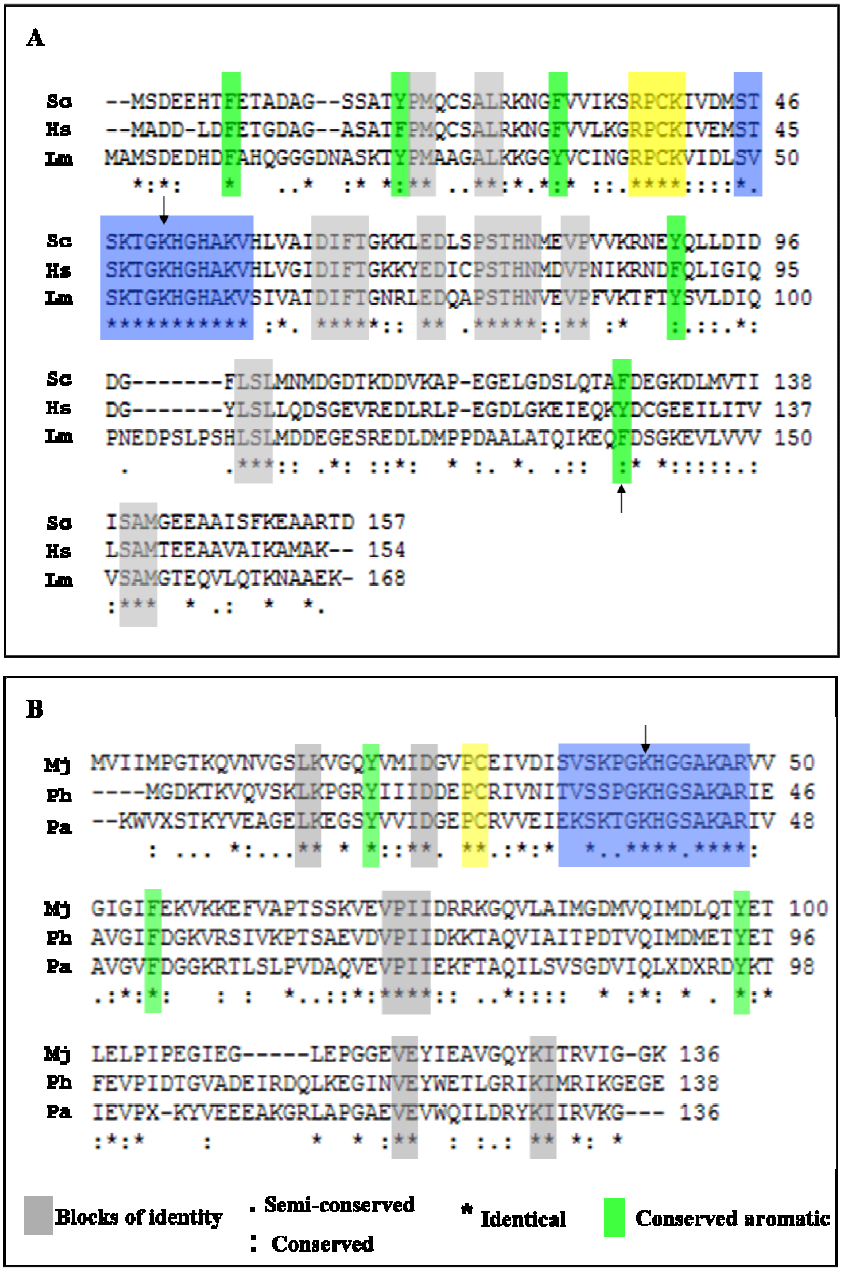

Figure 2.1: Sequence alignment of eIF5A proteins and aIF5Aa proteins. (A) CLUSTAL W multiple sequence alignment of yeast eIF5A (Sc) (Accession code NP010880), human eIF5A (Hs) (Accession code NP001961) and eIF5A from *L. mexicana* (Lm) (Accession code 1XTDA). (B) CLUSTAL W multiple sequence alignment of aIF5Aa proteins *M. jannaschii* (Mj) (2EIFA), *P. horikoshii* (Ph) (050089 and *P. aerophilum* (Pa) (P56635). Blocks of identity are boxed in grey and the lysine residue that is hypusinated is marked by a downward arrow. The "RPCK" or "PC" motifs are highlighted in yellow and the highly conserved stretches of residues surrounding the lysine are highlighted in blue. Conserved aromatic residues are boxed in green. The arrow pointing up represents Phe 128 residue in yeast eIF5A. Identical residues are marked by an asterisk and semi-conserved and conserved residues are indicated by either a full-stop or a colon, respectively.

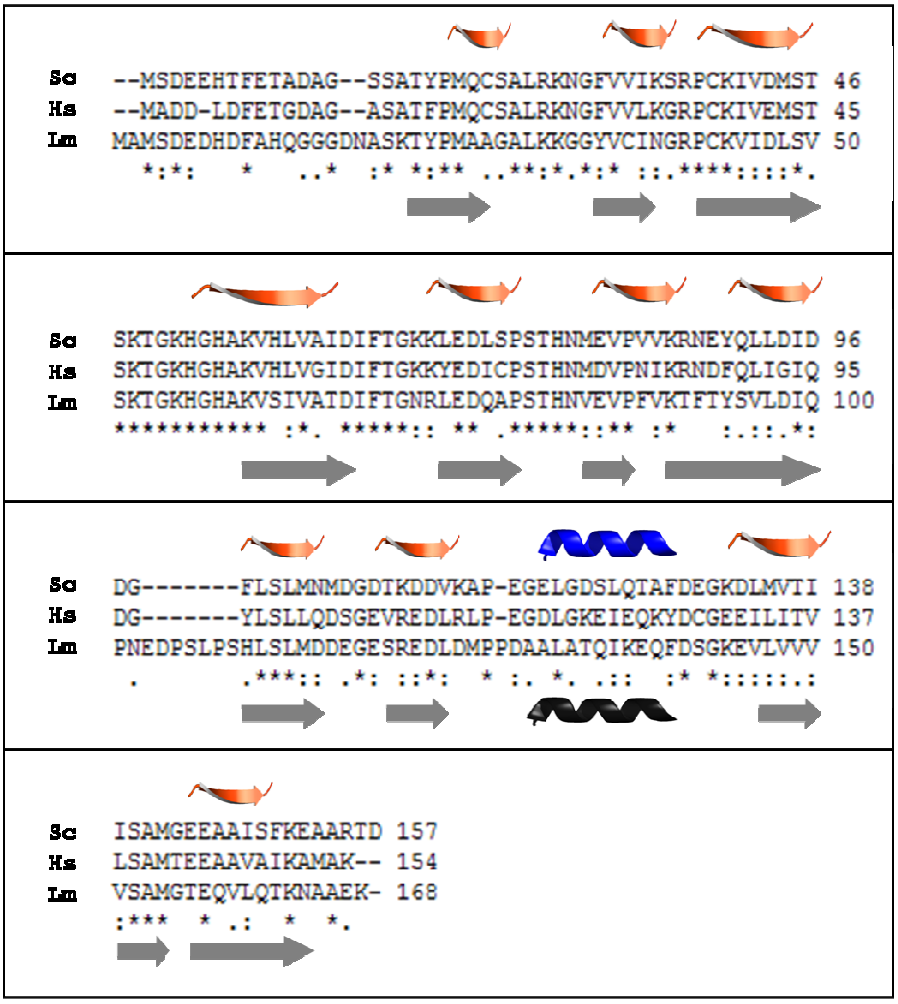

Figure 2.2: Secondary structure prediction of yeast eIF5A. Annotated above on the sequence of yeast eIF5A (Sc) (Accession code NP010880) aligned with human eIF5A (Hs) (Accession code NP001961) and *L. mexicana* eIF5A (Lm) (Accession code 1XTDA), are the predicted β-strands (red) or α-helical region (blue) as determined by JPred. Below the aligned sequences are the known secondary structures (β-sheets in grey block arrows and α-helix in black) for *L. mexicana*.

2.3.2 Homology modeling of the yeast eIF5A monomer

A comparison of the crystal structures of aIF5Aa from *M. jannaschii* (PDB entry 2EIF) and eIF5A from *L. mexicana* (PDB entry 1XTD) showed similar β-sheet arrangement at the N-terminus but the archaeal homologue lacked an α-helix at the C-terminus that was present in *L. mexicana* eIF5A (Figure 2.3 A and C). This α-helix was also predicted in the human homology model produced by Costa-Neto *et al*., (2006). Molecular modeling of the yeast eIF5A was performed using the Swiss Model first approach mode (Guex & Pietsch, 1997; Schwede *et al*., 2003) using either *M. jannaschii* aIF5Aa or *L. mexicana* eIF5A with sequence identities of 25 % and 48 % to yeast eIF5A respectively, as templates.

There was greater confidence in the model generated using *L. mexicana* eIF5A as a template, due to the stronger degree of sequence identity and better alignment between the two proteins as compared with the archaeal protein. The yeast eIF5A model, using *L. mexicana* eIF5A as the template indicated the presence of an α-helix in a similar position to that of the template (Figure 2.3 C and D). The model generated using *M. jannaschii* as a template was significantly different in that it did not show this α-helix and (Figure 2.3 A and B). The poor sequence identity between yeast eIF5A and aIF5A, and hence limited confidence in the model, was reflected in the resulting three-dimensional molecular model. Thus it was concluded that the yeast eIF5A structure, produced using *M. jannaschii* aIF5A as a template, was not inclusive enough to support major extrapolations of potential functionally important regions.

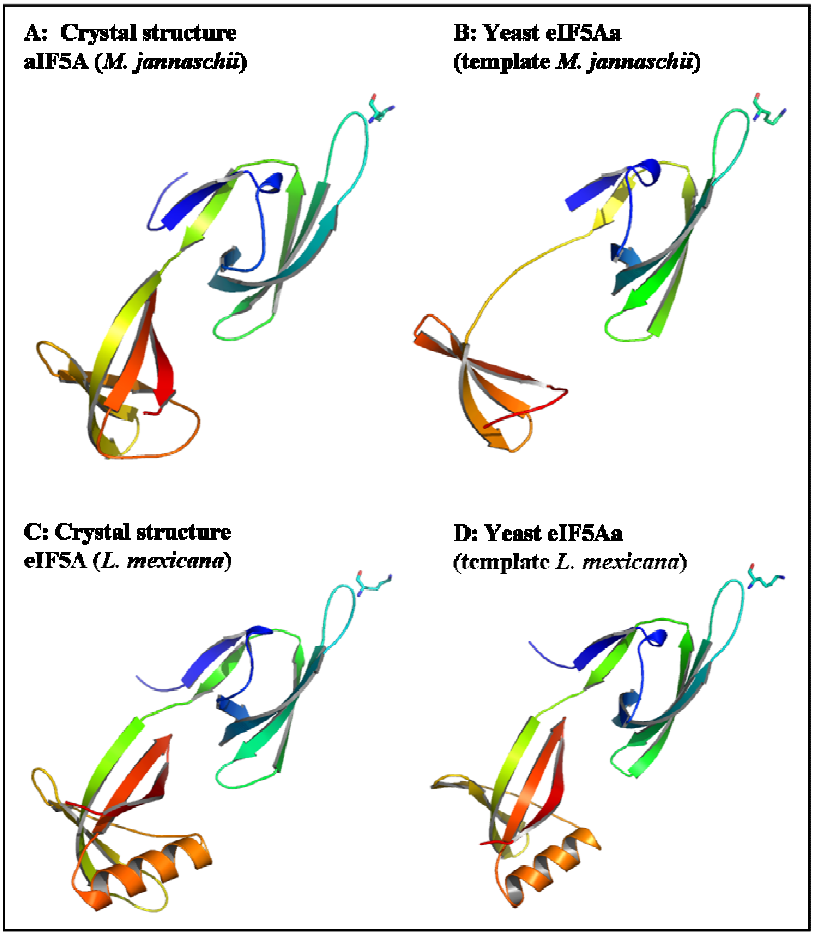

Figure 2.3: Homology modeling of eIF5A. Cartoons depicting the structures of (A) aIF5Aa from *M. jannaschii* (PDB entry 2EIF), (B) yeast eIF5A modeled on *M. jannaschii*, (C) eIF5A from *L. mexicana* (PDB entry 1XTD) and (D) yeast eIF5A modeled on *L. mexicana*. Swiss Model was used to generate the homology models (Guex & Pietsch, 1997; Schwede *et al*., 2003). Shown as sticks on the N-terminal domain in each case, is the lysine residue that is hypusinated.

To assess the validity of the highly automated approach used in the Swiss Model algorithm, the WHAT IF modeling tool was employed and model quality was determined using WHAT_CHECK to produce yeast eIF5A models (Guex & Pietsch, 1997; Schwede *et al*., 2003; Vriend, 1990; Hooft *et al*., 1996). When superposed, the WHAT IF model (Figure 2.4A) based on the *L. mexicana* eIF5A structure (Figure 2.4A and 2.4B Red), compared favourably with the model produced using Swiss Model (Figure 2.4B Blue). Differences were apparent in the loop structures, which are highly conserved. Costa-Neto *et al*., (2006) reported in their human eIF5A homology model based on *L. brasiliensis* eIF5A, that the conformation of the loop structure bearing the hypusination site was variable, which suggested an increased flexibility in this region. The variability of the yeast eIF5A models in the same region was also apparent in the superposed structures of the models generated using

different modeling tools (Figure 2.4B Boxed). In the case of human eIF5A, it was proposed this loop region may assume a regular structure in a more hydrophobic environment, such as that provided by the hydrophobic surface pocket of DHS (Costa-Neto *et al*., 2006). This proposal is plausible in that the DHS enzyme has been shown to complex with eIF5A precursor (Lee *et al*., 1999; Wolff *et al*., 2000). More recently, Gly 49 and Lys 47 in human eIF5A were identified as being critical for eIF5A function in yeast, presumably because the G49A and K47A mutant proteins act as suitable substrates for DHS (Cano *et al*., 2008). The equivalent residues in yeast (Gly 50 and Lys 48 respectively) also occur in the loop of conformational variability.

The human eIF5A homology model was based on the *L. brasiliensis* eIF5A (Costa-Neto *et al*., 2006) using the MODELLER (Sali *et al*., 1995) algorithm and validated with PROCHECK (Laskowski *et al*., 1993). For this reason, a similar yeast eIF5A homology model, using MODELLER (Sali *et al*., 1995) and PROCHECK (Laskowski *et al*., 1993) was produced using the *L. brasiliensis* eIF5A as a template (Figure 2.4C). The sequence identity between yeast eIF5A and *L. brasiliensis* eIF5A is 48 % (alignment not shown), comparable to the 48 % sequence identity between yeast eIF5A and *L. mexicana* eIF5A. The yeast eIF5A structure produced compared favourably with the human eIF5A homology model generated by Costa-Neto *et al*. (2006). Even when using the Swiss Model algorithm (Guex & Pietsch, 1997; Schwede *et al*., 2003) to model yeast eIF5A on the eIF5A from *L. brasiliensis* (Figure 2.4D blue) and superposing it with the MODELLER (Sali *et al*., 1995) version (FIGURE 2.4D red), it became apparent that variation in the models occurred only in the unstructured regions (particularly the loop region surrounding the site of hypusination). Given that the yeast eIF5A models based on either *L. mexicana* or *L. brasiliensis* eIF5A, using all of the three modelling programs, produced a similar output, the *L. mexicana* eIF5A model was chosen for further study.

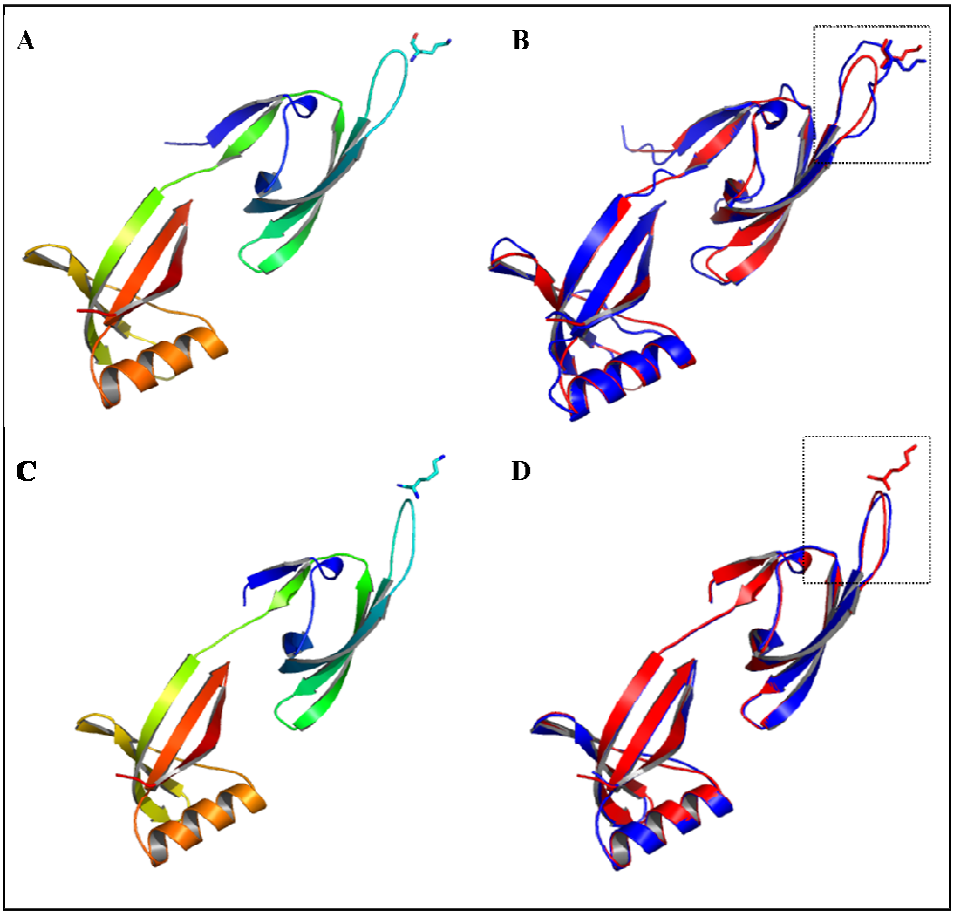

Figure 2.4: Comparison of homology models of eIF5A generated using different modeling tools. (A) Yeast eIF5A homology model generated using WHAT IF (Vriend, 1990) with *L. mexicana* eIF5A (PDB entry 1XTD) as the template. (B) Superposition of yeast eIF5A homology models generated using Swiss Model (Guex & Pietsch, 1997; Schwede *et al*., 2003) in blue and using WHAT IF (Vriend, 1990) in red. (C) Yeast eIF5A homology model generated using MODELLER (Sali *et al.*, 1995) using *L. brasiliensis* eIF5A (PDB entry 1X6O) as the template. (D) Superposition of yeast eIF5A homology models using Swiss Model (Guex & Pietsch, 1997; Schwede *et al*., 2003) in blue and using MODELLER (Sali *et al*., 1995) in red. The conserved lysine that becomes hypusinated is represented as sticks and the boxed region indicates the loop of conformational variability.

2.3.3 The eIF5A oligonucleotide binding fold

Since RNA is known to bind hypusinated eIF5A (Xu & Chen, 2001), the presence of an oligonucleotide binding fold (OB-fold) in yeast eIF5A was investigated. Murzin (1993) defined this novel folding motif as a five-stranded β-sheet folding in a coil to form a closed β-barrel, which is capped by an α-helix between the third and fourth strands. Features of the barrel-helix interface include the helix packing perpendicular to the barrel axis and the presence of a large hydrophobic residue in the cavity formed by the barrel (Murzin, 1993).

When the yeast eIF5A C-terminal domain was analysed, it was clear that the five anti-parallel β-strands formed a barrel conforming to the OB-fold criteria (Figure 2.5A). In addition, a phenylalanine residue was present in the cavity. This Phe 128 (or at least another aromatic residue) is highly conserved between eIF5As in the same position (Figure 2.1A, highlighted in green, upward arrow), indicating that eIF5A houses a structural feature to allow for nucleic acid binding. The aIF5A proteins from *M. jannaschii*, *P. horikoshii*, *P. aerophilum* and *Halobacterium sp*. lack the α-helix and the conserved aromatic residue and thus do not contain a true OB-fold (Figure 2.5B) (Kim *et al*., 1998; Peat *et al*., 1998; Yao *et al*., 2003; Wagner & Klug, 2007). However, aIF5A from *Halobacterium sp*. has been shown to bind RNA, suggesting an alternate mode of RNA-binding in archaeal homologues of eIF5A.

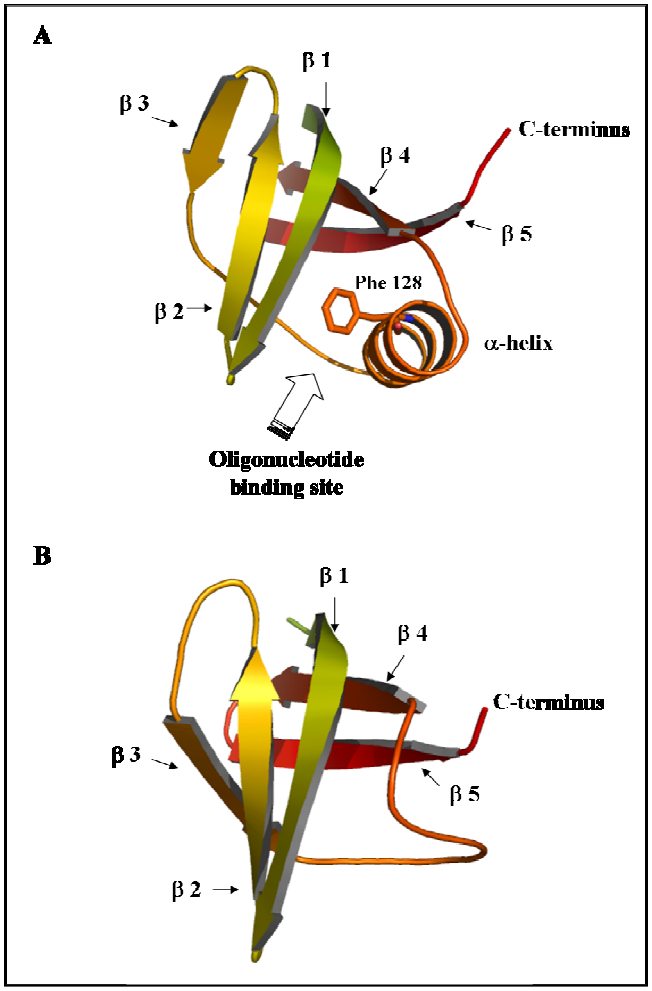

Figure 2.5: Defining the yeast OB-fold. Cartoon depicting the C-terminal domain of: yeast eIF5A (A) yeast eIF5A (modeled on the *L. mexicana* eIF5A template), and (B) aIF5Aa from *M. jannaschii* (PDB entry 2EIF). The five β-strands and the α-helix are labeled. The hydrophobic phenylalanine (Phe 128) is shown as sticks in the oligonucleotide binding cavity (A only). The oligonucleotide binding site is shown by an arrow.

2.3.4 Structural analogues of eIF5A

Since HEX-1 protein from *N. crassa* was found to be structurally analogous to yeast eIF5A in the initial homology modeling analysis, it was thought that this structural analogue may help to refine the homology model, particularly in terms of quaternary structure. HEX-1 is known to dimerise in three distinct conformations (Group I, II and II) to ultimately form a functional lattice, and because HEX-1 is structurally analogous to eIF5A (Yuan *et al*., 2003), it was rationalised that the dimerisation mechanisms employed by HEX-1 could be mirrored in yeast eIF5A. It has previously been proposed that human eIF5A exists in a number of oligomeric states, with a preference for a dimeric form in solution (Chung *et al*., 1991). In addition, the activity of *Halobacterium sp*. aIF5A depends on its oligomeric state (Klug & Wagner, 2007).

The 26 % sequence identity between HEX-1 and yeast eIF5A was not sufficient to produce a homology model of yeast eIF5A using either Swiss Model or WHAT IF (despite the stringent energy minimisation algorithm employed by the latter). Instead an alternative approach was used to model the dimer configurations of yeast eIF5A, using the HEX-1 dimer configurations as a starting point. This *in silico* approach could be used to identify potential structurally critical residues, or regions within eIF5A that are involved in dimerisation.

The HEX-1 protein was aligned with the yeast and *L. mexicana* eIF5A (identical residues indicated with asterisks in Figure 2.6). Next, residues corresponding to those involved in contacts in each of the HEX-1 three dimer configurations were identified and compared with conserved residues in the yeast and *L. mexicana* eIF5A proteins (Figure 2.6 yellow, green and orange shading). Only Ser 61 in HEX-1, corresponding to Ser 47 in yeast, was identified as being identical in all three sequences. Ser 61 is important as a stabilising residue in the Group II dimer configuration of HEX-1 (Yuan *et al*., 2003). Residues of similar charge in all three sequences were also considered as potential candidates at inter- and intra-subunit interfaces.

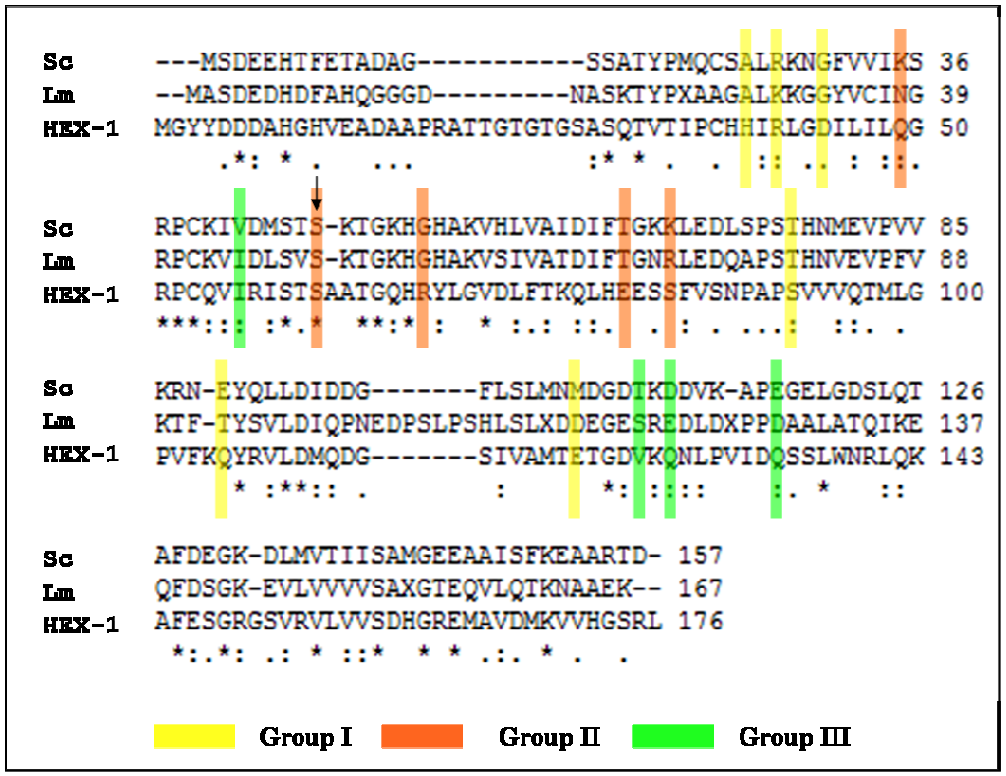

Figure 2.6: Protein alignment of eIF5A and HEX-1 indicating potential residues involved in dimeric interaction. CLUSTALW alignment of eIF5A from yeast (Sc) and *L. mexicana* (Lm) with HEX-1. Identical residues are marked by an asterisk, while the yellow, orange and green bars represent contact residues involved in the dimerisation of HEX-1 Group I, II and III configurations, respectively. The position of serine 61 (HEX-1) or the corresponding serine 47 (yeast) is marked by a downward arrow.

Next, monomeric models of both HEX-1 and yeast eIF5A were structurally compared. The serine residue identified as being conserved in both eIF5A and in HEX-1, while also being a stabilising residue in the dimerisation of HEX-1 Group II interactions is identified on the models (Figure 2.7 A and B). In addition, the Lys 51 residue that becomes hypusinated on eIF5A is marked (Figure 2.7 B). The residue corresponding to Lys 51 in HEX-1 was identified by alignment as Gln 66 (Figure 2.7A).

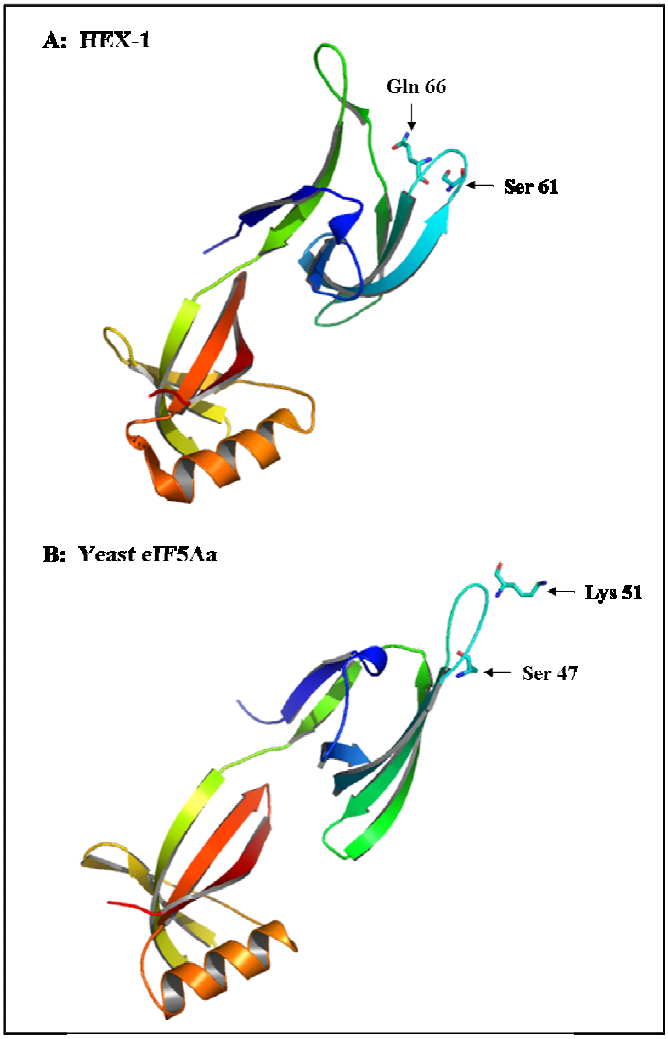

Figure 2.7: Monomeric models of the HEX-1 and yeast eIF5A proteins. (A) Crystal structures of the monomer of HEX-1 (PDB entry 1KHI). (B) Homology model of yeast eIF5A (modeled on *L. mexicana* eIF5A, PDB entry 1XTD). Marked as sticks on the models are the relevant positions of the conserved lysine residue (yeast eIF5A) corresponding to glutamine 66 (HEX-1) and the serine residue that is conserved at the same position of both proteins (Ser 47 in yeast eIF5A or Ser 61 in HEX-1).

2.3.5 Dimerisation of analogues and homologues of eIF5A

The three HEX-1 dimeric configurations (Groups I, II and III) with their relevant contacting residues were reproduced. In HEX-1, these dimer configurations alternate to ultimately form a vast crystal lattice to allow for Woronin body function in *N. crassa*. Yuan *et al*. (2003) identified critical residues for the function and/or structure of the crystal lattice. The residues involved in each of the dimer configurations are summarised in Table 2.1. The Group I dimer configuration is achieved by salt bridging of Arg 41 and Asp 44, stabilised by His 39, as well as additional hydrogen bonding involving Ser 92, Glu 121 and Gln 105 (Figure 2.8 A). The Group II dimer also involves salt bridges, but between Arg 68 and Glu 81, with additional

hydrogen bonding and stabilisation between Ser 84 and Gln 49 and Ser 61 and Glu 81 (Yuan *et al*., 2003) (Figure 2.8 B and C). The dimer, held together by a series of hydrogen bonds (Group III configuration), involves interaction of Gln 127 and Ile 56, as well as between Val 125 and Gln 134 (Figure 2.8 D). In addition to these interactions, a number of water-mediated hydrogen bonds stabilise the dimers (Yuan *et al*., 2003).

Table 2.1: Contact residues involved in dimerisation of the archaeal eIF5A homologue M. jannaschii aIF5A and the N. crassa HEX-1 protein.

Homologue/Analogue of eIF5A	Type of bond	Residues involved	Equivalent aligned residues in yeast eIF5A
***N. crassa* HEX-1** (Yuan *et al*., 2003)	Group I: Salt bridges and hydrogen bonding	**Arg 41** Asp 44 His 39 Ser 92 Glu 121 Gln 105	**Arg 27** Gly 30 Ala 25 Thr 76 Met 105 Glu 89
***N. crassa* HEX-1** (Yuan *et al*., 2003)	Group II: Salt bridges and hydrogen bonds	Arg 68 Glu 81 Ser 84 Gln 49 **Ser 61**	Gly 53 Thr 66 Lys 69 Lys 35 **Ser 47**
***N. crassa* HEX-1** (Yuan *et al*., 2003)	Group III: Hydrogen bonds	Gln 127 Ile 56 Val 125 Gln 134	Asp 111 Val 42 Thr 109 Glu 117
***M. jannaschii* aIF5Aa** (Kim *et al*., 1998)	Hydrogen bonds	**Lys 38** Pro 39 Gln 96 **Ser 35**	**Lys 48** Thr 49 Asp 106 **Ser 45**

Note: Residues in bold are conserved at similar positions.

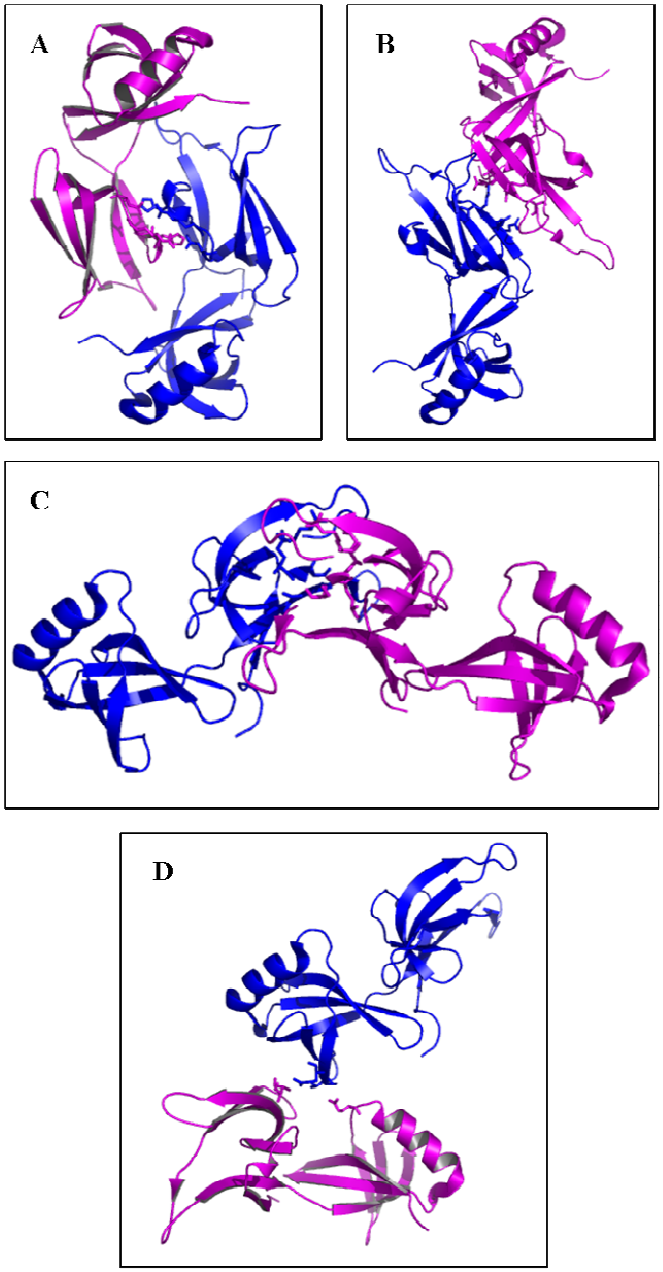

Figure 2.8: Models of the HEX-1 dimer configurations. Cartoons depicting the overall view of the interacting molecules in each of the three dimer configurations of the HEX-1 (PDB entry 1KHI; *Yuan et al*., 2003) protein that ultimately form a crystal lattice, namely the Group I (A), Group II (B) and Group III (D) interactions. The Group II dimer is also shown by a view down the crystallographic axis to reveal the 6_5 screw symmetry (C).

Crystals produced in solving the structures of aIF5As and eIF5A (Kim *et al*., 1998; Peat *et al*., 1998; Yao *et al*., 2003; Sun *et al*., 2005) routinely involved the addition of reducing agents, presumably to stabilise the protein and thus aid the crystallisation process. Kim *et al*. (1998) reported that *M. jannaschii* aIF5A may form a dimer connected by intermolecular hydrogen bond interactions, summarised in Table 2.1, involving Lys 38, Pro 39 and Gln 96 (equivalent

to Lys 48, Thr 49 and Asp 106 in yeast eIF5A, respectively). The three-dimensional aIF5Aa dimer structure observed by Kim *et al*. (1998) in some crystals was therefore reproduced (Figure 2.9). Although less ordered than crystal form II (PDB entry 2EIF), the structure solved from crystal form I (PDB entry 1EIF) was used, since it was the crystal that displayed a dimeric configuration. The two aIF5A molecules are connected by intermolecular hydrogen-bond interactions, involving Ser 35 (equivalent to Ser 45 in yeast eIF5A) and additional water mediated hydrogen bonding.

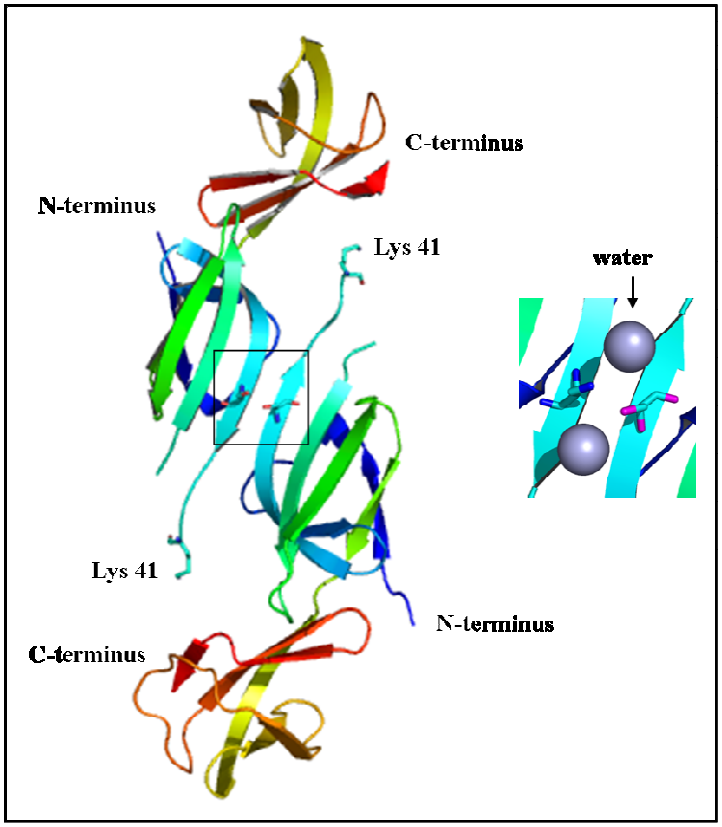

Figure 2.9: M. jannaschii aIF5A dimer model. Cartoon representation of the overall view of the aIF5A dimer model, with the conserved lysine residue near the disordered part of the loop structure. A close-up view of the dimer interaction site (boxed) is shown on the right. The interaction site involves a highly conserved serine residue (Ser 35) on each monomer, further facilitated by hydrogen bonding mediated by the presence of water (Kim *et al*., 1998).

2.3.6 Putative yeast eIF5A dimer models

Potential eIF5A dimer models were constructed by producing within one unit cell, the symmetry mates associated with the monomeric form, to within 4 Å. Although functionally divergent from eIF5A, HEX-1 dimer configurations could be used to derive inferences as HEX-1 bears such remarkable structural similarity to eIF5A. The *M. jannaschii* aIF5A protein has a greater degree of functional equivalence and identity to eIF5A, although it is

structurally more divergent. The aIF5A dimer was also compared to potential eIF5A dimer configurations. Residues thought to be involved in each of the proposed dimer interactions were also analysed for the degree of conservation, particularly if the residues occurred in highly conserved motifs, such as the "PCK", "DIFT", "PSTHN" or the "LSL" motifs (from the alignment in Figure 2.1A).

Three putative dimer models, named Type I, II and III, were generated. The Type I dimer model (Figure 2.10A), bearing similarities to the Group I HEX-1 dimer (Figure 2.10A) as well as to the *M. jannaschii* aIF5A dimer (Figure 2.9), was plausible in that there was potential for salt bridges to be formed between Asp 43 and Lys 48, as well as water-mediated hydrogen bonding involving Ser 45 (Figure 2.10B). The space-fill model of this potential dimer configuration also indicated that the conserved Lys 51 residue was exposed. Following hypusination (and thus extension), this residue could be in contact with the C-terminal domain of the protein near the α-helical region (Figure 2.10C).

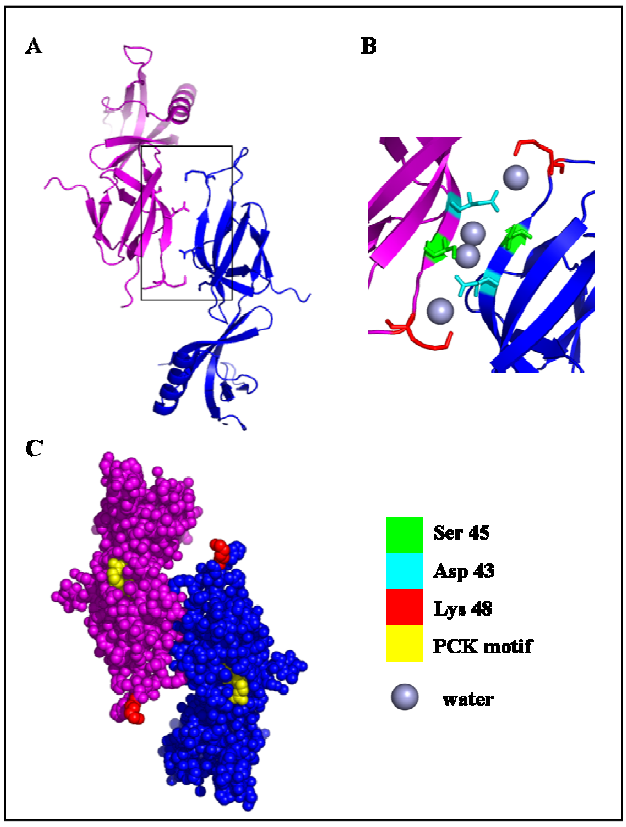

Figure 2.10: Predicted Type I eIF5A dimer. Cartoon representation of a putative eIF5A dimer configuration bearing similarity to the Group I dimer of HEX-1 and the *M. jannaschii* aIF5A dimer. (A) Overall view of the dimer model showing putative contact points. (B) Close-up view of putative salt bridging of Asp 43 and Lys 48, as well as water-mediated hydrogen bonding involving Ser 45. (C) Space-fill model of this dimer configuration.

The Type II dimer model (Figure 2.11A) was similar to the dimer belonging to Group II configuration of HEX-1 (Figure 2.8B). This configuration was the most plausible in that numerous predicted contact points between the monomeric units were observed. Salt-bridging involving Asp 61, Glu 69 and Asp 70 with His 54, His 52 and Lys 51, respectively (Figure 2.11B), could occur in this configuration. The space-fill (Figure 2.11C) shows this putative dimer model as having numerous contact points that would result in a highly stable configuration. Alternative views of the overall dimer model down the crystallographic axis (Figure 2.11D) show the extent to which the N-terminal domains of the two molecules would interact. The extensive N-terminal domain linkages are reiterated in the space model from the same crystallographic axis (Figure 2.11E).

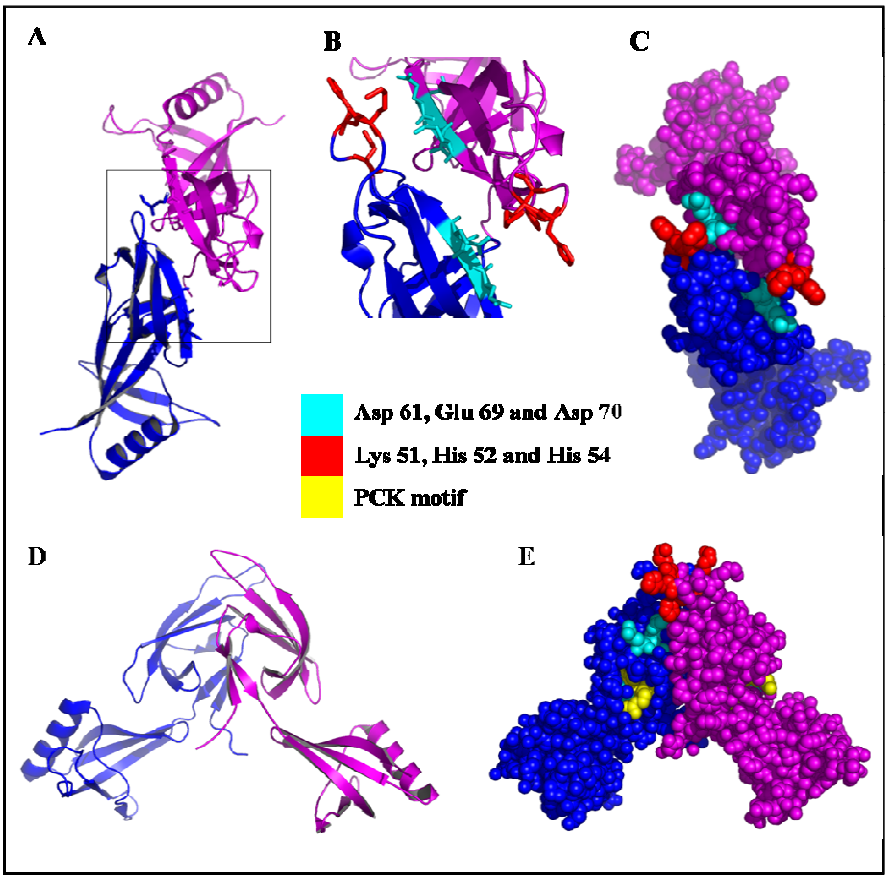

Figure 2.11: Putative Type II eIF5A dimer. Cartoons of a possible yeast eIF5A dimer configuration displaying similarities to the Group II dimer of HEX-1. (A) Overall dimer configuration with putative contact points marked as sticks. (B) Close-up view of possible eIF5A dimer contact region involving salt bridging between the residues indicated in the colour key. (C) Space-fill model of the overall putative dimer configuration. (D) View of the dimer down the crystallographic axis. (E) Space-fill model of the dimer down the crystallographic axis.

The Type III dimer model the least plausible in that so few potential contact points exist in this configuration, bore similarity to the Group III HEX-1dimer. This putative dimer (Figure 2.12A) seemed to be mediated by a single salt bridge between Asp 106 and Lys 67, with potential co-ordination of Thr 64 (Figure 2.12B). Since this dimer configuration in HEX-1 was required for the completion of the crystal lattice, something not observed in yeast eIF5A, it is unlikely that eIF5A dimerises in this configuration. The space-fill model (Figure 2.12C) echoes the weak feasibility of this dimer, showing a loose contact zone.

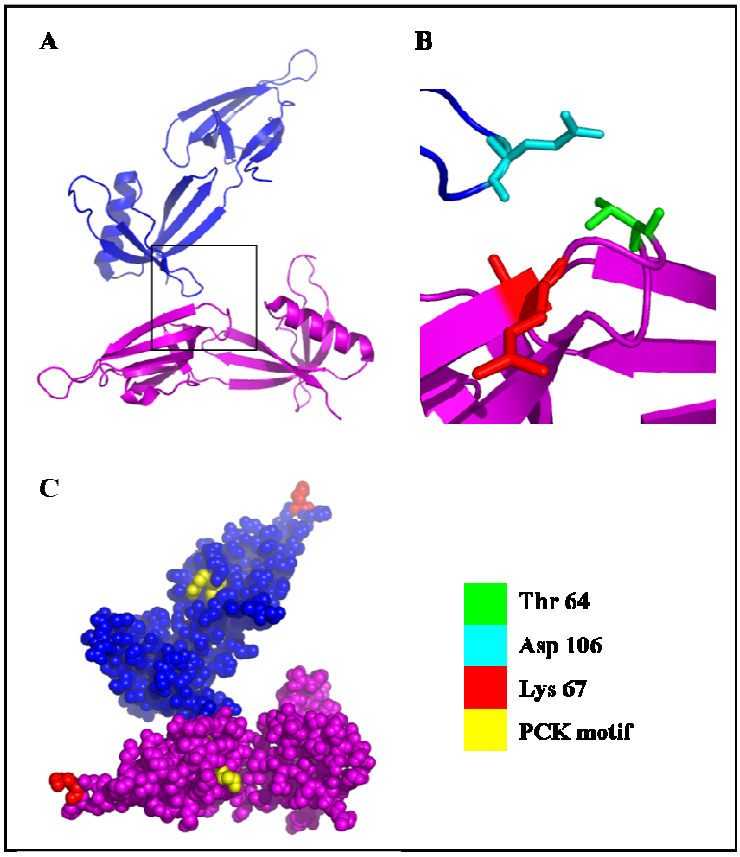

Figure 2.12: Putative Type III eIF5A dimer. Cartoon representations of the putative yeast eIF5A dimer model Type III. (A) Overall view of this dimer configuration with the putative contact points boxed. (B) Close-up view of the potential salt-bridging between the residues indicated in the colour key. (C) Space-fill model of this dimer configuration.

Summarised in Table 2.2 are the residues in yeast eIF5A postulated to play a role in structure of yeast eIF5A should it occur as a dimer. Interestingly, eight of these residues (Table 2.2, bold) occur within highly conserved eIF5A motifs and reinforce the sentiment that these residues are of structural importance. The most unstructured regions of eIF5A appear to be highly conserved, and the structured regions appear to have evolved to present the unstructured region (presumably so that they can take part in function and/or inter-subunit interactions).

Table 2.2: Summary of the residues thought to be important for the structural integrity of the yeast eIF5A dimer.

Type I Dimer	Type II Dimer	Type III Dimer	OB-Fold	Highly conserved eIF5A motifs
Ser 45	**Asp 61**	**Thr 64**	**Phe 128**	PCK (38-40)
Asp 43	Glu 69	Asp 106		**S**TS**K**TG**KH**G**H**AKV (45-57)
Lys 48	Asp 70	Lys 67		**D**IF**T** (61-64)
	His 54			ED (71-72)
	His 52			PSTHN (74-78)
	Lys 51			**F**D (128-129)

Note: In bold are the putative dimer-contact residues that occur within highly conserved motifs.

2.4 Conclusions

The main objective of the research discussed in this Chapter was to produce a suitable model of yeast eIF5A using currently available structural data. This objective was achieved by using the eIF5A homologue from *L. mexicana* as a template. The new model, along with secondary structure predictions revealed that yeast eIF5A contains an α-helix on the C-terminal domain. This finding was in accordance with the homology model of human eIF5A (Costa-Neto *et al*., 2006). Low confidence molecular models were produced using aIF5A as the template, echoing the sentiment that there may be too many structural and hence functional differences that one cannot extrapolate information across the major domains of living organisms. All crystallographic data involving homologues of eIF5A have been solved using heterologously-produced (unhypusinated) protein. To accurately determine the functional and higher order structural effects (such as the potential for oligomerisation and hypusination), it will be necessary to solve the structure of hypusinated protein. Also, since it is known that the presence of hypusine is required to bind RNA, the data generated to date is further restricted by the absence of RNA in solving the structure of activated eIF5A (Xu & Chen, 2001).

The presence of both hypusine and RNA may result in substantial conformational changes in the protein, which could provide clues about its functional mechanism. The credibility of the yeast eIF5A dimer models can only be confirmed once such crystal structure data is generated. It must be stressed that inferences drawn from the HEX-1 and aIF5Aa dimer models, are purely conjectural at this stage. The following chapters include the characterisation of yeast eIF5A using biochemical analyses and functional studies. It is expected that these analyses could be used to validate the models proposed in this Chapter.

Chapter 3: Development of an experimental system for studying the biological activity of eIF5A

Chapter 3: Development of an experimental system for studying the biological activity of eIF5A

3.1 Introduction

Substantial information on eIF5A has been generated through studies conducted in *S. cerevisiae* (yeast). The primary reason is that this simple eukaryote has the best characterised genome that unlike higher eukaryotes, is easy to manipulate. In addition, yeast experimental systems allow for robust functional gene analysis because unlike *E. coli*, yeast cells support *in vivo* post-translational modification of eIF5A such as hypusination and phosphorylation (discussed in Chapter 1, Section 1.1.2).

As discussed earlier (Chapter1, Section 1.1.1) the yeast genome encodes two eIF5A homologues, Tif51a and Tif51b. *TIF51A* (*HYP2*/*YEL034W*) is situated on Chromosome V and has been the best characterised, while less is known about *TIF51B* (*ANB1*/*YJR047C*), which is situated on Chromosome X (Mehta *et al*., 1990; Schnier *et al*., 1991). The *TIF51A* and *TIF51B* genes share over 90 % nucleotide sequence identity (Schwelberger *et al*., 1993). Expression of Tif51a and Tif51b results in two isoelectric variants, the more acidic eIF5A (20 kDa) and more basic eIF5Ab (18 kDa), expressed under aerobic or anaerobic conditions, respectively (Mehta *et al*., 1990; Scwelberger *et al*., 1993). Although both variants undergo hypusination, eIF5A is also phosphorylated on one or more serine residues, accounting for the difference in M_R of these two highly homologous proteins (Kang *et al*., 1993).

The hypusinated gene products of either *TIF51A* or *TIF51B* are able to support growth interchangeably under aerobic and anaerobic conditions in yeast strains lacking *TIF51B* or *TIF51A*, respectively (Schwelberger *et al*., 1993). When cell free lysates from wild-type yeast cells grown aerobically were analysed, it was found that eIF5A is more abundant than eIF5Ab and that a natural proteolytic breakdown of eIF5A, but not of eIF5Ab, occurred following cell lysis (Kang *et al*., 1993). Human eIF5A, which shares about 63 % amino acid sequence identity with the yeast eIF5A, can substitute for either of the yeast homologues, eIF5A or eIF5Ab (Schwelberger *et al*., 1993).

The overall aim of the experiments described in this chapter was to develop an experimental system for the functional and biochemical characterisation of yeast eIF5A. Important components of this system include: (1) the availability of anti-eIF5A antibodies that can be

used to track the presence of the protein in cells and during purification procedures; (2) the ability to over-express and efficiently purify native eIF5A from both *E. coli* and yeast cells; (3) an *in vivo* assay system for testing biological activity of mutant eIF5As. This chapter describes the over-expression and affinity purification of 6 x His-tagged eIF5A and the use of this protein to raise anti-eIF5A rabbit polyclonal antibodies. Also included is the design and construction of the yeast experimental system for *in vivo* assays. This involved the insertion of a chromosomal copy of *TIF51A* under the control of the *GAL1* promoter (P_{GAL1}*TIF51A*), followed by successive disruption of the *TIF51B* and *TIF51A* genes by integrative transformation, resulting in a strain that was viable in media containing galactose, but unable to grow with glucose as a carbon source.

3.2 Materials and Methods

3.2.1 Strains and culture conditions

The parent yeast strain, INVScI (Table 3.1), was grown in YPD (complete) medium (Appendix A) and competent cells were prepared using the Frozen-EZ Yeast Transformation II™ Kit (Zymo Research). Knockout yeast strains (Table 3.1) were grown at 28^{o}C in selective minimal medium (SMM) broth containing galactose as a carbon source, supplemented with the required amino acids for each strain as well as uracil where required (Appendix A, Kaiser *et al*., 1994). Recombinant plasmids were hosted in *E. coli* DH5α cells while heterologous expression of eIF5A was carried out in *E. coli* BL21 (DE3) (Table 3.2). All *E. coli* cultures were grown in Luria Bertani (LB) medium and competent cells were prepared using the method of Hanahan (1985) (Appendix B).

Table 3.1: Genotypes of yeast strains used in this study.

Strain	Genotype	Source
INVScI	*MATa his3Δ leu2 trp1-289 ura3-52*/	Invitrogen
	Matα his3Δ leu2 trp1-289 ura3-52	
PGY1	*MATa his3Δ1 trp1-289 ura3-52* P_{GAL1}*TIF51A::LEU2*/	This study
	Matα his3Δ1 trp1-289 ura3-52 P_{GAL1}*TIF51A::LEU2*	
PGY7	*MATa his3Δ1 trp1-289* P_{GAL1}*TIF51A::LEU2 TIF51B::hisG-URA3-hisG* /	This study
	Matα his3Δ1 trp1-289 P_{GAL1}*TIF51A::LEU2 TIF51B::hisG-URA3-hisG*	
PGY8	*MATa his3Δ1 trp1-289 ura3-52* P_{GAL1}*TIF51A::LEU2 TIF51B::hisG*/	This study
	Matα his3Δ1 trp1-289 ura3-52 P_{GAL1}*TIF51A::LEU2 TIF51B::hisG*	
PGY9	*MATa his3Δ1 trp1-289* P_{GAL1}*TIF51A::LEU2 TIF51B::hisG TIF51A::hisG-URA3-hisG*/	This study
	Matα his3Δ1 trp1-289 P_{GAL1}*TIF51A::LEU2 TIF51B::hisG TIF51A::hisG-URA3-hisG*	
PGY10	*MATa his3Δ1 trp1-289 ura3-52* P_{GAL1}*TIF51A::LEU2 TIF51B::hisG TIF51A::hisG*/	This study
	Matα his3Δ1 trp1-289 ura3-52 P_{GAL1}*TIF51A::LEU2 TIF51B::hisG TIF51A::hisG*	

Table 3.2: Genotypes of *E. coli* strains used in this study.

Strain	Genotype	Reference
E. coli DH5α	F^- *Φ80lacZΔM15 Δ(lacZYA-argF)U169 deoR recA1 endA1 hsdR17(*r_k^-, m_k^+*) phoA supE44 thi-1 gyrA96 relA1* λ^-	Hanahan, 1983
E. coli BL21 (DE3)	F^- *omptT* $hsdS_B$ (r_B^-; m_B^-) *gal(DE3) dcm plyS* Cm^r	Studier & Moffat, 1986

3.2.2 Recombinant DNA techniques

Recombinant plasmid DNA was isolated from *E. coli* DH5α cells either using the method of Berghammer and Auer (1993) for initial diagnostic purposes, or the High Pure Plasmid Isolation Kit (Roche). The integrity of all PCR products and recombinant plasmids resulting from the cloning of oligonucleotides or site-directed mutagenesis was routinely determined by DNA sequencing using the ABI Prism® Big Dye™ Terminator v 3.1 Cycle Sequencing Kit (Applied Biosciences) with the specified sequencing primers (Appendix C) and analysed using the ABI Prism 3100 Genetic Analyser (Applied Biosystems). Chromatograms of sequences were visualised using the Chromas v. 2 (Technelysium Pty Ltd.) and analysed using Vector NTI DeLuxe v. 4.0 or v. 5.0 (Informax Inc.) software packages. The sequences of all DNA primers used in this and following chapters can be found in Appendix C.

3.2.3 INVScI genomic DNA isolation and PCR amplification of *TIF51A*

INVScI cells were inoculated into YPD broth (Appendix A) and grown at 28°C to mid-log phase ($OD_{600\ nm}$ = 0.8) before being harvested by centrifugation at 1000xg. Genomic DNA was extracted using the phenol/chloroform method described by Kaiser *et al*. (1994)

(Appendix D). Primer pair PG5F and PG2R (Appendix C), which exclude the UAG (stop) codon and introduce flanking 5' *Nde* I and 3' *Bam* HI and *Sma* I sites, were used to amplify the *TIF51A* coding sequence from genomic DNA. The PCR product was gel purified using Glassmilk® (GeneClean® II kit, QBiogene) and ligated into the pGEM® T Easy vector (Promega) and transformants screened by restriction analysis. The recombinant plasmid, pPG5, containing the correct insert was sequenced using the pUCF and pUCR primers (corresponding to flanking pGEM®-T-Easy vector sequences) to verify the integrity of the PCR amplification product.

3.2.4 Construction of the *E. coli TIF51A* –His expression vector, pPG6

Ten micrograms each of oligonucleotides PG3F and PG4R (Appendix C) were annealed in 200 mM Tris-HCl pH 7.6, 100 mM $MgCl_2$ (final volume 20 µl) and incubated at 100^{o}C for 5 minutes and then cooled at room temperature. The double-stranded oligonucleotide, PG3, (Figure 3.1) encoding a 6 x polyhistidine (6 x His) tag followed by an UAG (stop) codon, flanked by *Bam* HI and *Sma* I sites on its 5' end and an *Eco* RI site on the 3' end, was used to fuse a 6 x His tag to the 3' end of *TIF51A* coding sequence in pPG5. A *Nde* I - *Eco* RI restriction fragment carrying the *TIF51A*-His coding sequence was then ligated into pT7-7 (Tabor, 1990) resulting in the *TIF51A*-His expression vector, pPG6 (Figure 3.1).

3.2.5 Heterologous expression of eIF5A-His in *E. coli*

E. coli BL21 (DE3) cells transformed with pPG6 or pT7-7, were inoculated into LB broth (supplemented with 200 µg/ml ampicillin) and grown at 37^{o}C until the $OD_{600\ nm}$ reached 0.4 after which expression was induced by the addition of IPTG to a final concentration of 1 mM. Aliquots of cells were collected at hourly intervals and analysed by sodium dodecyl sulphate-polyacrylamide gel electrophoresis (SDS-PAGE) using a 15 % polyacrylamide gel (Appendix E) followed by staining with Coomassie. To determine solubility, samples containing 2 $OD_{600\ nm}$ units of cells were disrupted by sonication at a frequency of 400 mHz at 10 second intervals (10 seconds sonication followed by 10 seconds on ice) for a total of 2 minutes. Lysates were centrifuged at 1000xg for 10 minutes at 4^{o}C. The resulting supernatant and pellet fractions were analysed by SDS-PAGE.

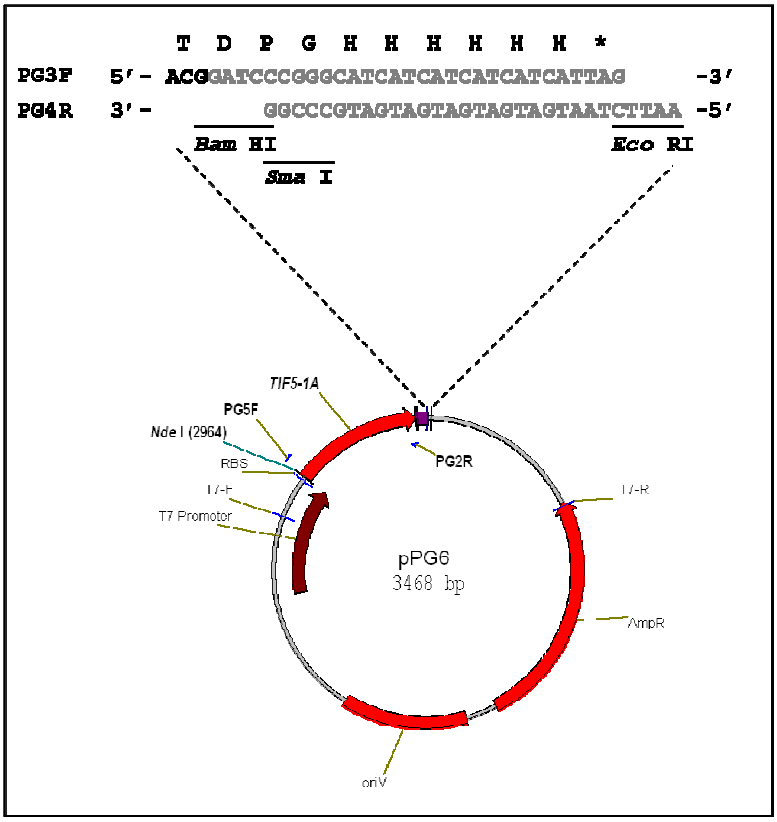

Figure 3.1: Schematic map of the E. coli eIF5A-His expression vector pPG6. Annealed oligonucleotides PG3F and PG4R, encoding a 6 x His tag flanked by the overhanging *Bam* HI and *Sma* I sites on the 5' end and an *Eco* RI site at the 3' end, preceded by a UAG (stop) codon (*). The annealed oligonucleotides were ligated into the pT7-7 derived plasmid, pPG5, bearing the *TIF51A* gene excluding the UAG (stop) codon, such that the *TIF51A* would encode eIF5A-His (C-terminal 6 x His tag) resulting in the expression vector, pPG6. The pT7-7 vector makes use of the T7 promoter system in *E. coli* (Studier & Moffat, 1986) and bears an *E. coli* origin of replication (oriV) and β-lactamse gene encoding ampicillin resistance (AmpR).

3.2.6 Nickel affinity purification of eIF5A-His

E. coli BL21 (DE3) cells expressing eIF5A-His (pPG6) were harvested at 2000xg and resuspended in Lysis Buffer (50 mM Tris-HCl, pH 8.0, 300 mM NaCl, 10 mM imidazole). The cell suspension was sonicated as described above, followed by a clearing centrifugation step at 1500xg for 10 minutes at 4^{o}C. The supernatant was loaded onto equilibrated Qiagen Ni-NTA Spin columns and the manufacturer's native purification protocol was followed with changes in the wash buffer (50 mM Tris-HCl, pH 8, 300 mM NaCl, 20 mM imidazole) and elution buffer (50 mM Tris-HCl, pH 8, 300 mM NaCl, 250 mM imidazole). The flow-through, washes and elutions collected during the purification procedure were analysed by SDS-PAGE and Coomassie staining to detect the presence of eIF5A.

3.2.7 Western analysis

One milligram of purified eIF5A-His protein was used to raise rabbit polyclonal antibodies (Prof D.U. Bellstedt, Department of Biochemistry, Stellenbosch University). Serum was collected from the rabbit before inoculation of the protein ("Day 0" Pre-bleed) and on Day 39, following a series of booster inoculations on Days 28, 30 and 32 post-inoculation.

Antibody concentrations were optimised for Western analysis as follows. Crude protein extracts from *E. coli* BL21 (DE3) cells transformed with pPG6 or pT7-7 were resolved using a 15 % SDS-polyacrylamide gel and transferred to Hybond C+ (Amersham Biosciences) nitrocellulose membranes using the standard Western blotting procedure (Appendix F). Varying dilutions of antiserum ("Day 0" Pre-bleed, or "Day 39" serum) were used as primary antibodies while the secondary antibody used was the recommended 1:12 500 dilution of the Roche BM Chemiluminescence Western Blotting Kit secondary antibody. Antibodies were diluted in TBS-Tween 20 solution containing 1 % BSA (Appendix F).

To test the specificity of the "Day 39" serum whole cell protein extracts derived from *E. coli* BL21 (DE3) cells transformed with pPG6 or pT7-7 were resolved by SDS-PAGE, followed by Western analysis. Sensitivity of the antiserum was tested by probing known concentrations of purified eIF5A-His with the optimised serum dilution. After the appropriate dilutions of antiserum were determined, a pre-adsorption procedure was followed to remove non-specific antibodies (method adapted from Harlow and Lane (1988), Appendix G). This was done by incubating serum with lysates of cells transformed with pT7-7, in a ratio of 1:3 at 4^{o}C for 12 hours at 50 rpm, followed by a clearing spin at 2000xg for 20 minutes. The supernatant (pre-adsorbed antiserum) was analysed using lysates of cells harbouring either pPG6 or pT7-7 to determine the specificity to eIF5A.

Finally, the sensitivity of the pre-adsorbed antiserum was determined by Western analysis of dilutions of known concentrations of purified eIF5A-His. In the case of detection of eIF5A expressed in yeast strains, cells were grown at 28^{o}C in SMM broth, supplemented with the required amino acids for each strain as well as uracil (Appendix A, Kaiser *et al.*, 1994) containing galactose as a carbon source until the $OD_{600\ nm}$ reached 0.8. Two $OD_{600\ nm}$ units of cells were harvested and protein was extracted using the method of Kaiser *et al.* (1994) (Appendix H). Protein extracts were resolved by SDS-PAGE followed by Western analysis using anti-eIF5A pre-adsorbed antiserum.

3.2.8 Construction of yeast strain with P_{GAL1}-dependent eIF5A expression

TIF51A was amplified from INVScI genomic DNA (as in Section 3.2.3) using primers PG1F (introducing a 5' *Hind* III site) and PG6R (introducing a 3' *Bam* HI site) (Appendix C) and the product inserted between the *GAL1* promoter and *CYC1* terminator in the YipLac128-derived plasmid, YipLacVCAPB320 (Venter, 2001). YipLac128 carries a *LEU2* selectable marker and is used to insert recombinant genes into the *leu2* locus on chromosome III in INVScI by homologous recombination (Gietz and Sugino, 1988). The resulting plasmid, pPG13, was linearised with *Cla* I, and used to transform INVScI cells. Leu^+ transformants were selected after incubation for 4 days at 28 ^oC on SMM agar plates supplemented with uracil, tryptophan, histidine and glucose as the carbon source (Appendix A, Kaiser *et al*., 1994). Genomic DNA was extracted from potential recombinants and the presence of the P_{GAL}-eIF5A expression cassette confirmed by PCR using primers sets: PG1F (specific to 5' *TIF51A*) and AI1R (specific to 3' T_{CYC1}); AI2F (specific to 5' P_{GAL1}) and PG6R (specific to 3' *TIF51A*); and AI2F and AI1R.

3.2.9 Construction of the *TIF51A*-disruption plasmid (pPG14)

The *TIF51A* gene (including its endogenous promoter) was amplified from INVScI genomic DNA using primers PG8F and PG6R (Appendix C), which introduce flanking *Age* I and *Bam* HI sites at the 5' and 3' ends of the gene, respectively. The PCR product was inserted into pGEM®T-Easy (pPG9) and the integrity of the PCR product was confirmed by DNA sequencing. Site-directed mutagenesis (QuikChange SDM Kit, Stratagene) was used to introduce a *Bgl* II site in the middle of the *TIF51A* gene of pPG9 (into the Asp 63 codon), using primers PG17F and PG18R (Appendix C). The resulting plasmid, pPG18 (Figure 3.2A), was confirmed by restriction analysis and DNA sequencing. Next, pNKY51 (Alani *et al*., 1987, Figure 3.2B) was digested with *Bam* HI and *Bgl* II, releasing a 3.8 kbp fragment carrying the *URA3* gene flanked by *hisG* repeats, which was ligated into pPG18 linearised with *Bgl* II in the middle of the *TIF51A* gene producing the *TIF51A*-disruption vector, pPG14 (Figure 3.2C).

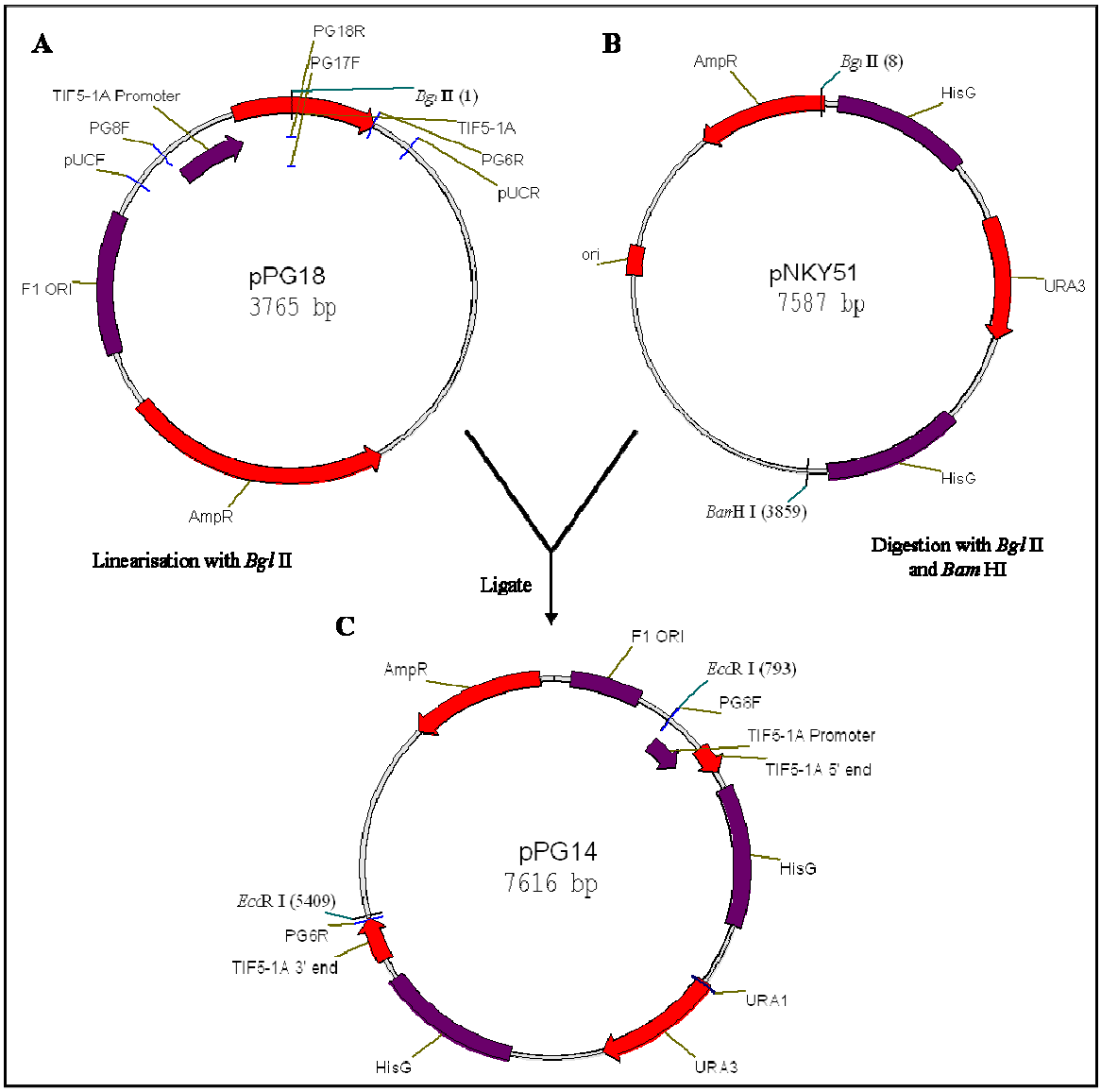

Figure 3.2: Schematic representation of the construction of the TIF51A-disruption vector, pPG14. (A) pPG18 with an engineered *Bgl* II site at the Asp63 codon of the *TIF51A* gene was digested with *Bgl* II and ligated with a 3.8 kbp fragment obtained by the digestion of pNKY51 digested with *Bgl* II and *Bam* HI (B). The resulting plasmid, pPG14 (C), bearing a β-lactamase gene encoding ampicillin resistance and a phage f1 origin of replication (F1 ori), was used for the disruption of *TIF51A*.

3.2.10 Construction of the *TIF51B*-disruption plasmid (pPG16)

The *TIF51B* gene and its endogenous promoter were amplified from INVScI genomic DNA using primers PG13F and PG14R (Appendix C) and the PCR product cloned into pGEM®T-Easy (pPG15). Site-directed mutagenesis was used to introduce a *Bam* HI site into the middle of the *TIF51B* gene (into the Pro 75 codon), using primers PG15F and PG16R (Appendix C). This resulting plasmid, pPG19 (Figure 3.3A), was selected by restriction analysis and the introduction of the *Bam* HI site further confirmed by DNA sequencing. Next, a 3.8 kbp

Bam HI-*Bgl* II fragment carrying the *hisG-URA3-hisG* cassette from pNKY51 (Figure 3.3B), was ligated into the pPG19 *Bam* HI site. The resulting *TIF51B*-disruption vector, pPG16 (Figure 3.3C), was confirmed by restriction analysis and the disruption region was sequenced using primers PG13F, URA1, HISG and PG14R (Appendix C).

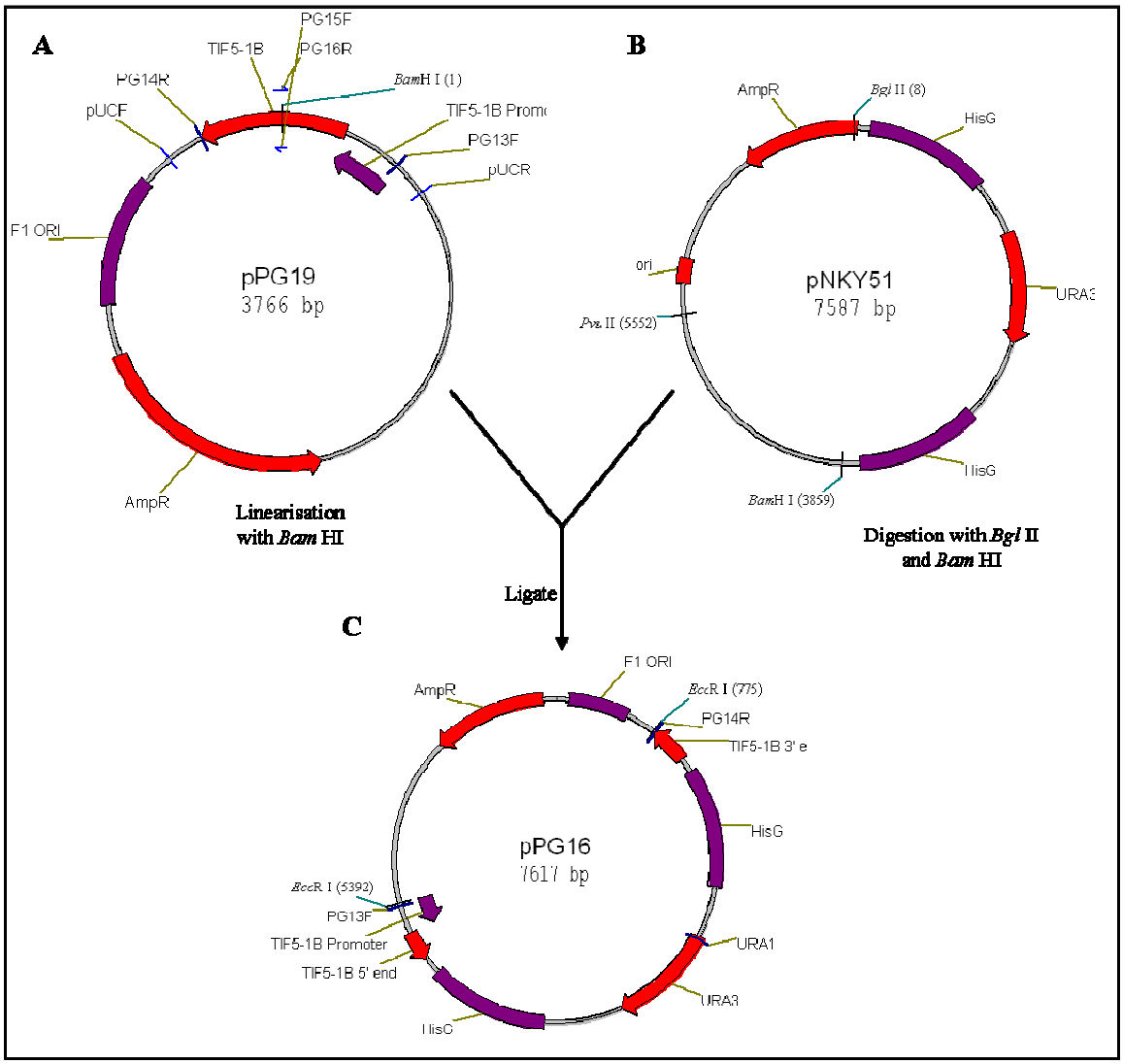

Figure 3.3: Schematic representation of the construction of the TIF51B-disruption vector, pPG16. (A) pPG19, with an engineered *Bam* HI site at Pro^{75} of the *TIF51B* cassette was digested with *Bam* HI and ligated with a 3.8 kbp fragment obtained by the digestion of pNKY51 digested with *Bgl* II and *Bam* HI **(B)**. The resulting plasmid, pPG16 **(C)**, housing a phage f1 origin of replication (F1 ori) and a β-lactamase gene encoding ampicillin resistance (AmpR), was used for the disruption of *TIF51B*.

3.2.11 Construction of yeast knockout strains

Construction of the TIF51B-disruption strain, PGY8. The 4.6 kb *Eco R1* fragment from pPG16, carrying the *hisG-URA3-hisG* cassette flaked by the 5' and 3' regions of *TIF51B* gene, (Figure 3.3C) was used for the transformation of PGY1 competent cells. Ura^+ transformants

were selected on SMM agar plates (supplemented with each histidine and tryptophan and glucose as carbon source) after growth at 28^{o}C for 4 days. Genomic DNA was extracted and analysed for the integration of the *TIF51B* disruption cassette by PCR amplification with primer sets PG13F (specific to 5' *TIF51B*) and PG14R (specific to 3' *TIF51B*) or PG13F and URA1 (specific to 5' *URA3*) (Appendix C). Since yeast strains INvSc1 and thus PGY1 are diploid strains, transformants in which both copies of *TIF51B* had been disrupted were selected (PGY7, Table 3.1). This was done by plating transformants onto SMM agar plates, supplemented with histidine, tryptophan, uracil and 0.001 % 5-fluoroorotic acid (5-FOA) together with glucose as a carbon source. The cells were incubated at 28^{o}C for 4 days, to allow for the deletion of the *hisG* repeat together with the *URA3* marker by homologous recombination, resulting in reversion to the Ura^{-} phenotype. Genomic DNA was extracted from Ura^{-} colonies and analysed for curing of the Ura^{+} phenotype together with the disruption of both copies of *TIF51B* using PCR amplification with primers PG13F and PG14R (Appendix C). The resulting strain, PGY8 (Table 3.1) contained a copy of *TIF51A* under control of the *GAL1* promoter with both copies of the *TIF51B* disrupted by insertion of the *hisG* coding sequence.

Construction of the TIF51B-TIF51A-disruption strain, PGY10. The 4.6 kb *Eco* RI restriction fragment from pPG14 (Figure 3.2C), carrying the *hisG-URA3-hisG* cassette inserted into the *TIF51A* gene sequence, was transformed into PGY8 competent cells. Ura^{+} transformants were selected on SMM agar plates (supplemented with histidine and tryptophan and galactose as a carbon source) as described above. Genomic DNA was extracted and analysed for homologous integration of the disruption cassette into the two *TIF51A* genes using PCR amplification with primers PG8F (specific to 5' *TIF51B*) and URA1 (specific to 5' *URA3*) (Appendix C). Transformants in which both copies of *TIF51A* had been disrupted (PGY9), were plated onto SMM agar plates, supplemented with histidine, tryptophan, uracil and 5-FOA together with galactose as a carbon source. The plates incubated, at 28^{o}C for 4 days, to allow for the removal of the *hisG* repeat by homologous recombination and reversion to a Ura^{-} phenotype.

Genomic DNA was extracted and analysed to confirm the removal of the *URA3* marker and disruption of *TIF51A* using PCR amplification with primers PG8F and PG6R, which are specific to 3' *TIF51A* (Appendix C). The resulting strain, PGY10 contained a copy of *TIF51A* under control of the *GAL1* promoter with two copies each of *TIF51B* and *TIF51A* disrupted by the insertion of the *hisG* coding sequence.

3.2.12 Southern Blot analysis

Genomic DNA was extracted from strains INVScI, PGY1, PGY8 and PGY10 digested with *Eco* RV and resolved using a 1 % agarose gel. The DNA was transferred to a Hybond N+ (Amersham Biosciences) nylon membrane using the method described in Appendix I (Sambrook *et al*., 1989). A pGEM®T-Easy construct, carrying the *TIF51A* coding sequence (pPG30, Appendix J), was linearised using *Hin*d III and used to generate a negative sense [^{32}P]-dCTP-labelled RNA probe with T7 RNA polymerase according to the manufacturer's recommendations (MBI Fermentas). Since *TIF51A* and *TIF51B* coding sequences share over 90% nucleotide sequence identity, this probe would hybridise to both genes. Hybridisation was performed at 42^{o}C (with formamide) and stringent washes were carried out to remove unbound and non-specifically bound probe (Ausubel *et al*., 1983; Appendix I).

3.2.13 Construction of the *TIF51A* complementation vectors

The coding region of *TIF51A*, as well as its endogenous promoter was amplified from INVScI genomic DNA using primer pair PG8F and PG6R (Appendix C), which introduced a 5' *Age* I and a 3' *Bam* HI site. The product was inserted into the pGEM® T Easy vector and the recombinant plasmid selected by restriction analysis and DNA sequencing using the pUCF and pUCR primers (Appendix C). Digestion with *Age* I and *Bam* HI released a 738 bp fragment carrying the *TIF51A* coding region preceded by its native promoter, which was ligated into *Age* I/*Bam* HI-digested pYES2 (Invitrogen). The integrity of the resulting construct, pPG10, was confirmed by restriction analysis and DNA sequencing using primers AI2F and AI1R (Appendix C). Plasmid pPG10, (Figure 3.4) was used for complementation assays in the *TIF51A*-*TIF51B*-disrupted strain, PGY10.

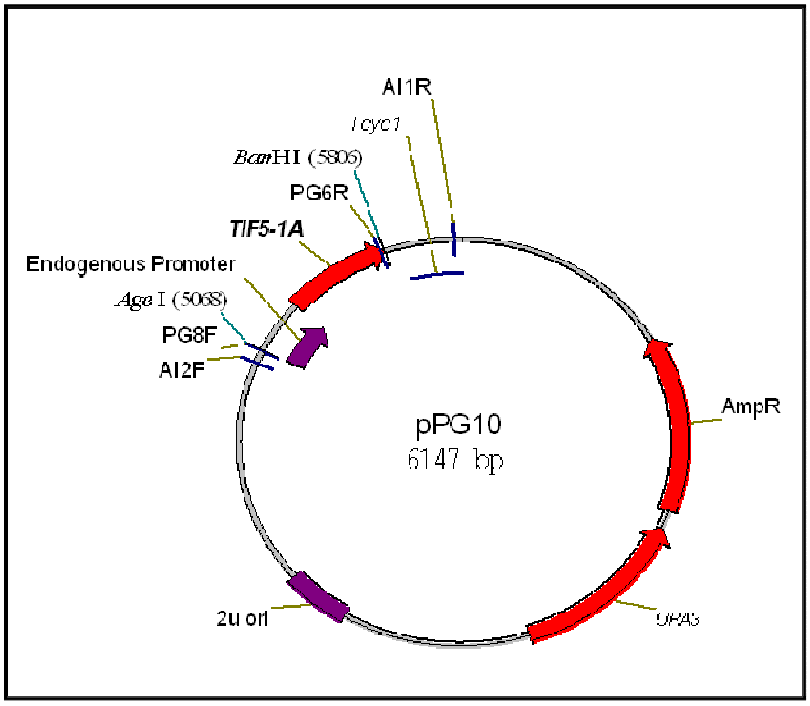

Figure 3.4: The *TIF51A* complementation vector pPG10. Schematic representation of the pYES2-derived vector, pPG10, which bears the *URA3* auxotrophic marker, and has, in place of the *GAL1* promoter, the *TIF51A* coding region preceded by the endogenous promoter. In addition, pPG10 bears the yeast 2 micron origin of replication (2 μ ori), the β-lactamase gene encoding ampicillin resistance (AmpR) and a T_{cyc1} transcriptional terminator.

An N-terminal 6 x His tag was then introduced upstream of the *TIF51A* AUG start codon in the vector pPG10. This was achieved by PCR amplification using the overlapping primers PG30 and PG31 (Appendix C), which introduce a *Pvu* II site followed by the 6 x His tag immediately upstream from the eIF5A ORF. The PCR product was digested with *Pvu* II and ligated with T4 DNA ligase. The resulting His-eIF5A complementation plasmid, pPG20 (Figure 3.5), bearing the His-*TIF51A* sequence was confirmed by restriction analysis and the integrity of the DNA sequence confirmed using primers AI2F and AI1R (Appendix C) that bind to the 5' P_{GAL1} and 3' T_{CYC1} regions respectively. Plasmid pPG20, (Figure 3.5) was used for complementation assays in the *TIF51A*-*TIF51B*-disrupted strain, PGY10.

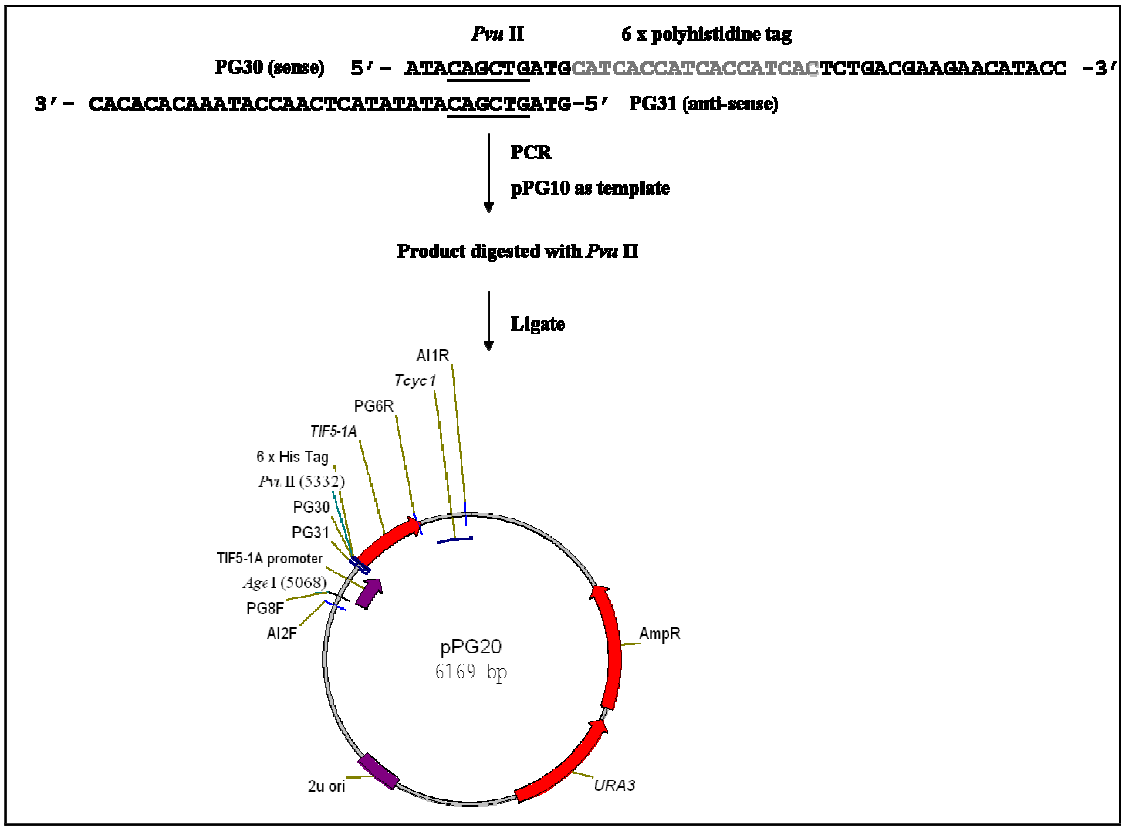

Figure 3.5: Construction of His-eIF5A complementation plasmid, pPG20. Schematic representation of primers PG30 (sense) and PG31 (anti-sense) that were used in the inverse PCR of pPG10, digested with *Pvu* II and ligated to produce pPG20, the His-eIF5A complementation vector for strain PGY10. The construct bears a β-lactamase gene encoding ampicillin resistance and a *URA3* auxotrophic marker.

Furthermore, a C-terminal 6 x His tag version of the complementation vector was generated. This was achieved by removing a 400 bp fragment following digestion with *Sal* I/*Eco* RI from pPG6 (Section 3.2.4) and replacing the 3' portion of *TIF51A* from pPG10 with the same 3' region, but containing the coding sequence for the 6 x His tag at the C-terminus. Plasmid pPG10-His (Appendix J) was also used for complementation assays in the *TIF51A*-*TIF51B*-disrupted strain, PGY10.

3.2.14 Complementation of the *TIF51A*-*TIF51B*-disruption strain, PGY10

Strain PGY10 was transformed with either pYES2 (Invitrogen) or with pPG10 and grown on SMM agar plates supplemented with histidine, tryptophan and galactose but no uracil, at 28°C for 4 to 6 days. Following patching, 4 $OD_{600\ nm}$ units of cells were scraped from the agar plates, washed in sterile distilled water and inoculated into either YPD or YPGal broth. After 24-36 hours of growth with shaking at 28°C, cells were harvested by centrifugation at 1000xg and resuspended to an $OD_{600\ nm}$ of 1.0 in water. Five-fold serial dilutions were performed and

5 µl of each dilution were spotted onto either YPD or YPGal agar plates. These plates were incubated for a further two days at 28°C.

3.3 Results and Discussion

The two most important requirements of an experimental system for studying eIF5A were: (1) to track the presence of the protein during purification and biochemical characterisation and (2) to assay for eIF5A function *in viv*o. Thus the focus in this chapter was to produce good quality anti-eIF5A antibodies and to construct a knockout yeast strain for complementation assays to detect eIF5A function.

3.3.1 Over-expression and purification of eIF5A-His from *E. coli*

The construct, pPG6, which carries a copy of the *TIF51A* coding sequence downstream of the T7 promoter, was used for over-expression of eIF5A in *E. coli*. Cells expressing eIF5A were induced and analysed for the presence of the protein by SDS-PAGE. A protein migrating at approximately 21 kDa was observed in cells transformed with pPG6, with maximum levels of this protein produced after 2 hours of induction (Figure 3.6, lanes 3-6). This is consistent with the M_R of eIF5A-His (20 kDa plus the 6 x His tag). Since no equivalent protein was detected in extracts from cells transformed with the vector, pT7-7 (Figure 3.6, compare lane 1 with lane 6), the 21 kDa protein was attributed to the presence of eIF5A-His. Nearly all of eIF5A-His was present in the soluble fraction, with a significantly lower amount visible in the insoluble fraction (Figure 3.6, lanes 7 and 8), indicating that the recombinant protein was soluble.

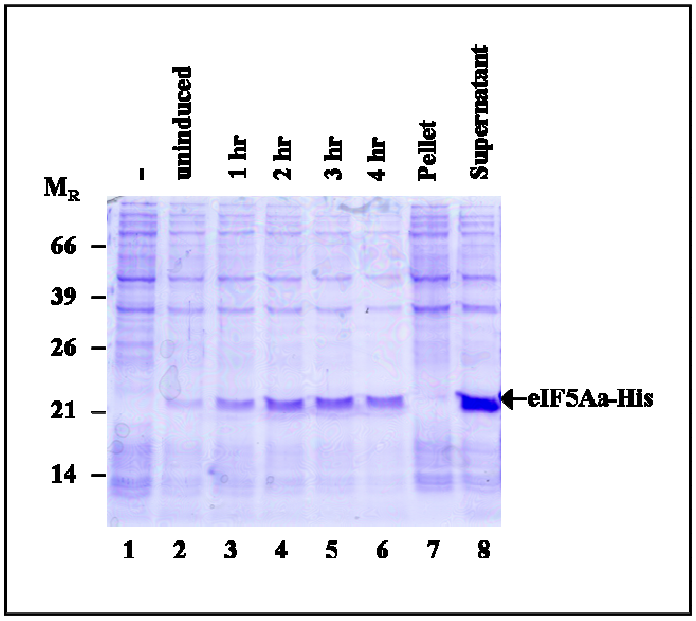

Figure 3.6: Expression and solubility of recombinant eIF5A-His in *E. coli*. Coomassie-stained 15 % SDS-polyacrylamide gel with the following resolved proteins. Lane 1: protein extract from cells transformed with pT7-7 (-) sampled 4 hours post-induction; Lanes 2–6: protein extracts from cells transformed with pPG6 (eIF5A-His) at hourly intervals from 0 to 4 hours after induction; Lane 7: insoluble fraction (pellet) and Lane 8: soluble fraction (supernatant) of cell free extract derived from cells expressing eIF5A-His after four hours of induction. The position of the eIF5A-His protein is shown on the right (arrow), while the relative molecular weights are indicated on the left in kDa.

Since the majority of recombinant eIF5A-His appeared to be soluble, it was decided to proceed with native purification of the protein. Cell-free extracts derived from 10 $OD_{600\ nm}$ units of *E. coli* cells expressing eIF5A-His (pPG6) were used for nickel-affinity purification of eIF5A-His. Analysis of eluted fractions using SDS-PAGE revealed little eIF5A-His in the flow-through fraction, indicating that the protein had bound to the column (Figure 3.7, lane 2). Similarly, no eIF5A-His could be detected in the wash fractions (Figure 3.7, lanes 3-5), which contained an increase in the imidazole concentration when compared with the binding buffer (from 10 mM to 20 mM, respectively). A buffer containing 250 mM imidazole was used to elute the eIF5A-His. The elution fractions comprised mainly of purified eIF5A protein (migrating at approximately 21 kDa), with the presence of a small amount of higher molecular weight proteins, at about 70 kDa in size, (Figure 3.7, lanes 6-8). Since the contaminating proteins represented a minor fraction of the total protein, the sample was used to raise polyclonal antibodies.

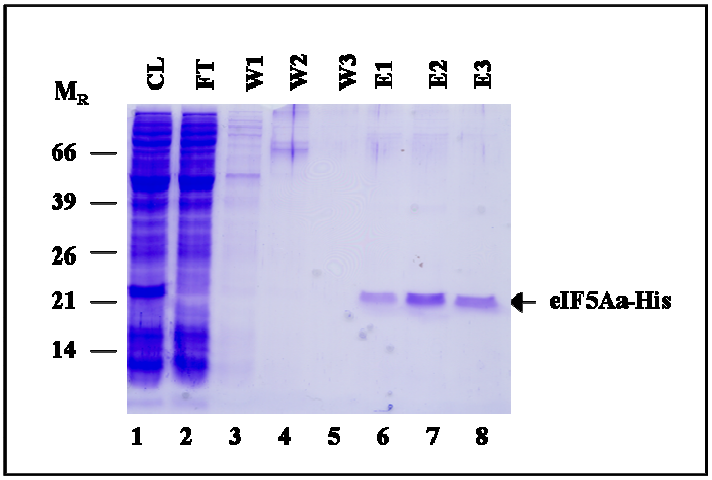

Figure 3.7: Nickel affinity purification of eIF5A-His. Coomassie-stained 15 % SDS-polyacrylamide gel with the following resolved protein samples: Lane 1: Cell-free lysates (CL) of cells transformed with pPG6 following induction for 4 hours; Lane 2: Flow-through (FT) obtained after binding of CL to the column; Lanes 3-5: Wash fractions (W1-3) collected using 20 mM imidazole buffer; Lanes 6-8: Elutions of purified eIF5A-His (E1-3) collected using 250 mM imidazole buffer. eIF5A-His is indicated by the arrow (right) and the size of the molecular weight markers are indicated on the left in kDa.

3.3.2 Optimisation of Western analysis with anti-eIF5A polyclonal antibodies

Western analysis was used to confirm the absence of anti-eIF5A antibodies in the rabbit serum prior to immunisation with purified eIF5A-His. Protein extracts from *E. coli* cells expressing eIF5A-His (pPG6) and whole cells transformed with pT7-7 were probed with "Day 0" serum. At a dilution of 1:250 000, neither eIF5A nor other cellular proteins could be detected (Figure 3.7A, lanes 1 and 2). To confirm that antibodies present in the antiserum had been raised against eIF5A, the "Day 39" anti-eIF5A-His serum was used to detect eIF5A in cell-free extracts at dilutions of either 1:250 000, 1:500 000 or 1:1 000 000. eIF5A was detected in cell-free extracts derived from cells transformed with pPG6, but not with pT7-7 (Figure 3.8A, lane 4 vs. lane 3) indicating the presence of anti-eIF5A antibodies in the serum.

Some cross-reaction with other *E. coli* proteins was observed, especially with a protein migrating at 14 kDa. Dilution of the antiserum to 1:500 000 or 1:1 000 000 resulted in reduction, but not elimination of cross-reaction with *E. coli* cellular proteins, (Figure 3.8A, lanes 5 to 8). To reduce the degree of cross-reaction with *E. coli* proteins, it was decided to immunoprecipitate these non-eIF5A-specific antibodies by pre-adsorbing the antiserum with cell-free protein extracts derived from *E. coli* cells harbouring the vector pT7-7. Western analysis of whole cells transformed with either pPG6 (+) at or pT7-7 (-), using the pre-absorbed antiserum resulted in substantially reduced levels of cross-reactivity with *E. coli* cellular proteins (Figure 3.8B lanes 1 and 2). Finally, the sensitivity of the anti-eIF5A

antiserum was determined using dilutions of purified eIF5A-His showing that the antibodies could detect 7.5 ng of purified eIF5A-His (Figure 3.8C, lane 4).

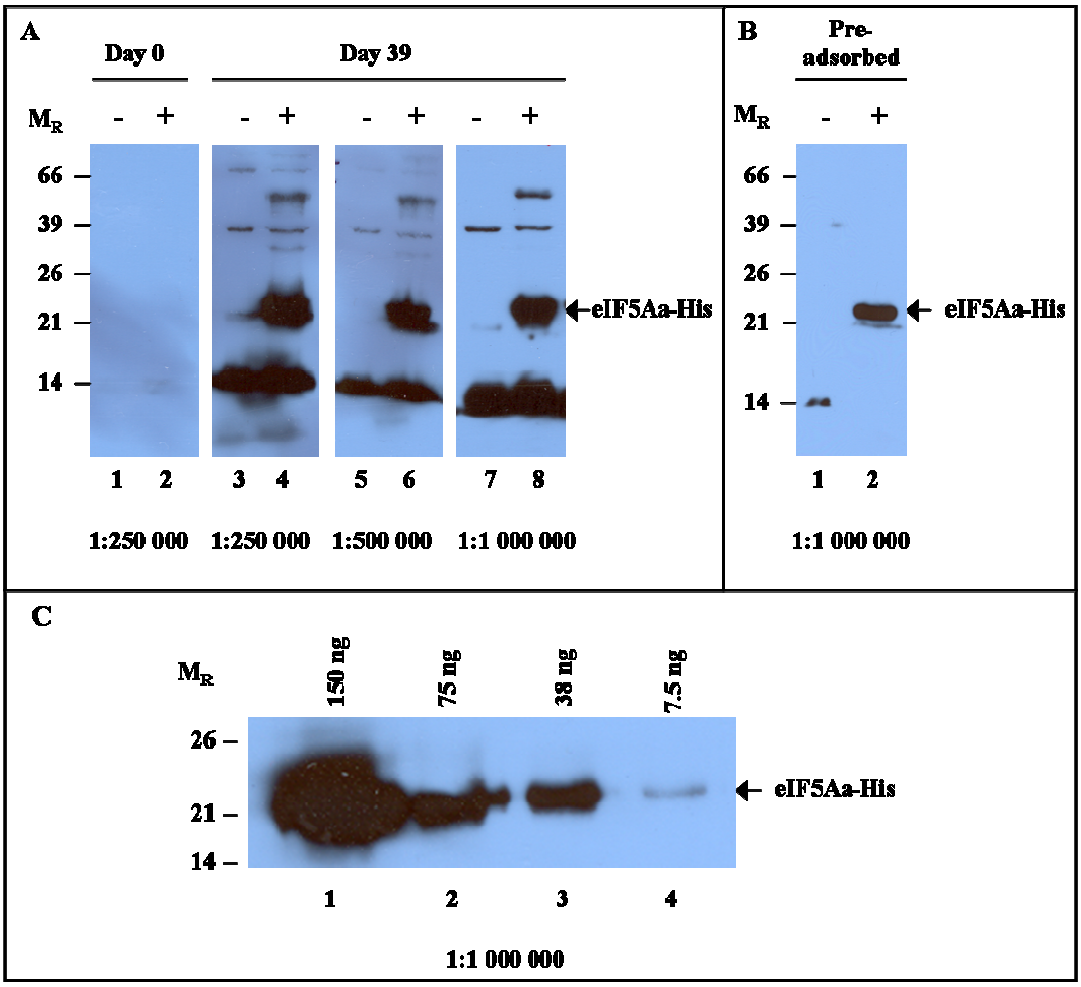

Figure 3.8: Optimisation of anti-eIF5A antiserum for Western analysis. (A) Western analysis of whole cells transformed with pPG6 (+) or pT7-7 (-) using "Day 0" antiserum at a dilution of 1:250 000 (lanes 1 and 2) or using the "Day 39" antiserum at dilutions of 1:250 000 (lanes 3 and 4), 1:500 000 (lanes 5 and 6) and 1: 1 000 000 (lanes 7 and 8). **(B)** Western analysis of protein extracts from cells harbouring either pT7-7 (-) or pPG6 (+) using the "Day 39" anti-eIF5A serum at a dilution of 1:1 000 000 after pre-adsorption. **(C)** Western analysis of purified eIF5A-His proteins at concentrations of 150 ng, 75 ng, 38 ng and 7.5 ng (lanes 1 to 4 respectively), using the pre-adsorbed "Day 39" anti-eIF5A serum at a dilution of 1:1 000 000. The autorad exposure time in each case was 1 minute. Sizes of the relative protein molecular weight markers are indicated on the left of the blots in kDa, and the relative size of eIF5A-His is indicated on the right (arrow).

3.3.3 Construction of the *TIF51A-TIF51B* knockout yeast strain, PGY10

The strategy for assaying for eIF5A function by complementation was to construct a knockout yeast strain in which the endogenous *TIF51A* and *TIF51B* genes had been disrupted, with a functional copy of *TIF51A* under control of the *GAL1* promoter inserted into the *leu2* gene. Thus expression of *LEU2::TIF51A* ("endogenous eIF5A") could thus be induced by growth in galactose and repressed in medium containing glucose, allowing for the ability to assay for biological function of "exogenous eIF5A" (expressed from a plasmid under control of the native *TIF51A* promoter).

3.3.3a The *LEU2::P_{GAL1}-TIF51A* strain, PGY1

In the first step, a copy of *TIF51A* under the control of the *GAL1* promoter (P_{GAL1}*TIF51A*), was inserted into the *leu2* locus of INVScI by homologous recombination. This was achieved by transforming pPG13, linearised using a single *Cla* I site within the *LEU2* coding sequence (Figure 3.9A and B) and selecting for Leu^+ transformants. Confirmation of integration of the *LEU2::P_{GAL1}-TIF51A* fragment was obtained by PCR analysis of genomic DNA extracted from recombinants using three primer pairs designed to recognise only the *LEU2::P_{GAL1}-TIF51A* sequence. The PCR analysis of five recombinants with the correct genotype is represented in Figure 3.8C. Recombinant 2 (Figure 3.9C, lanes 2, 7 and 12, marked by asterisks) was selected for further strain construction (PGY1). The sizes of all three PCR products from strain PGY1 corresponded with the expected sizes based upon the sequence (Figure 3.9B). It is unknown whether the homologous recombination event occurred in both copies of *leu2* in the diploid INVScI cells but it was certain that at least one copy of P_{GAL1}*TIF51A* had been inserted onto the chromosome at the *leu2* locus. It was expected that a single copy would be able to drive the production of sufficient *TIF51A* in the subsequent disruption strains in medium containing galactose as the sole carbon source, to ensure viability.

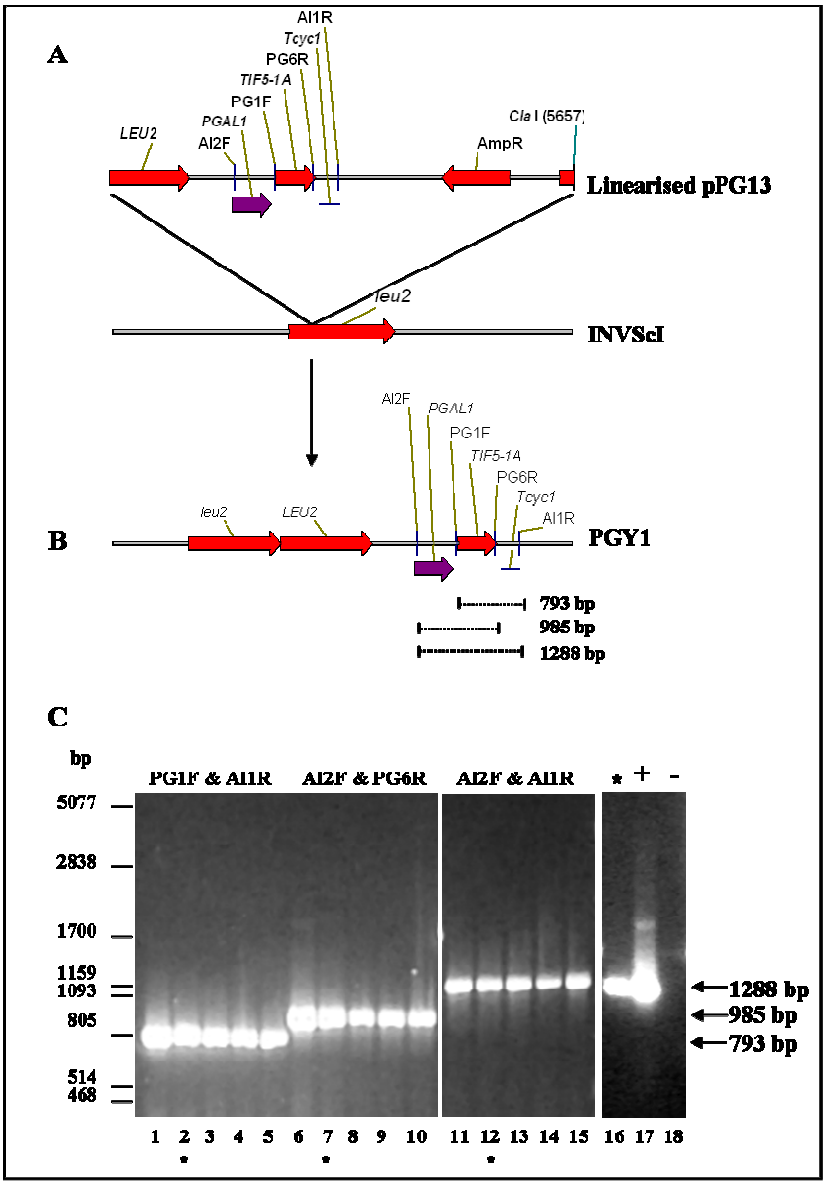

Figure 3.9: Construction and confirmation of the yeast strain, PGY1. (A) Schematic depicting the result of insertion of pPG13 into the *leu2* locus of yeast strain INVSc1. **(B)** Schematic of the integrated P_{GAL1}*TIF51A* with the functional *LEU2* and the non-functional *leu2* auxotrophic markers. The positions of primers, AI2F, PG1F, PG6R and AI1R are indicated. Sizes of amplified products with primer pairs PG1F and AI1R, AI2F and PG6R, as well as AI2F and AI1R are indicated as dotted lines below the map. **(C)** Analysis of PCR products by agarose gel electrophoresis: Lanes 1-5: Amplification products obtained using primers PG1F and AI1R; Lane 6-10: Amplification products obtained using primers AI2F and PG6R and Lanes 11-15: Amplification products obtained using primers AI2F and AI1R. Of the five samples, the second was chosen as the representative sample (marked *). Lane 16-18: Amplification products obtained using primers AI2F and AI1R of the representative sample (*) (lane 16), of the original plasmid, pPG13 (+) (lane 17) and of INVScI DNA (-) (lane 18). The relative sizes of the molecular markers are indicated on the left of the gel in base pairs and the positions of the bands corresponding to the expected sizes of the DNA fragments are indicated on the right (arrows).

3.3.3b The *TIF51B*-disrupted strain, PGY8

The integration of P_{GAL1}*TIF51A* into the *leu2* locus on chromosome III enabled the successive disruption of *TIF51A* and *TIF51B* by the integrative transformation process developed by Alani *et al*., (1987). This process involved the transformation of PGY1 cells with a linear DNA fragment carrying the *TIF51B* gene disrupted by a copy of *URA3,* flanked on either side by a *hisG* repeat (Figure 3.10A). Next, cells in which the *URA3* marker had been deleted via homologous recombination between the *hisG* repeats, were isolated by selecting for the Ura^- phenotype by growth on agar containing 5-FOA (Figure 3.10B). PCR analysis was used to confirm the initial disruption of the two copies of *TIF51B* and subsequent deletion of the *URA3* marker (Figure 3.10C). Of the 200 transformants screened, only 2 appeared to contain the *TIF51B* disruption cassette. A 4.5 kbp PCR amplification product representing the disrupted *TIF51B* gene, was obtained from one transformant as well as a 0.7 kbp fragment representing a wild-type *TIF51B* gene (Figure 3.10C, lane 1), suggesting that only one of the *TIF51B* genes were disrupted.

PCR analysis of a second transformant (PGY7), resulted in only the 4.5 kbp fragment (represented in Figure 3.10C, lane 4) suggesting that both *TIF51B* genes had been disrupted. Further PCR analysis of this transformant (PGY7) confirmed that only the 4.5 kbp fragment was amplified with primers PG13F and PG14R (Figure 3.10D, lane 1), Amplification with PG13F and URA1 resulted in the production of an expected 2.8 kbp fragment (Figure 3.10D, lane 2). These sizes corresponded with the control reactions using the pPG16 plasmid (Figure 3.10D, lanes 4 and 5, respectively).

The strain containing the double knockout of *TIF51B,* PGY7, was used to select for Ura^- revertants by selecting for 5-FOA resistance. Cells with a Ura^- phenotype are resistant to 5-FOA, while Ura^+ cells are 5-FOA sensitive (Boeke *et al*., 1984; Umezu *et al*., 1971). Genomic DNA from 5-FOA resistant cells was subjected to PCR analysis to confirm the deletion of the *URA3* marker as a result of homologous recombination between the *hisG* repeats (Figure 3.9D, lane 3). The presence of a 1.8 kbp PCR product (representing a single copy of *hisG*) in Ura^- cells as compared with the 4.5 kbp fragment corresponding to the *hisG-URA3-hisG* fragment, confirmed the correct genotype (Figure 3.10D, lane 1) in strain PGY8, which was used to create the *TIF51B-TIF51A* knockout strain.

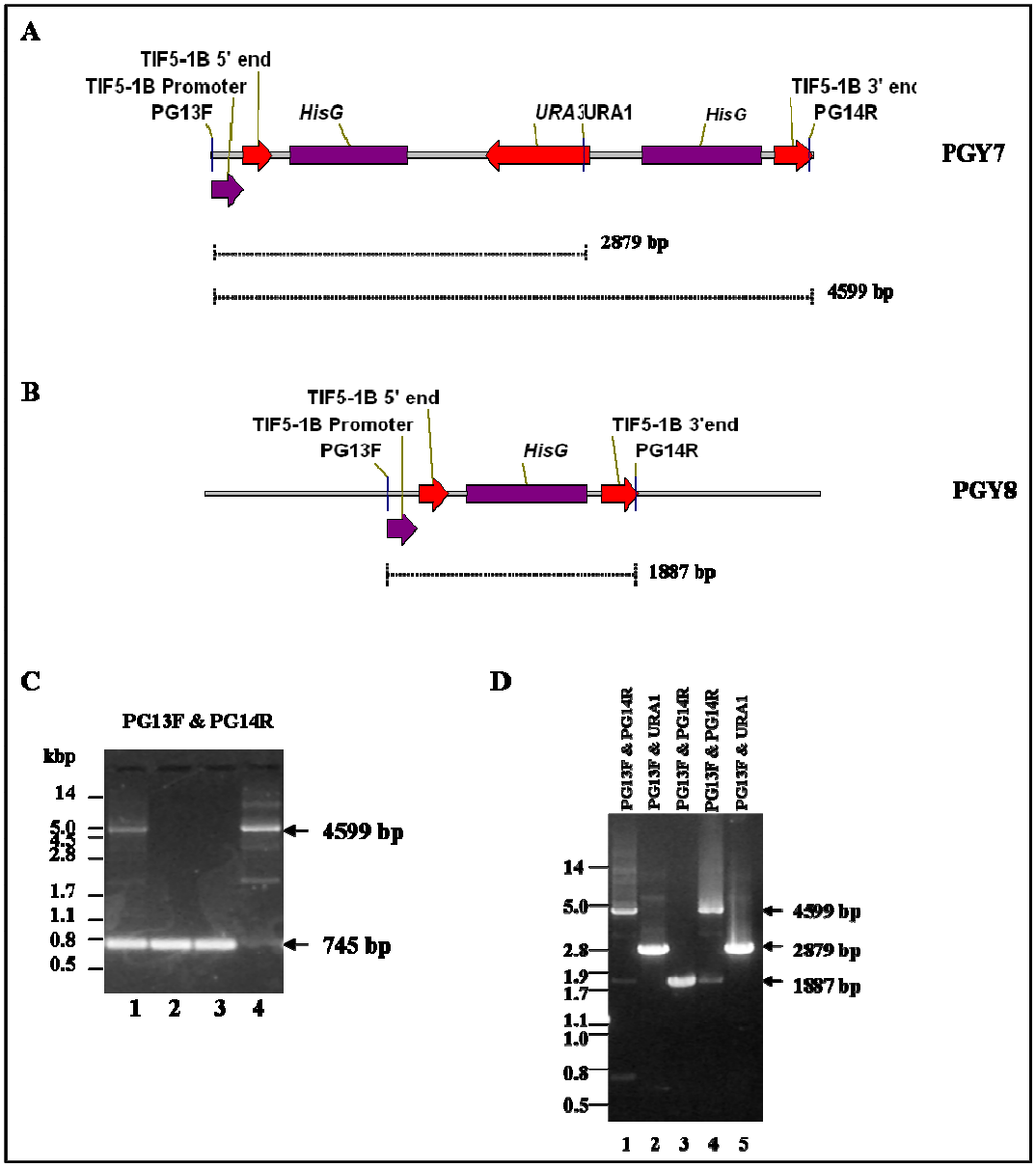

Figure 3.10: Construction and confirmation of the disrupted TIF51B yeast strain, PGY8. (A) Schematic of the *TIF51B* disruption fragment bearing *URA3* flanked by *hisG* repeats. Below the map (dotted lines) are the expected fragment sizes expected upon amplification with the indicated primer sets. **(B)** Schematic of the disrupted *TIF51B* following homologous recombination of the *hisG* repeats and subsequent reversal to Ura$^-$ phenotype. **(C)** 1 % agarose gel with the amplified products of four potential transformants selected for the Ura$^+$ phenotype using primers PG13F and PG14R (lanes 1-4). **(D)** 1 % agarose gel with the amplified products using the primer sets indicated to confirm integration prior to 5-FOA treatment (PGY7) (Lanes 1 and 2): and post-5-FOA treatment (PGY8) (Lane 3) of the selected transformant. Lanes 4 and 5 represent the control reactions performed using the disruption vector pPG16. The sizes of the molecular weight markers are shown on the left of the gels in kbp and the positions of the bands corresponding to the expected sizes of the DNA fragments are indicated on the right (arrows). Primers used for the PCR amplifications are indicated above the lanes.

3.3.3c The *TIF51B*-*TIF51A*-disrupted strain, PGY10

To disrupt *TIF51A*, strain PGY8 was transformed with an *Eco* RI-digested DNA fragment from pPG14 carrying the *TIF51A* 5' coding sequence disrupted by *URA3*, flanked on either side by a copy of *hisG* (Figure 3.11A). As with the disruption of *TIF51B*, the *hisG-URA3-hisG* cassette was inserted into *TIF51A* by homologous recombination between the 5' and 3' *TIF51A* flanking sequences. Since disruption of both *TIF51A* loci results in loss of viability, Ura^+ transformants were grown on agar plates containing galactose to induce expression of P_{GAL1}-*TIF51A* inserted into the *leu2* locus in this strain. Transformants were screened by PCR analysis to determine whether or not the *hisG-URA3-hisG* cassette had been inserted into the two *TIF51A* loci. Of the 500 transformants screened, only 2 had at least one of the two *TIF51A* loci disrupted (Figure 3.11C, lanes 1 and 7). These two transformants, were subjected to selection for reversion of the Ura^+ phenotype by selecting for 5-FOA resistance. The Ura^- colonies were analysed for the *TIF51A* disruption using PCR primers PG8F and PG6R. It was discovered that only one of the two strains initially selected had both copies of *TIF51A* disrupted, while the other still carried one wild-type copy of the gene (Figure 3.11D, lanes 1 and 2, respectively).

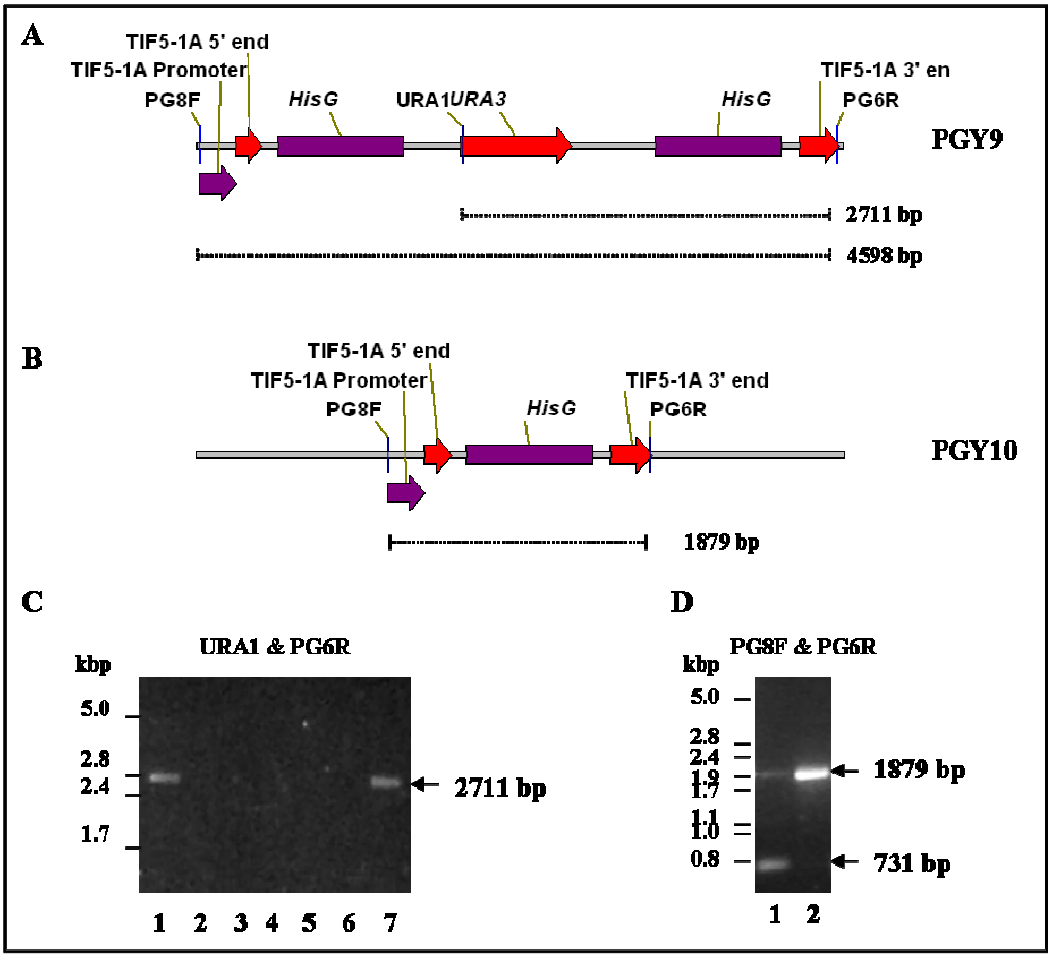

Figure 3.11: Construction of the disrupted TIF51A yeast strain, PGY10. (A) Schematic representation of the *TIF51A* disruption fragment bearing *URA3* flanked by *hisG* repeats. Below the map (dotted lines) are the expected fragment sizes expected upon amplification with the indicated primer sets. (B) Schematic representation of the disrupted *TIF51A* following homologous recombination of the *hisG* repeats and subsequent reversal to Ura$^-$ phenotype. (C) 1 % agarose gel with the amplified products of seven potential transformants selected for the Ura$^+$ phenotype using the primer set indicated (lanes 1-7). (D) 1 % agarose gel with the amplified products of two potential integrants, following reversion of the Ura$^+$ phenotype. The sizes of the molecular weight markers are shown on the left of the gels in kbp, the positions of the bands corresponding to the expected sizes of the DNA fragments are indicated on the right (arrows) and the primers used in the amplification are indicated above the lanes.

Finally, a series of PCR amplifications were conducted to confirm the genotypes of the *TIF51B-TIF51A* knockout yeast strain. To verify the presence of the *LEU2::*P_{GAL1}*-TIF51A* fragment, DNA primers AI2F and AI1R, which correspond to sequences in P_{GAL1} and T_{CYC1} were used to amplify a 1.2 kbp product containing the *TIF51A* coding sequence, from genomic DNA. The PCR fragment was obtained from all strains excepting the wild type parental strain, INVSc1 (Figure 3.12A, lanes 2-4 vs. lane 1). To confirm the disruption of *TIF51B*, a 1.8 kbp fragment, corresponding to the sequence flanked by primers PG13F and

PG14R, was amplified. The PCR product was detected in strains PGY8 and PGY10, but not in strain INVSc1 or PGY5. (Figure 3.12B, lanes 3 and 4). The wild-type *TIF51B* gene (present in strains INVScI and PGY1) was represented by a 0.7 kbp fragment (Figure 3.12B, lanes 1 and 2). Lastly, to verify the disruption of *TIF51A*, primers PG8F and PG6R, corresponding to the 5' and 3' regions of *TIF51A*, respectively, were used to amplify a 1.8 kbp fragment indicating disruption of *TIF51A* by *hisG* from genomic DNA extracted from strain PGY10 (Figure 3.12C, lane 4). As expected, a 0.7 kbp fragment, indicating the wild-type sequence, was amplified from genomic DNA isolated from strains INVScI, PGY1 and PGY8 (Figure 3.12C, lanes 1-3).

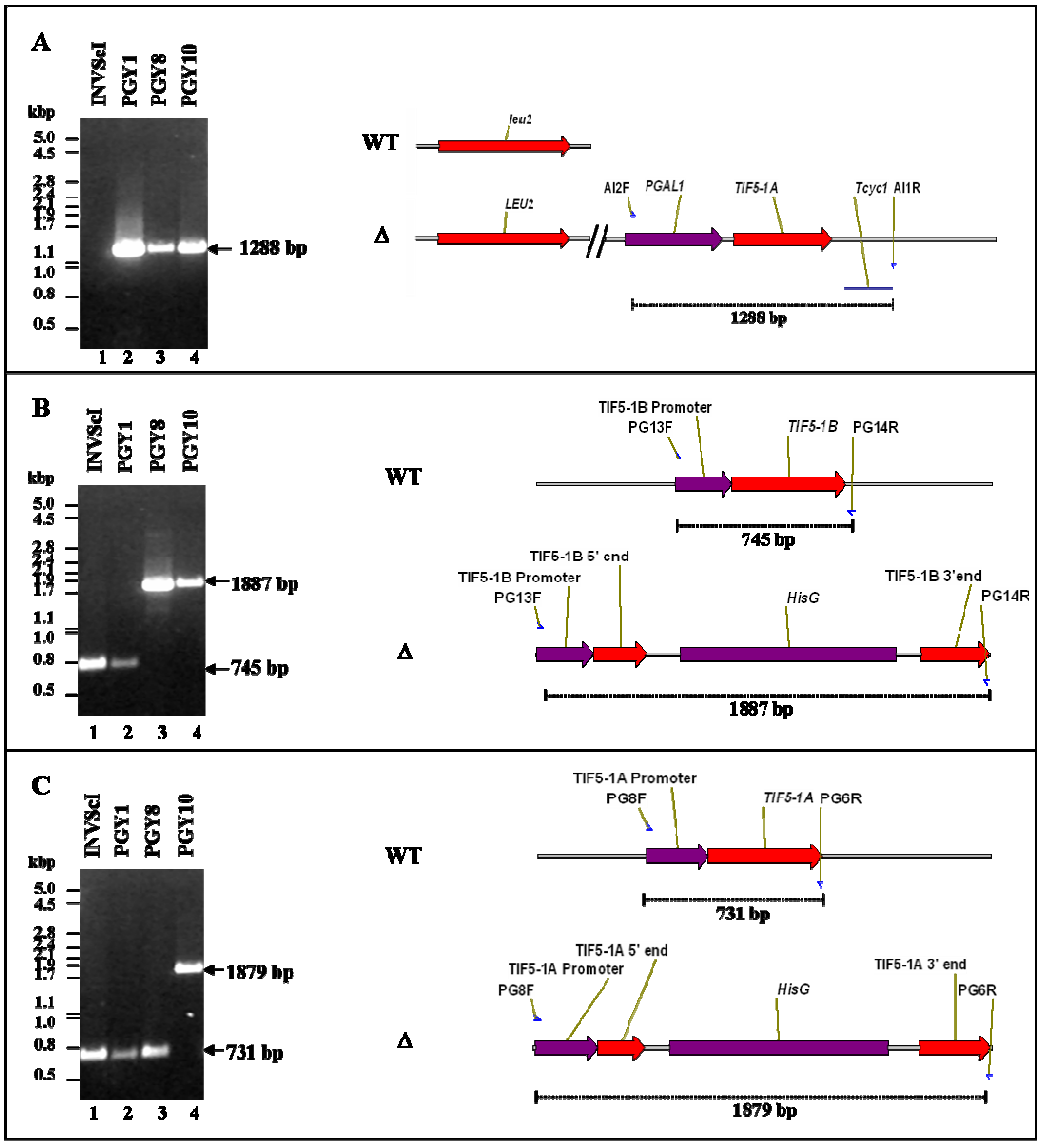

Figure 3.12: Genotypic confirmation of the yeast strains used in this study using PCR. Genotypic confirmation of strains PGY1 (A), PGY8 (B) and PGY10 (C) by PCR analysis (left) using primers AI2F and AI1R, PG8F and PG6R, and PG13F and PG14R, respectively. On the right in each case is a corresponding representation of the wild-type strain (INVScI) and the integrated strains PGY1 (A), PGY8 (B) and PGY10 (C). Indicated below each schematic (dotted lines) are the expected fragment sizes upon amplification with the indicated primers above the lanes. The sizes of the molecular weight markers are indicated on the left of the gels (in kbp) and the positions of the bands corresponding to the expected sizes of the DNA fragments are indicated on the right (arrows).

3.3.4 Southern blot analysis of yeast genomic DNA

Genomic DNA extracted from all the strains, including the wild-type, INVScI, was digested with *Eco* RV and probed with a radio-labelled RNA transcript that would recognise the coding sequences of both *TIF51A* and *TIF51B*. The *LEU2::*P_{GAL1}*-TIF51A* sequence, detected as a 1.6 kbp RE fragment, was present in strains PGY6, PGY8 and PGY10 (Figure 3.13A,

lanes 1-3, fragment “a”), but not in the parental strain, INVScI (Figure 3.13A, lane 4). The disrupted *TIF51B* sequence was confirmed by the shifting of a 0.6 kbp fragment in strains INVSc1 and PGY6 (Figure 3.13A, lanes 3 and 4, fragment “b”) to a 0.8 kbp fragment in strains PGY8 and PGY10 (Figure 3.13A, lanes 1 and 2, fragment “c”). The fragment indicated by the asterisk (*) is produced by the digestion of the 5’ *TIF51B* region, that is not as readily recognised by the probe, since the regions upstream of *TIF51B* and *TIF51A* are not well conserved. Finally, the *TIF51A* knockout was confirmed by a shift from a band of 2.1 kbp in strain INVSc1, PGY6 and PGY8 (Figure 3.13A, lanes 2-4, “d”) to 3 kbp in strain PGY10 (Figure 3.13A, lane 1, fragment “e”). The restriction fragment sizes observed on the Southern blot corresponded with the sizes expected as indicated for each strain by the schematic maps in Figure 3.13B (“a”–“e”).

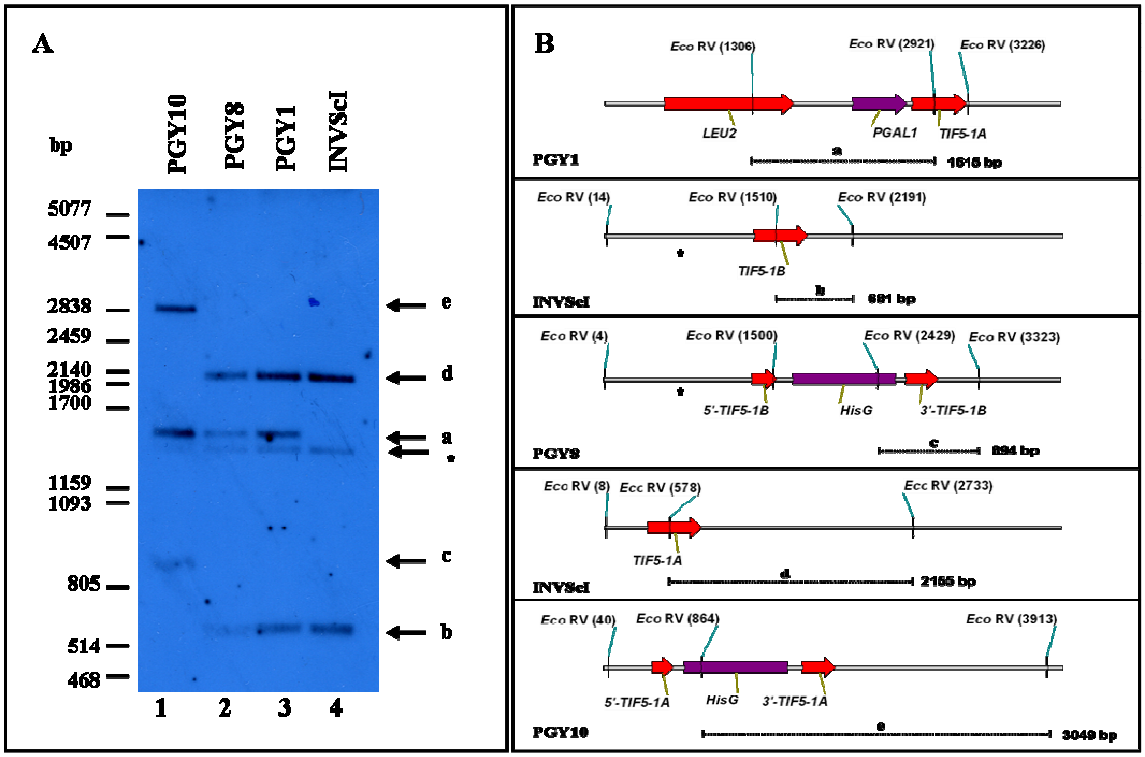

Figure 3.13: Genotypic confirmation of yeast strains by Southern blot analysis. (A) Southern Blot of *Eco* RV-digested genomic DNA extracted from all yeast strains probed with an RNA transcript binding the CDS of both *TIF51A* and *TIF51B*. The relative sizes of the molecular weight markers are indicated on the left of the blot, and the positions of the DNA fragments of interest (“a” – “e”) are indicated on the right (arrows). **(B)** Schematic maps of the wild-type (INVScI), P_{GAL1}*TIF51A* integrated (PGY1), *TIF51B*-disrupted (PGY8) and *TIF51A*-disrupted (PGY10) strains, indicating the expected sizes of the DNA fragments to which the RNA probe would bind below (dotted lines).

3.3.5 Phenotypic confirmation of knockout yeast strains

With the genotypes of the yeast strains confirmed by both PCR and Southern blot analysis, it was necessary to determine the phenotypes of the yeast strains. This was achieved by the growing the strains in complete medium containing galactose as the sole carbon source (YPGal), followed by growth on YP agar containing either galactose or glucose. All the yeast strains grew on medium containing galactose as the carbon source due to the integration of P_{GAL1}-*TIF51A*. In contrast to the other strains, PGY10 did not grow on medium containing glucose, (Figure 3.14). The loss of viability in the absence of galactose indicated both *TIF51A* and *TIF51B* loci were successfully disrupted, resulting in a strong phenotype in this diploid knockout, which corresponds to the phenotypes observed by Schnier *et al*., (1991) and Schwelberger *et al*., (1993).

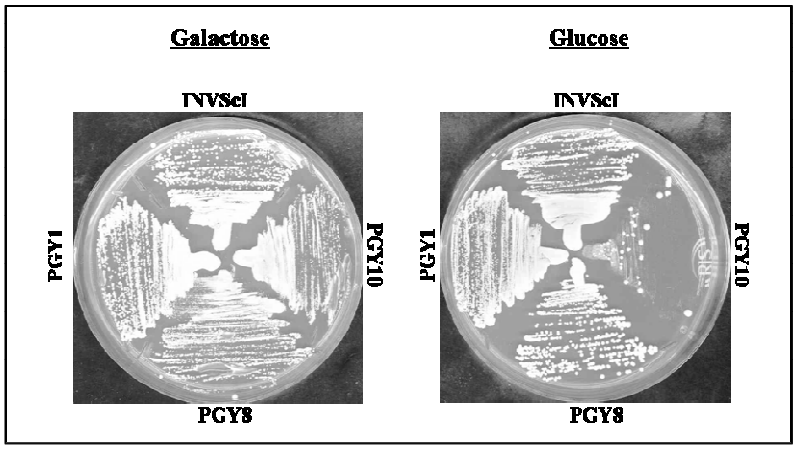

Figure 3.14: Phenotypic analysis of the yeast strains used in this study. Phenotypic analysis of the strains INVScI, PGY1, PGY8 and PGY10 (positioned on the top, left, bottom and right of the plates, respectively, as indicated) on complete medium containing either galactose (left) or glucose (right) as the sole carbon source.

3.3.6 Protein profile analysis of the yeast strains using Western analysis

Western analysis was conducted to examine the expression of eIF5A and eIF5Ab in all the yeast strains, using the anti-eIF5A antibodies (Section 3.3.2). eIF5A (approximate M_R of 20 kDa) and eIF5Ab (approximate M_R of 18 kDa) were present in the wild-type strain, INVScI (Figure 3.15 lane 1). Although equivalent amounts of total protein were loaded in each lane (determined using Bradford's assay and Coomassie staining), there appeared to be more eIF5A as compared with eIF5Ab in strain PGY6, consistent with the increase in expression as a result of the presence of *LEU2::*P_{GAL1}-*TIF51A* (Figure 3.15, lane 2).

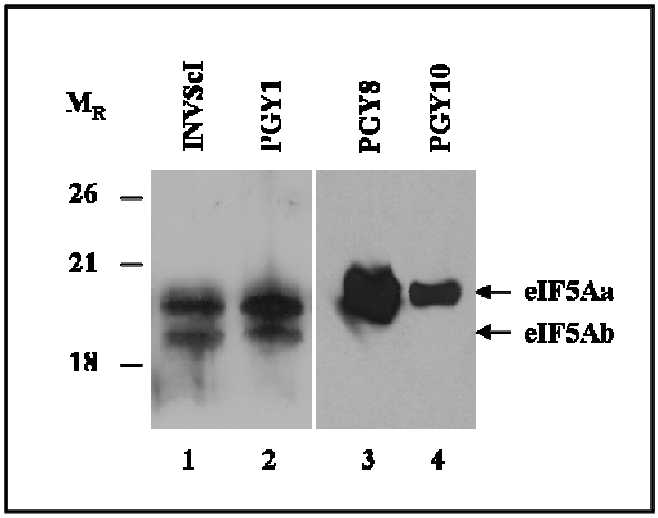

Figure 3.15: Protein profile analysis of strains used in this study. Western analysis of eIF5A and eIF5Ab present in the total protein extracts of strains INVScI (lane 1), PGY1 (lane 2), PGY8 (lane 3) and PGY10 (lane 4), grown in complete medium containing galactose as the carbon source. The relative positions of eIF5A and eIF5Ab are indicated by arrows on the right, and the relative molecular weight markers are indicated on the left of the blot in kDa.

As expected, the disruption of *TIF51B* (strain PGY8), resulted in the loss of eIF5Ab in protein extracts (Figure 3.15, lane 3). Upon further disruption of *TIF51A* (strain PGY10), a reduction in the levels of eIF5A suggested that only the eIF5A expressed from P_{GAL1} was detected (Figure 3.15, lane 4).

3.3.7 Complementation of PGY10

To test the functionality of the knockout strain PGY10, serial dilutions of washed cells transformed with either pYES2 (vector) or pPG10 (bearing *TIF51A* under the control of its endogenous promoter) were plated onto SMM (supplemented with histidine and tryptophan) agar plates containing either galactose or glucose as the carbon source. Cells transformed with either pYES2 (-) or pPG10 (+) grew on medium containing galactose as the sole carbon source, due to the presence of the *LEU2::*P_{GAL1}*-TIF51A* on the chromosome (Figure 3.16 left). Cells transformed with pYES2 (empty vector) exhibited a lethal phenotype on plates containing glucose, but complementation of growth was observed for cells transformed with pPG10 (Figure 3.16 right).

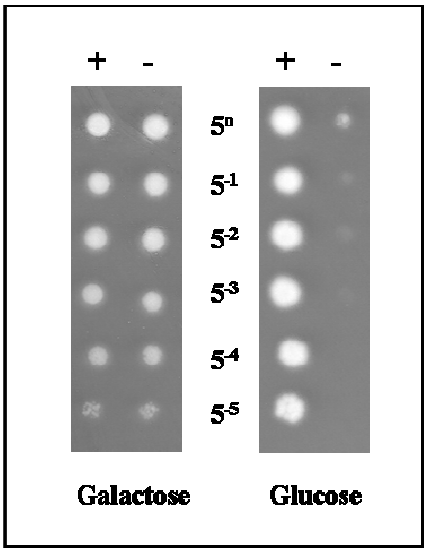

Figure 3.16: Complementation of PGY10 growth by exogenously-supplied eIF5A. Serial dilutions of strain PGY10 transformed with either pYES2 (-) or with pPG10 (+) plated onto SMM containing galactose (left) or glucose (right). A non-lethal phenotype of PGY10 is observed on galactose while a lethal phenotype is observed on glucose (-) which is reversed upon the addition of plasmid borne eIF5A (+) from the pPG10 plasmid.

3.3.8 Assay for biological function of His-eIF5A and eIF5A-His

Next, yeast strain PGY10 was used for complementation assays to determine whether an amino or carboxyl terminal 6 x His tag affected the biological function of eIF5A. Plasmids pPG10 (expressing wild-type *TIF51A* under the control of its endogenous promoter), pPG20 (His-*TIF51A* preceded by the endogenous promoter), pPG10-His (*TIF51A*-His preceded by the endogenous promoter) and pYES2 (no *TIF51A*) were transformed into PGY10 cells. Following growth in galactose, the transformants were diluted and plated onto medium containing either glucose or galactose. Cells expressing the wild type *TIF51A* were able to grow on glucose medium while those containing the vector, pYES2 were not viable (Figure 5.3). Cells expressing His-eIF5A or eIF5A-His were equally able to grow on glucose medium, indicating that the presence of the 6 x His tag on either terminus of eIF5A was not interfering with the function of the protein. Thus any biochemical data derived from the following studies using His-eIF5A or eIF5A-His will be derived from functional protein.

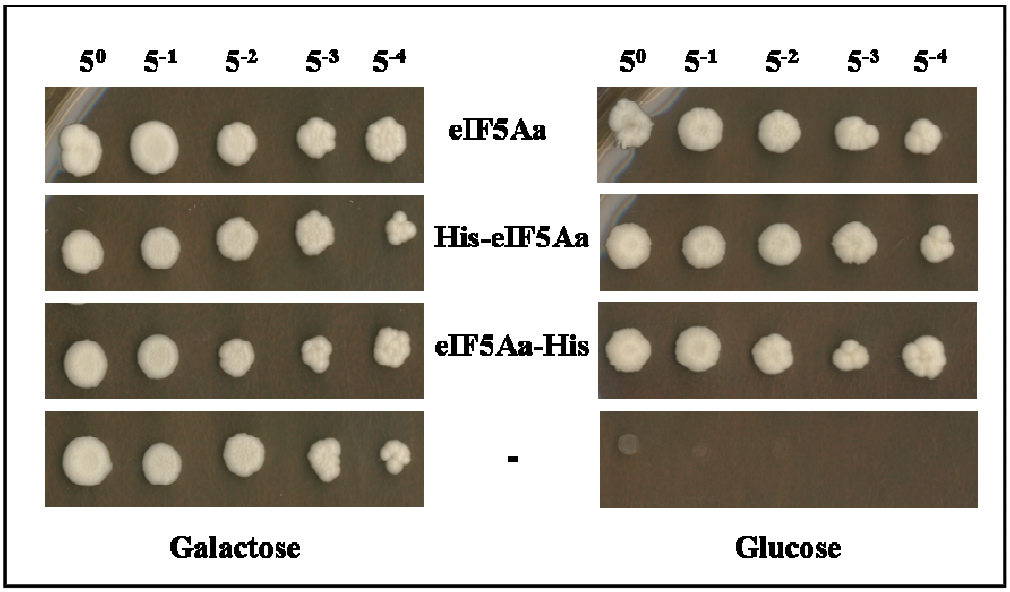

Figure 3.17: Functional complementation assays to determine the biological activity of His-eIF5A. Five-fold serial dilutions of PGY10 cells transformed with either pPG10 (eIF5A), pPG20 (His-eIF5A), pPG10-His (eIF5A-His) or with pYES2 (-) and plated on medium containing either galactose (left) or glucose (right) as the sole carbon source.

3.4 Conclusions

The first of the objectives for this chapter was to raise eIF5A-specific polyclonal antibodies which could be used for detecting eIF5A and eIF5Ab. Following pre-absorption to remove non-specific antibodies, the substantially diluted antiserum was able to detect as little as 7.5ng of purified eIF5A-His, which indicates that the antiserum would be useful in detecting low quantities of eIF5A and eIF5Ab. The second objective was to develop a yeast experimental system that would enable the functional and biochemical characterisation of eIF5A. This objective was partially accomplished by constructing a yeast strain, PGY10 through the successive disruption of *TIF51A* and *TIF51B* and insertion of P_{GAL1}*TIF51A* onto the chromosome, such that cells grown in medium containing galactose as the carbon source would remain viable. However, a lethal phenotype was observed for PGY10 cells grown in medium containing glucose which could be rescued by exogenously-supplied eIF5A. This experimental system was used in subsequent experiments to explore functional and biochemical characterisation of eIF5A.

Although it might have been easier and probably a more practical genetic approach to have used a haploid yeast strain for the construction of a *TIF51A*/*TIF51B*-knockout with a phenotype in glucose, the diploid strain PGY10 does potentially offer advantages in that the starting INVScI strain was originally designed as a fast-growing expression strain to be used

in conjunction with the pYES2 plasmid system (Invitrogen). This allows for the expression of wild-type and mutant proteins from pYES2-derived plasmids (to be discussed in Chapter 4). And lastly, although it proved to be an inefficient system to develop, with an integrative transformation frequency as low as 0.2 %, it was still possible to construct a homozygous diploid yeast strain with a lethal disruption in both copies of the *TIF51A* and *TIF51B* genes that displays a lethal phenotype in glucose.

Chapter 4: Biochemical characterisation of recombinant eIF5A

Chapter 4: Biochemical characterisation of recombinant eIF5A

4.1 Introduction

The main aim of the experiments described in this chapter was to characterise recombinant eIF5A. Since current information about the structure of eIF5A has been derived from the recombinant protein purified from *E. coli* cells (Kim *et al*., 1998; Peat *et al*., 1998; Yao *et al*., 2003; Sun *et al*., 2005), it was decided to use this experimental system developed to produce His-tagged eIF5A (Chapter 3, Section 3.2.6). Gel filtration, native PAGE and cross-linking studies were then conducted to determine the oligomeric status of the native, purified protein.

4.2 Materials and Methods

4.2.1 Strains, culture conditions and recombinant techniques

As in Section 3.2.1, recombinant plasmids were hosted in *E. coli* DH5α while heterologous expression of eIF5A was carried out in *E. coli* BL21 (DE3) cells. *E. coli* cells were grown in LB medium and competent cells were prepared using the method of Hanahan (1985) (Appendix B). Recombinant plasmid DNA was isolated from *E. coli* DH5α cells either using the methods described in Section 3.2.2. The integrity of all PCR products and recombinant plasmids resulting from the cloning of oligonucleotides or site-directed mutagenesis was routinely determined by DNA sequencing as in Section 3.2.2. The sequences of all primers used in this chapter are listed in Appendix C.

4.2.2 Construction of *E. coli* expression vector pPG8

Primers PG5F and PG6R, introducing flanking *Nde* I and *Bam* HI sites, were used to amplify the *TIF51A* ORF from INVScI genomic DNA (as isolated in Section 3.2.3). The PCR product was ligated into the pGEM T-Easy vector (pPG7) The *TIF51A* gene was then excised from pPG7 by digestion with *Nde* I and *Bam* HI and inserted into the *Nde* I and *Bam* HI sites of expression vector pIVEX2.4b (Roche), which encodes an N-terminal His-tag preceded by an AUG (start) codon followed by a *Nde* I site. The expression vector, pPG8 (Figure 4.1), which contained a copy of *TIF51A* fused to a His-tag at its amino terminal end, was used in the over-expression of His-eIF5A.

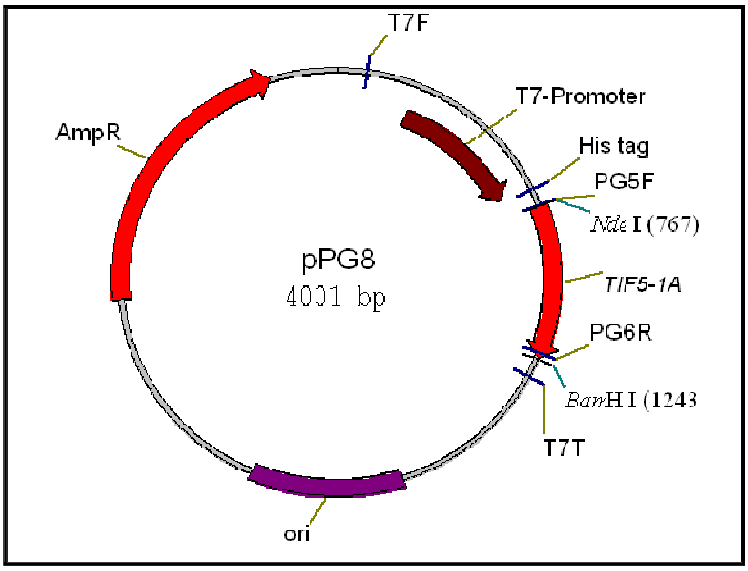

Figure 4.1: *E. coli* His-eIF5A expression vector, pPG8. Schematic representation of the T7-based expression vector pPG8, encoding an N-terminal His-tagged eIF5A. The vector bears the β-lactamase gene encoding ampicillin resistance (AmpR) and an *E. coli* origin of replication (ori). The binding sites for sequencing primers T7F and T7T, flanking the 5' region of the T7 RNA polymerase and the 3' end of the *TIF51A* ORF, respectively, are also indicated.

4.2.3 Expression and purification of His-eIF5A

Expression of His-eIF5A in *E. coli* was performed as described in Section 3.2.5. Cell lysates were prepared by sonication (Section 3.2.5) before being subjected to nickel affinity chromatography using the ÄKTA 900 FPLC series (Amersham Biosciences) system (His-Trap columns). The native purification procedure (according to the Qiagen 5 ml His-Trap recommended protocol, Appendix K) was followed for the purification of His-eIF5A with an increase in the imidazole concentration from 0-500 mM. The eluted fractions (500 µl) were analysed by reading the absorbance at $OD_{280\ nm}$ and then by SDS-PAGE. Fractions containing His-eIF5A protein were pooled and dialysed against a buffer containing 100 mM Tris-HCl pH 7.5, 100 mM NaCl and concentrated using Amicon® Ultr-15 centrifugal filter units (Millipore) to the desired concentration. Finally, protein concentrations were determined using the Bradford's Assay (Bradford, 1976) and Abs_{280nm} readings.

4.2.4 Site directed mutagenesis of His-eIF5A

Primer pair PG36 and PG37 (Appendix C) was used to generate mutant pPG8-C39S using site-directed mutagenesis (QuikChange Site-directed Mutagenesis kit, Stratagene). The bases encoding the Cys 39 residue within the *TIF51A* gene were altered to encode serine (C39S), while also removing a *Hinc* II site. Similarly, primer pair PG34 and PG35 (Appendix C) was

used to generate pPG8-C23S that encodes a serine residue at Cys 23 (C23S) in eIF5A. Primers PG1F and PG6R (Appendix C) were used to determine the DNA sequence of mutated *TIF51A* genes to confirm the presence of the appropriate C39S or C23S mutation. Expression and purification of the mutant His-eIF5A proteins was performed as in Section 4.2.3.

4.2.5 Gel filtration and native PAGE

Gel filtration was performed using a Tricorn 10/30 column (Amersham Biosciences) packed with Superdex 200 pg matrix according to the manufacturer's recommendations. The volume of the packed column was determined to be 27.5 ml with a 14 900 theoretical plate number per metre and a peak symmetry of 0.95 as determined from the manufacturer's recommended acetone test. The column was calibrated using 2 mg/ml each of Myoglobin, Carbonic anhydrase, Ovalbumin and Bovine serum albumin proteins (Sigma). Gel filtration of all protein samples was performed with 100 mM Tris-HCl, pH 7.5, 100 mM NaCl buffer (except for high salt testing that made use of a buffer containing 100 mM Tris-HCl, pH 7.5, 500 mM NaCl).

Either 100 µl or 200 µl loops were used for the injection of protein and eluted protein fractions were analysed by readings at $OD_{280\ nm}$. Native PAGE (Appendix E) analysis involved the electrophoresis of protein samples, resuspended in non-reducing tracking buffer (Appendix E), using a 10 % continuous polyacrylamide gel and resolving at 150 V for a period of 50 minutes, followed by staining with Coomassie stain.

4.2.6 Chemical treatment of His-eIF5A with glutaraldehyde and dithiothreitol (DTT)

Chemical cross-linking of His-eIF5A was performed by adding glutaraldehyde (0-2 % final concentration in 0.5 % increments) (Sigma) to purified protein (2 mg/ml) in a final volume of 30 µl buffer containing 50 mM Tris-HCl, pH 7.5, 50 mM NaCl and 1 mM EDTA. The mixture was incubated at room temperature for 2 minutes before adding 10 µl of 1 M Tris-HCl, pH 8.0, to stop the reaction. Glutaraldehyde-treated protein was then resolved by SDS-PAGE and stained with Coomassie stain. Reducing conditions were obtained by adding DTT (Sigma) to a final concentration of 1 mM to approximately 2 mg/ml purified His-eIF5A (in a final volume of 100 µl) for a period of 15 minutes at room temperature, and then analysed by gel filtration and native PAGE.

4.3 Results and Discussion

4.3.1 Purification of native His-eIF5A

In reports in the literature, structural characterisation of eIF5A has been largely performed on recombinant protein with an engineered fusion tag (predominantly His-tags) on the N-terminus (Kim *et al*., 1998; Peat *et al*., 1998; Yao *et al*., 2003; Sun *et al*., 2005). Accordingly the vector, pPG8, was constructed to facilitate the expression of His-eIF5A (as opposed to eIF5A-His in the previous chapter). His-eIF5A was over-expressed in *E. coli* BL21 (DE3) cells and the protein was then purified from cell lysates using a 5 ml His-Trap column. The cell-free lysates (CL), the flow-through (FT) following binding to the column as well as the eluting fractions (E) absorbing in the 280 nm range were then analysed by SDS-PAGE. His-eIF5A protein present in the CL fraction (Figure 4.2 lane 1), was not observed in the FT fraction (Figure 4.2 lane 2) following the binding step, indicating that complete binding to the column of the His-tagged proteins had occurred. Eluted fractions, E40-E65 (Figure 4.2 lanes 4-9), corresponding to a 250-300 mM imidazole concentration, contained relatively pure quantities of His-eIF5A, with an apparent molecular weight of about 19 kDa. Co-eluting with His-eIF5A were small amounts of a protein approximately 43 kDa in size (Figure 4.2 lanes 7-9). The elution fractions containing His-eIF5A were pooled, resulting in a total of 20 ml of purified protein that was dialysed against 100 mM Tris-HCl (pH 7.5), 50 mM NaCl and concentrated to 22 mg/ml (Figure 4.2 lane 10). The co-eluted 43 kDa protein represented a minor portion of the total yield of His-eIF5A.

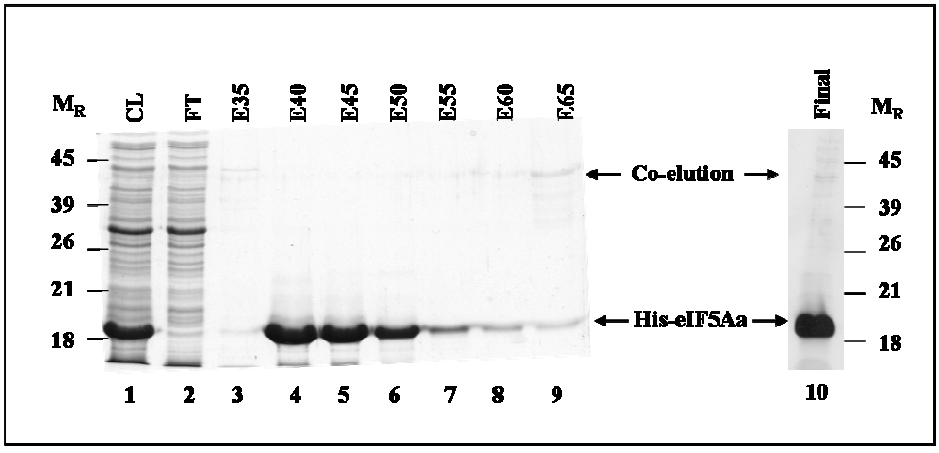

Figure 4.2: Purification of His-eIF5A from *E. coli*. PAGE analysis of the fractions collected during the purification of His-eIF5A from *E. coli*. Lane 1: The cell-free lysate (CL) obtained by the over-expression of His-eIF5A; Lane 2: The flow-through (FT) obtained following binding of the tagged protein to the His-Trap column; Lanes 3-9: The elution fractions collected with increasing levels of imidazole; and Lane 10: Purified His-eIF5A following dialysis and concentration. The sizes of the molecular weight markers are indicated in kDa and the position of His-eIF5A is shown.

4.3.2 Oligomeric analysis of His-eIF5A

Gel filtration (size-exclusion chromatography) and native (non-reducing) PAGE were used to determine the oligomeric state of the purified His-eIF5A. An integrated elution volume of 16.9 ml, corresponding to a protein of approximately 37 kDa in size, was obtained following gel filtration (Figure 4.3). Since the apparent molecular weight of the reduced form of His-eIF5A was determined to be about 19 kDa, (Figure 4.2), the gel filtration data suggested that the protein exists as a dimer under non-reducing conditions. Native PAGE analysis showed that His-eIF5A resolved as two species; the protein at higher mobility was attributed to the dimeric form of eIF5A, while the lower order species probably represents the monomeric form (Figure 4.3 inset).

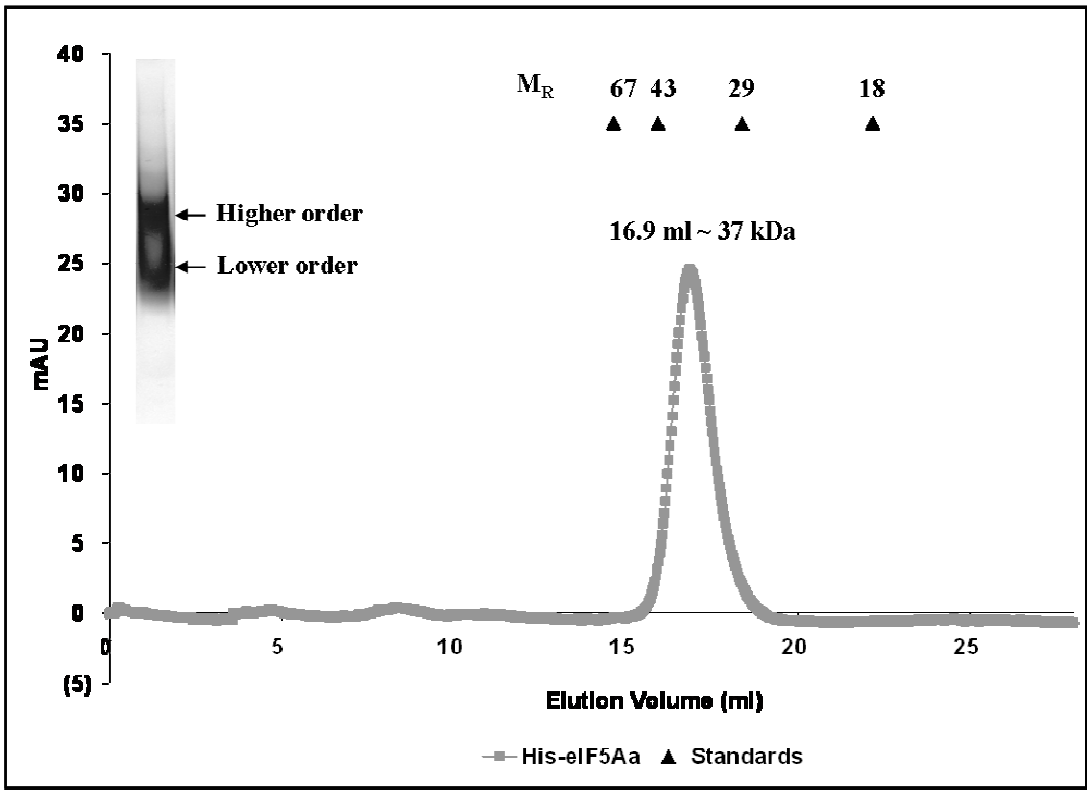

Figure 4.3: Oligomeric state of His-eIF5A as determined by size exclusion chromatography and native PAGE. Chromatogram obtained following gel filtration or native PAGE analysis (inset) of purified His-eIF5A. The sizes of the protein standards are represented by triangles, corresponding to Myoglobin (18 kDa), Carbonic anhydrase (29 kDa), Ovalbumin (43 kDa) and Bovine serum albumin (67 kDa).

4.3.3 Capturing the oligomers of eIF5A

To confirm that the higher order species observed in the previous experiment could be a dimer, chemical cross-linking of His-eIF5A with glutaraldehyde, which is commonly used as a small inter- and intra-molecular cross-linker, was employed. The process of this cross-linking is induced by an initial reaction of glutaraldehyde with amine groups within close molecular contacts (Cheung & Nimni, 1982; van der Spuy *et al*., 2001). Varying concentrations of glutaraldehyde (from 0 – 2 % in increments of 0.5 %) were used to capture the oligomeric states of His-eIF5A. SDS-PAGE analysis of the cross-linked protein samples at each of the glutaraldehyde concentrations indicated that His-eIF5A has the ability to exist in a monomeric (approximately 20 kDa), dimeric (approximately 40 kDa) or in a higher order state (approximately 55 kDa) (Figure 4.4). This result provided evidence that the species migrating at a higher mobility following native PAGE analysis (Figure 4.3 inset), and the protein eluting at approximately 37 kDa eluted by gel filtration analysis was a dimeric form of His-eIF5A.

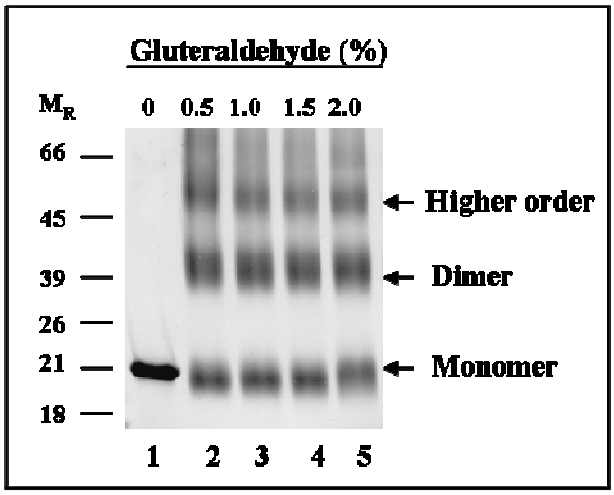

Figure 4.4: Cross-linking of His-eIF5A with glutaraldehyde. Purified His-eIF5A from *E. coli* was subjected to varying concentrations of glutaraldehyde (from 0 to 2 %) and cross-linked products were analysed by SDS-PAGE. The relative positions of the monomeric, dimeric and higher order states of the protein are indicated on the right, while the sizes of the molecular weight marker are shown on the left.

4.3.4 Determination of His-eIF5A ionic interactions

To determine whether the various oligomeric states of the His-eIF5A protein are as a result of ionic interactions, high salt concentrations (500 mM NaCl) were used during gel filtration of His-eIF5A. The reasoning was that if ionic interactions were responsible for oligomerisation, then these interactions would be disrupted by an elution buffer with high ionic strength. No visible disruption of the His-eIF5A dimeric species was observed following gel filtration of

His-eIF5A under high salt conditions (Figure 4.5), with the original integrated elution volume of 16.9 ml being retained. This result suggested that stronger molecular force was at play in holding the dimeric and potential higher conformations of His-eIF5A together.

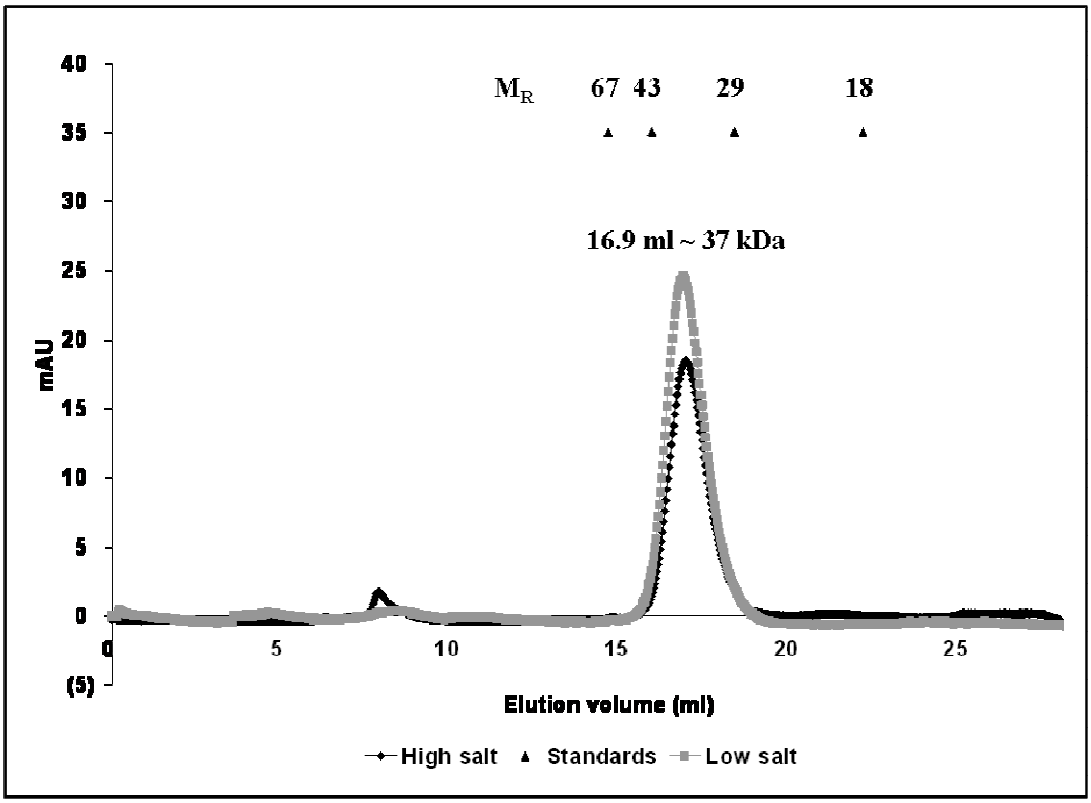

Figure 4.5: Effect of ionic strength on the dimeric state of His-eIF5A. Chromatogram obtained from the gel filtration of His-eIF5A using a high salt buffer or a low salt buffer. Calibration of the column was achieved using Myoglobin (18 kDa), Carbonic anhydrase (29 kDa), Ovalbumin (43 kDa) and Bovine serum albumin (67 kDa) (indicated by triangles).

4.3.5 Independence of dimerisation on protein concentration

To address the possibility that the dimeric state of His-eIF5A was the result of concentration-dependent aggregation, high (greater than 2 mg/ml) and low (less that 500 μg/ml) concentrations of His-eIF5A were analysed by gel filtration. The results revealed that dilution of His-eIF5A did not affect the presence of the dimeric state (Figure 4.6) with an integrated elution volume of 16.9 ml, corresponding to a protein of about 37 kDa in size. The possibility of aggregation in a concentration-dependent manner was thus excluded as no apparent shift from the dimeric state was observed. Also observed was a small protein peak in the low salt sample eluting near the void volume of 27 ml (approximately smaller than 14 kDa in size) which was attributed to a common His-eIF5A proteolytic product present in the protein

sample prior to gel filtration. This proteolytic product has also observed by Schwelberger *et al*. (1993), Kang *et al*. (1993) and Valentini *et al*. (2002).

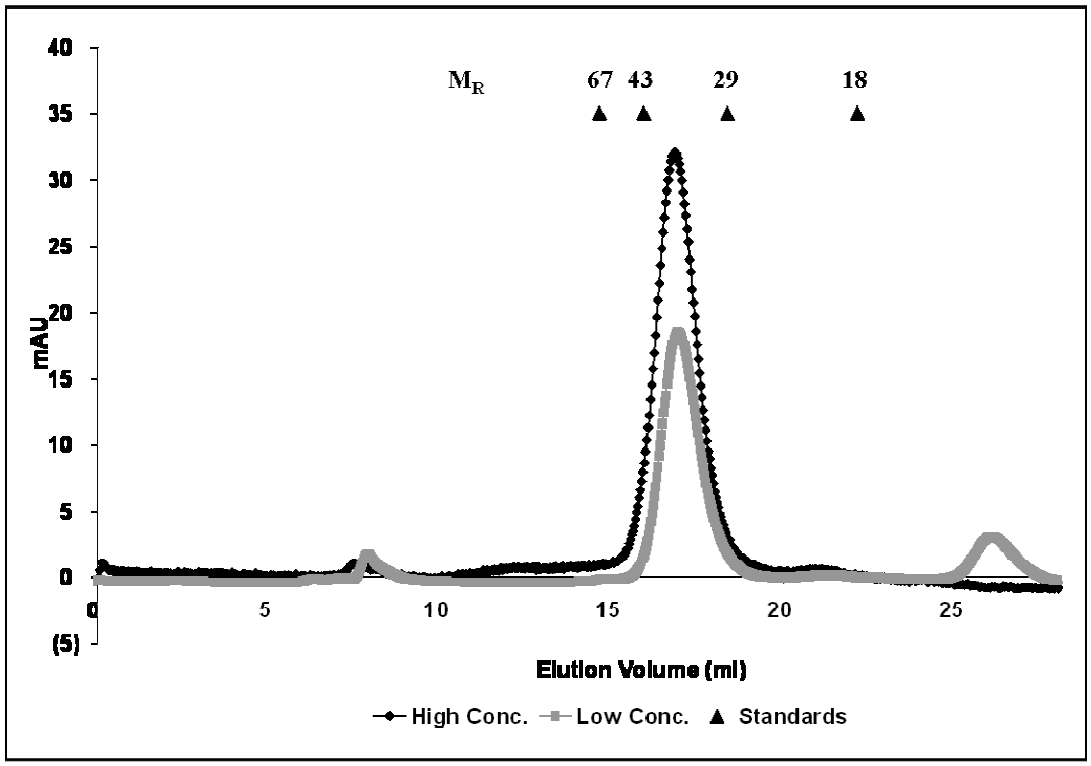

Figure 4.6: The concentration-independence of the dimeric state of His-eIF5A. Gel filtration profiles obtained for high and low concentrations of His-eIF5A protein. The triangles indicate the relative sizes of standard proteins Myoglobin (18 kDa), Carbonic anhydrase (29 kDa), Ovalbumin (43 kDa) and Bovine serum albumin (67 kDa).

4.3.6 Exposure of His-eIF5A to reducing agents and the role of Cys 39

To investigate whether disulphide bridging might be responsible for the dimeric state of His-eIF5A, protein samples were treated with the strong, specific reducing agent, DTT and subjected to gel filtration and native PAGE analysis. Interestingly, the dimeric state of the protein was disrupted by the addition of DTT, shifting the integrated elution volume from the previously-observed 16.9 ml to 23.07 ml, equivalent to the monomeric size of approximately 18 kDa (Figure 4.7). Native PAGE analysis showed the presence of only the monomeric form following the addition of DTT as opposed to dimeric and monomeric forms in untreated protein samples (Figure 4.7 inset). A similar shift from the dimeric state was observed following native PAGE analysis of His-eIF5A treated with 1 mM β-mercaptoethanol (data not shown). These results suggested that cysteine, methionine, serine and threonine residues in His-eIF5A might be important for the structural integrity of the dimer, either by forming intra- or inter-subunit disulphide bonds.

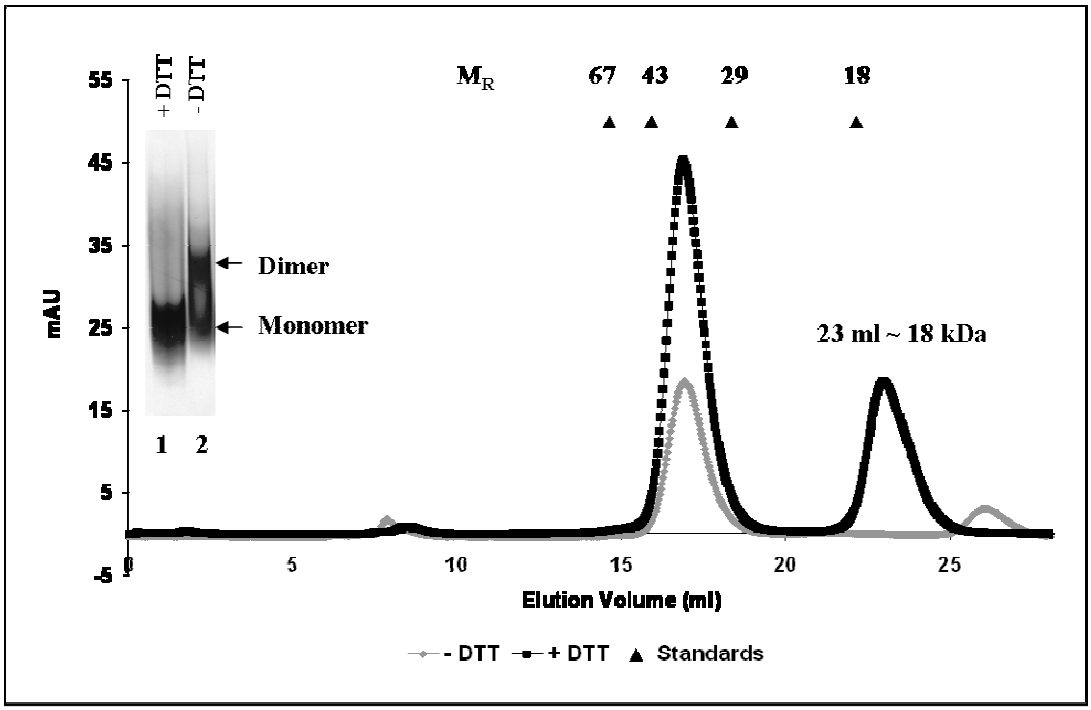

Figure 4.7: Effect of reducing agents on the dimeric state of eIF5A. Gel filtrations profiles of His-eIF5A in the presence and absence of DTT-treatment. Inset: Native PAGE analysis of His-eIF5A in the presence (lane 1) and absence (lane 2) of DTT. Proteins Myoglobin (18 kDa), Carbonic anhydrase (29 kDa), Ovalbumin (43 kDa) and Bovine serum albumin (67 kDa) were used to calibrate the column (represented by triangles).

Since the yeast *TIF51A* gene encodes only two cysteine residues (present at positions Cys 23 and Cys 39 near the N-terminus of the eIF5A protein), it was decided to investigate whether these residues were important for dimerisation of eIF5A, perhaps by the formation of disulphide bridges. With this in mind, the cysteine 39 residue was chosen as the most likely candidate because it is highly conserved among the eukaryotic and archaeal homologues of eIF5A. To test this hypothesis, plasmid pPG8-C39S, in which Cys 39 has been substituted with a serine residue, was used for the expression of mutant protein His-eIF5A-C39S. The mutant protein showed a similar Ni-affinity purification profile to that obtained for native His-eIF5A (in Section 4.3.1, Figure 4.2) and was dialysed and concentrated to 2 mg/ml.

Analysis by gel filtration revealed that the His-eIF5A-C39S protein (C39S) eluted predominantly as the monomeric form (Figure 4.8), which contrasted to the predominant dimeric form observed for His-eIF5A (WT). This was supported by the data obtained from native PAGE analysis (Figure 4.8 inset). The results showed that the Cys 39 residue is critical for stabilising the eIF5A dimer formed by protein purified from *E. coli*. The appearance of minor, indistinct higher molecular weight protein peaks (greater than 67 kDa in size)

indicated that the destabilisation of His-eIF5A may also have led to some aggregation. The expression of His-eIF5A-C23S, with Cys 23 substituted by a serine residue, was too poor to collect enough protein to continue with a similar investigation.

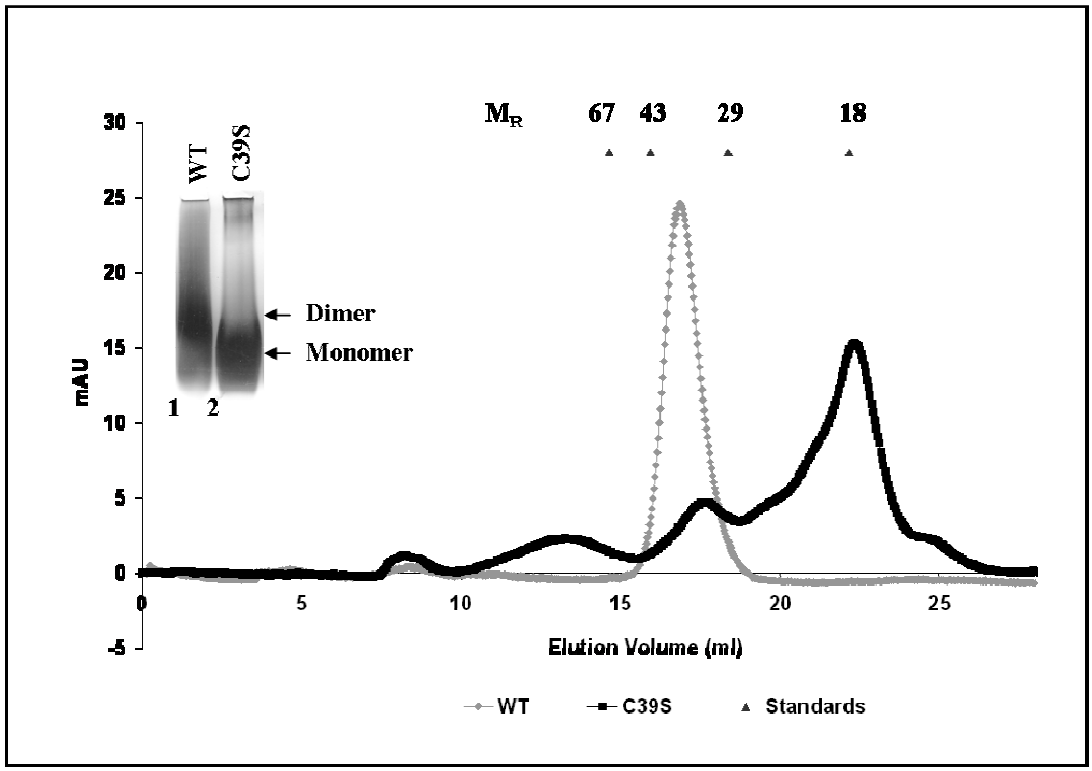

Figure 4.8: Effect of the C39S mutation on the dimeric state of His-eIF5A. Gel filtration of His-eIF5A (WT) and His-eIF5A-C39S (C39S) mutant proteins produced in *E. coli*. Inset: Migration of His-eIF5A (WT, lane 1) and His-eIF5A-C39S (C39S, lane 2) as resolved by native PAGE. The positions of the calibration proteins, Myoglobin (18 kDa), Carbonic anhydrase (29 kDa), Ovalbumin (43 kDa) and Bovine serum albumin (67 kDa) are indicated by triangles.

4.4 Conclusions

Although not shown, the same experiments were conducted on eIF5A with an engineered C-terminal His-tag to eliminate the possibility of involvement in the N-terminal His tag in dimerisation of eIF5A. In all cases, the results of these experiments with eIF5A-His were consistent with those obtained for eIF5A with the N-terminal His tag. This indicated that the His-tag, whether engineered upstream or downstream of the *TIF51A* ORF, was unlikely to be interfering with the folding of the protein during these analyses.

The biochemical analyses of heterologously-expressed eIF5A described in this chapter reveals that native eIF5A exists predominantly as a dimer in solution. This is in agreement with the finding by Chung *et al*., (1991) who proposed that mammalian eIF5A can exist in a monomeric, dimeric and trimeric form. The dimeric form or His-eIF5A was retained under high salt conditions, indicating that stabilisation of the dimer was not due to ionic interactions. The observation that addition of DTT and that mutant His-eIF5A-C39S exists as a monomer indicates that eIF5A probably undergoes a redox-controlled structural transition, involving Cys 39. The crystallisation procedures of heterologously-produced eIF5A and aIF5A involved the addition of a reducing agent, and this explains why the crystal structures of eIF5A and its homologues were solved in the monomeric form (Kim *et al*., 1998; Peat *et al*., 1998; Yao *et al*., 2003; Sun *et al*., 2005). The possibility that the dimer is stabilised by intra- or inter-subunit disulphide bridging was reinforced by the observation that His-eIF5A, under reducing conditions, was monomerised. Thus dimerisation of eIF5A expressed in *E. coli* is dependent on the oxidative state and the presence of the highly conserved cysteine residue. Whether or not this highly conserved residue is also important in the function of eIF5A in its native host, yeast, is one of the topics covered in the following chapters.

Although *E. coli* is the most widely used heterologous expression host, it has limitations in that no post-translational modification can take place. The biological function of eIF5A requires the presence of hypusine (Park *et al*., 1989) raising the question of whether or not hypusine plays a role in determining the oligomeric state of eIF5A. The next chapter describes the results of a similar investigation into the oligomeric state of hypusinated eIF5A produced via a homologous (yeast) expression system.

Chapter 5: Functional and biochemical analysis of native eIF5A

Chapter 5: Functional and biochemical analysis of native eIF5A

5.1 Introduction

All the currently available structural information on eIF5A and its archaeal homologues has been derived from recombinant protein produced in *E. coli*. Since eIF5A produced in *E. coli* is not hypusinated, these structures cannot account for how hypusine relates to the structure of the protein. While HEX-1 is structurally related to eIF5A, it is not hypusinated, so the data derived from crystallographic studies on this protein provide no further clues as to the structural implications of the presence of hypusine.

The *in silico* study described in Chapter 2 resulted in an homology model of yeast eIF5A based upon available data derived from the crystal structures of the *L. mexicana* and archaeal homologues. Further modeling informed by the structure of the HEX-1 analogue predicted that eIF5A could exist in solution as one of three potential dimers (Section 2.3.6). To test this hypothesis, His-tagged eIF5A was purified from *E. coli* and the oligomeric state of the native protein was characterised by gel filtration and native PAGE. The results confirmed the presence of a dimer which was disrupted under reducing conditions, leading to the identification of Cys 39 as being important for the formation of the dimeric species (Section 4.3.6).

The aim of the research described in this chapter was to determine whether hypusinated eIF5A also exists as a dimer and if so, whether as in *E. coli*, dimerisation was dependent upon Cys 39. The results revealed that hypusinated eIF5A (expressed in yeast) also exists as a dimer in solution but that dimerisation is dependent upon hypusination and RNA binding and not Cys 39.

5.2 Materials and Methods

5.2.1 Strains, culture conditions and recombinant DNA techniques

Recombinant plasmids were hosted in *E. coli* DH5α cells (as in Section 3.2.1) while heterologous expression of eIF5A was carried out in *E. coli* BL21 (DE3) cells. *E. coli* cells were grown in LB medium and competent cells were prepared using the method of Hanahan (1985) (Appendix B). The methods described in Section 3.2.2 were used to isolate recombinant plasmid DNA from *E. coli* DH5α cells and the integrity of all PCR products and

recombinant plasmids resulting from the cloning of oligonucleotides or site-directed mutagenesis was routinely determined by DNA sequencing.

5.2.2 Construction of yeast expression vector

The hybrid alcohol dehydrogenase 2-glyceraldehyde-3-phosphate dehydrogenase (*ADH2/GAPDH*) promoter was amplified from plasmid pMT9 (Tomasicchio *et al*., 2007) using primers PG32F and PG33R (Appendix C) which introduce flanking *Age* I and *Pvu* II sites at the 5' and 3' ends of the promoter, respectively. The $P_{ADH2/GAPDH}$ fragment was then used to replace the *GAL1* promoter in pPG20, using the same enzymes. The resulting plasmid, pPG39 (Figure 5.1), was used for the over-expression of His-eIF5A in yeast cells. Primers AI2F and AI1R were used to confirm the correct sequence of the *ADH2/GAPDH* promoter and the *TIF51A* ORF in pPG39.

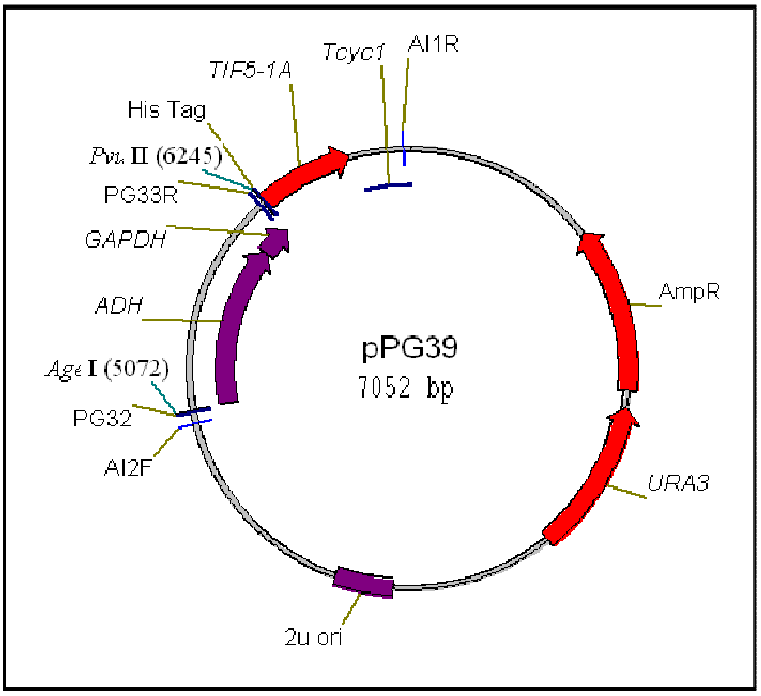

Figure 5.1: The vector, pPG39, used for over-expression of His-eIF5A in yeast. The 2μ-based multicopy expression vector contains a T_{CYC1} transcriptional terminator, a β-lactamase gene encoding ampicillin resistance and a uracil auxotrophic marker. The highly efficient dual-promoter system, $P_{ADH2/GAPDH}$ is fused to the 5' coding region of His-*TIF51A* (from pPG20). Primers AI2F and AI1R were used to were used to confirm the correct sequence of the *ADH2/GAPDH* promoter and the *TIF51A* ORF.

5.2.3 Site-directed mutagenesis of His-eIF5A

The procedure outlined in Chapter 4 (Section 4.2.4) was used to generate mutant eIF5A plasmids by site-directed mutagenesis. Tabulated below (Table 5.1) are the primer pairs used to introduce base substitutions into the *TIF51A* coding sequence to produce variants of pPG20 (used in complementation assays), pPG39 (used for native eIF5A over-expression) and pPG8 (used for heterologous expression in *E. coli*, from Section 4.2.2).

Table 5.1: Primers used to introduce base substitutions in *TIF51A* ORF. Primer sequences are listed in Appendix C.

Primers (sense & antisense respectively)	Substitution	Restriction site introduced	Name of plasmid variant produced
PG10a & PG10b	Lysine 51 to Arginine (K51R)	None	pPG20-K51R pPG39-K51R pPG8-K51R
PG36 & PG37	Cysteine 39 to Serine (C39S)	*Hinc* II	pPG20-C39S pPG39-C39S
PG34 & PG35	Cysteine 23 to Serine (C23S)	None	pPG20-C23S pPG39-C23S

5.2.4 His-eIF5A expression in yeast

INVScI cells were transformed with the relevant plasmids and plated onto selective agar plates (SMM supplemented with leucine, tryptophan and histidine, Appendix A) containing 2 % glucose. Following patching onto fresh selective plates,, cells were inoculated into SMM broth (supplemented with leucine, tryptophan and histidine) and 0.01 % glucose at an $OD_{600\ nm}$ of 0.05 and incubated with shaking at 28 ^{o}C for 36 hours. The depletion of glucose results in the activation of $P_{ADH2/GAPDH}$ (Cousens *et al*., 1987), resulting in the expression of His-eIF5A or the His-eIF5A mutants. Cells were harvested at 500xg for 10 minutes and washed in sterile distilled water before being resuspended in lysis buffer (Section 3.2.6). Cells were then lysed using 0.1 g of glass beads per 2 $OD_{600\ nm}$ units using a bead beater (bursts of 30 seconds on ice) for a total of 5 minutes. Lysed cells were centrifuged at 500xg for 10 minutes and the supernatants were used for nickel affinity purification of His-eIF5A.

5.2.5 Analysis of His-eIF5A and His-eIF5A mutants

Expression and purification of His-eIF5A and His-eIF5A mutants in *E. coli*, was performed as described in Section 4.2.3. Homologously-expressed His-eIF5A and mutant His-eIF5A were purified using the native purification procedure outlined in Section 4.2.3. The same methods from Sections 4.2.5 were used for analysis of proteins by gel filtration and native PAGE.

Proteins were subjected to glutaraldehyde and DTT treatment of protein as in Section 4.2.6. RNase (1 μM final concentration) (Merck) was added to 100 μl of purified proteins (2 mg/ml) and digested at 37 ^{o}C for a period of either 10 or 20 minutes, before analyzing by gel filtration and native PAGE. Proteins were re-purified following RNase digestion as above, using Qiagen Ni-NTA spin columns (as in Section 3.2.6). The protein extraction protocol and Western analysis of His-eIF5A was performed as in Section 3.2.7.

5.3 Results and Discussion

5.3.1 Purification of native His-eIF5A from yeast

To produce sufficient quantities of purified hypusinated His-eIF5A to allow for further biochemical analyses, His-eIF5A was over-expressed in INVScI cells transformed with pPG39 in which the *GAL1* promoter has been replaced with the hybrid *ADH2-GAPDH* promoter which supports several orders of magnitude higher levels of expression than P_{GAL1}. The His-eIF5A was then purified from the cell lysates using a 5 ml His-Trap column (Amersham Biosciences) under native purification conditions. The cell-free lysates (CL), the flow-through (FT) following binding to the column as well as the eluting fractions (E) absorbing in the 280 nm range were analysed by SDS-PAGE. His-eIF5A protein visible in the CL fraction (Figure 5.2 lane 1) was not observed in the FT fraction (Figure 5.2 lane 2) following the binding step, indicating that complete binding to the column of the His-tagged proteins had occurred. Eluted fractions E40-E60 (Figure 5.2 lanes 8-12), corresponding to a 200-250 mM imidazole concentration, all contained relatively pure quantities of His-eIF5A obtained from yeast (resulting in a total of 20 ml of purified protein that was dialysed against 100 mM Tris-HCl (pH 7.5), 50 mM NaCl and concentrated to 8 mg/ml (Figure 5.2 lane 13).

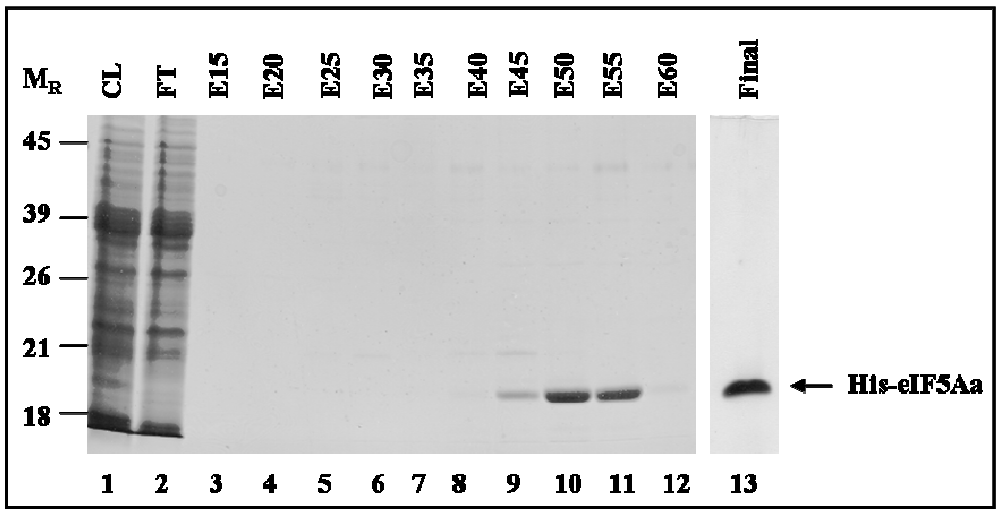

Figure 5.2: Ni Affinity purification of His-eIF5A from yeast. PAGE analysis of the fractions collected during the purification of His-eIF5A from yeast. Over-expression of His-eIF5A is observed in lane 1 containing the cell-free lysates (CL), while binding of the tagged protein to the His-Trap column is represented by the absence of the His-eIF5A protein in the flow-through fraction (FL) in lane 2. Purified protein eluted from fractions E45-E60 (lanes 9-12) was pooled, dialysed and concentrated. Lane 13 contains the final purified His-eIF5A. The sizes of the molecular weight marker are indicated on the left in kDa and the position of His-eIF5A on the right.

5.3.2 Oligomeric analysis of hypusinated His-eIF5A

To confirm that functional (hypusinated) His-eIF5A existed in the same oligomeric state as the protein produced in *E. coli* (non-hypusinated) in Chapter 4 (Section 4.3.2), similar biochemical analyses of His-eIF5A obtained from yeast were conducted. Gel filtration of His-eIF5A from yeast resulted in an integrated elution volume of 16.85 ml, which corresponded to a protein of approximately 40 kDa in size (Figure 5.3). This suggested that His-eIF5A from yeast may exist as a dimer. Native PAGE results (Figure 5.3 inset) showed that the protein migrated as a higher order and lower order species. The protein at higher mobility was assumed to be the dimeric form of eIF5A, while the lower order species may represent the monomeric form.

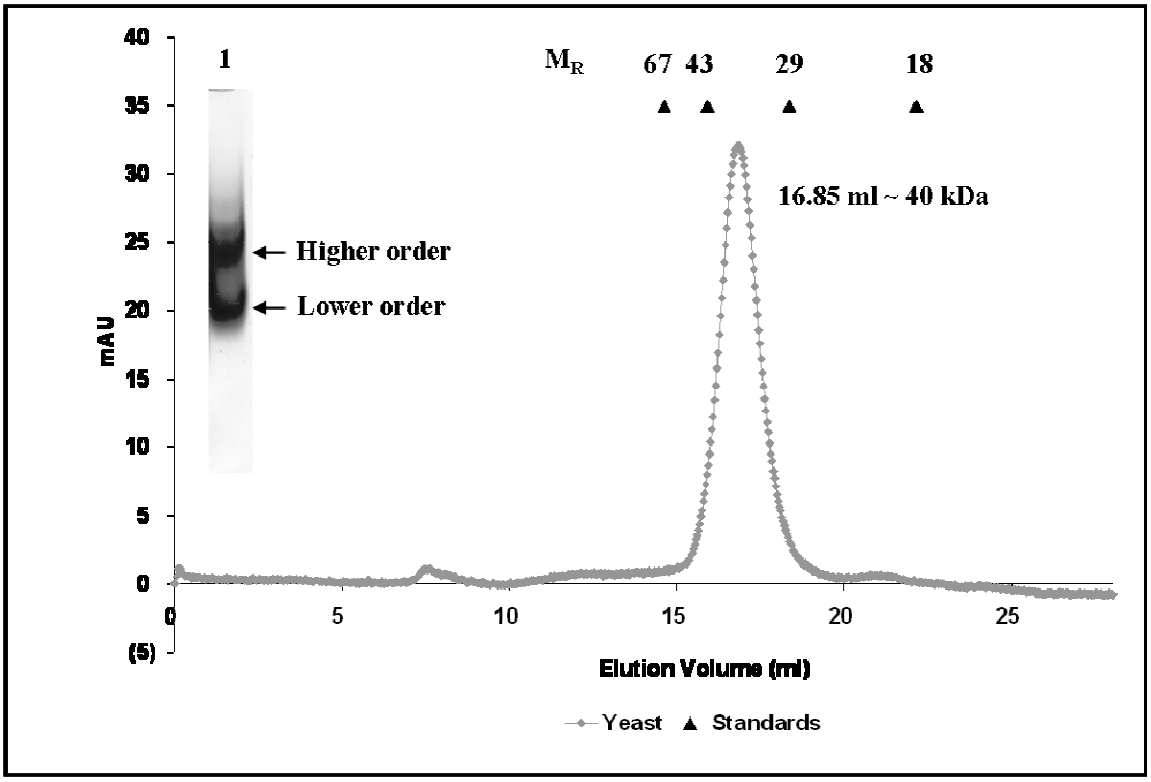

Figure 5.3: Oligomeric state of native, hypusinated His-eIF5A. Chromatogram obtained following gel filtration and native PAGE (inset) of purified His-eIF5A obtained from yeast. The sizes of the protein standards are represented by triangles, corresponding to Myoglobin (18 kDa), Carbonic anhydrase (29 kDa), Ovalbumin (43 kDa) and Bovine serum albumin (67 kDa).

To confirm that the higher order species, migrating at approximately 40 kDa could be a dimer, chemical cross-linking using glutaraldehyde was performed to capture the various oligomeric states of His-eIF5A from yeast. SDS-PAGE analysis of the cross-linked protein (Figure 5.4) indicated that hypusinated His-eIF5A has the ability to exist in a monomeric (approximately 20 kDa), dimeric (approximately 40 kDa) or in a higher order state (approximately 58 kDa).

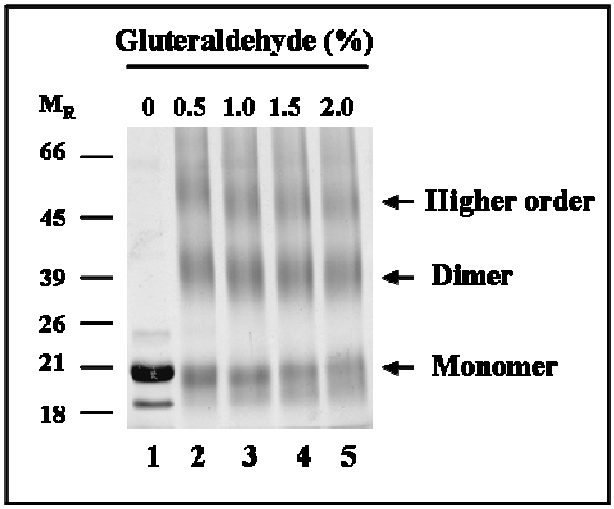

Figure 5.4: Cross-linking of His-eIF5A using varying concentrations of glutaraldehyde. Purified His-eIF5A from yeast was subjected to varying concentrations of glutaraldehyde (from 0 to 2 %) and cross-linked products were analysed by SDS-PAGE. The relative positions of the monomeric, dimeric and higher order states of the protein are indicated on the right, while the sizes of the molecular weight marker are shown on the left.

Gel filtration of His-eIF5A under the high salt (500 mM NaCl) conditions showed no visible disruption of the dimeric (Figure 5.5), and the original integrated elution volume of 16.85 ml was retained (corresponding to a protein of about 40 kDa in size). This result suggested that dimerisation of hypusinated His-eIF5A, similar to unhypusinated His-eIF5A purified from *E. coli* (Section 4.3.4), was not dependent on ionic interactions.

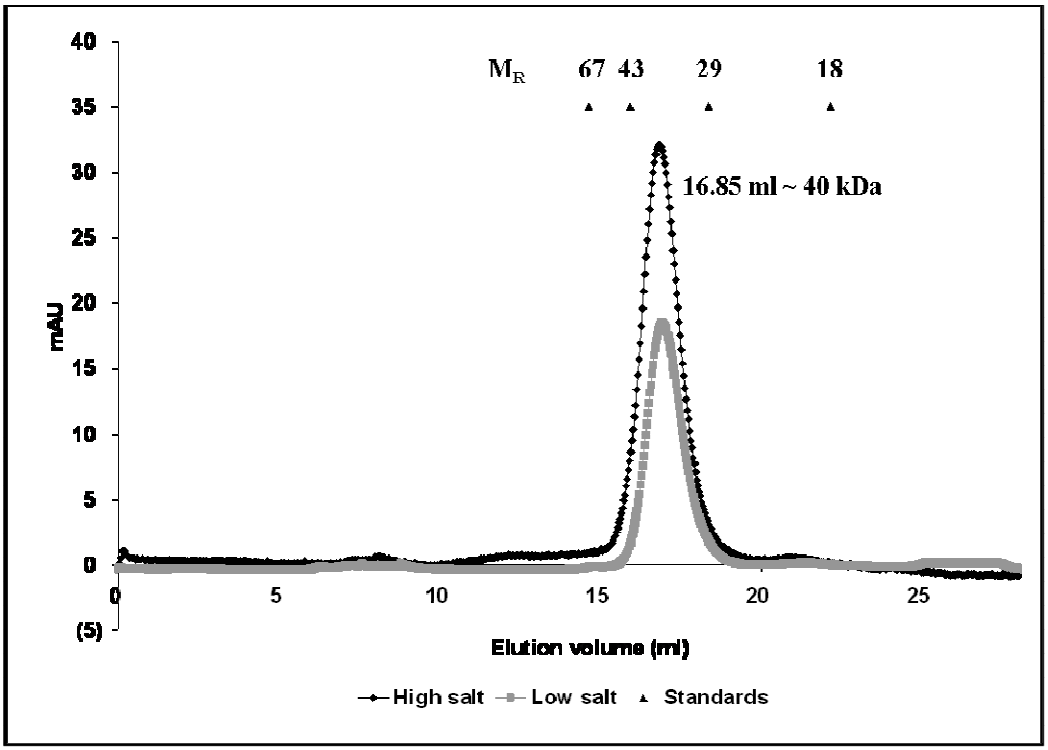

Figure 5.5: Effect of ionic strength on the oligomeric state of yeast His-eIF5A. Chromatograms obtained from the gel filtration of His-eIF5A purified from yeast using a high salt (500 mM NaCl) or low salt (100 mM NaCl) buffer. The position of standard proteins Myoglobin (18 kDa), Carbonic anhydrase (29 kDa), Ovalbumin (43 kDa) and Bovine serum albumin (67 kDa) are indicated by triangles.

Finally, to confirm that dimerisation of hypusinated eIF5A was independent of the protein concentration, high (greater than 2 mg/ml) and low (less than 500 μg/ml) concentrations of the protein were separated by gel filtration. The resulting chromatogram revealed that dilution of hypusinated His-eIF5A had no effect on its dimeric state (Figure 5.6), with an integrated elution volume of 16.85 ml corresponding to a protein of about 40 kDa in size. The possibility of aggregation in a concentration-dependent manner was therefore excluded as no apparent shift from the dimeric state was observed.

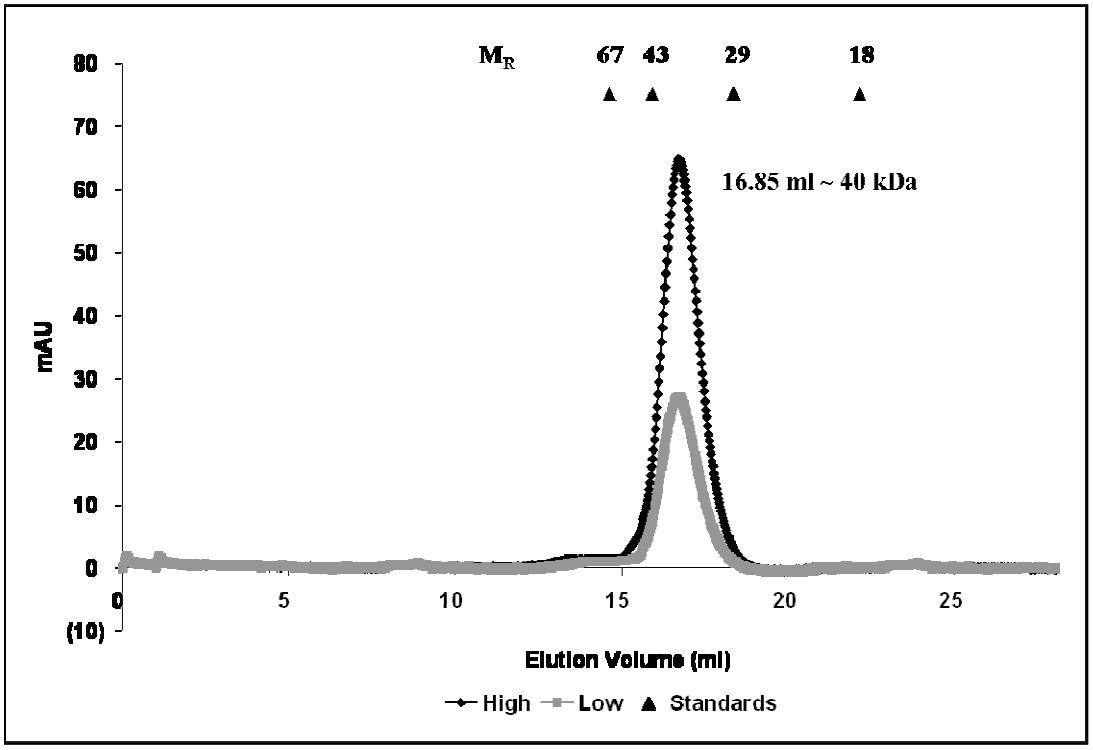

Figure 5.6: The concentration-independence on the oligomeric state of yeast His-eIF5A. Gel filtration profiles obtained for varying concentrations of His-eIF5A produced in yeast. The triangles indicate the relative sizes of standard proteins Myoglobin (18 kDa), Carbonic anhydrase (29 kDa), Ovalbumin (43 kDa) and Bovine serum albumin (67 kDa).

5.3.3 Effect of reducing agents on hypusinated His-eIF5A and the role of Cys 39 and Cys 23

To investigate whether disulphide bridging, involving Cys 39 or Cys 23 (the only two cysteine residues in yeast eIF5A) also played a role in the dimerisation of hypusinated His-eIF5A, the protein was treated with DTT (as in Section 4.2.6) and then analysed by gel filtration and native PAGE analysis. The His-eIF5A dimer was disrupted by the addition of DTT (Figure 5.7). The integrated elution volume of 16.85 ml (corresponding to approximately 40 kDa) shifted to 22.5 ml (corresponding to approximately 17 kDa) in the presence of DTT (Figure 5.7). This reduction or destabilisation of the dimer to a monomeric state following DTT treatment was also detected by native PAGE analysis (Figure 5.7 inset). These results suggested that, as in *E. coli*, dimerisation of hypusinated His-eIF5A might be dependent upon the formation of disulphide bridges.

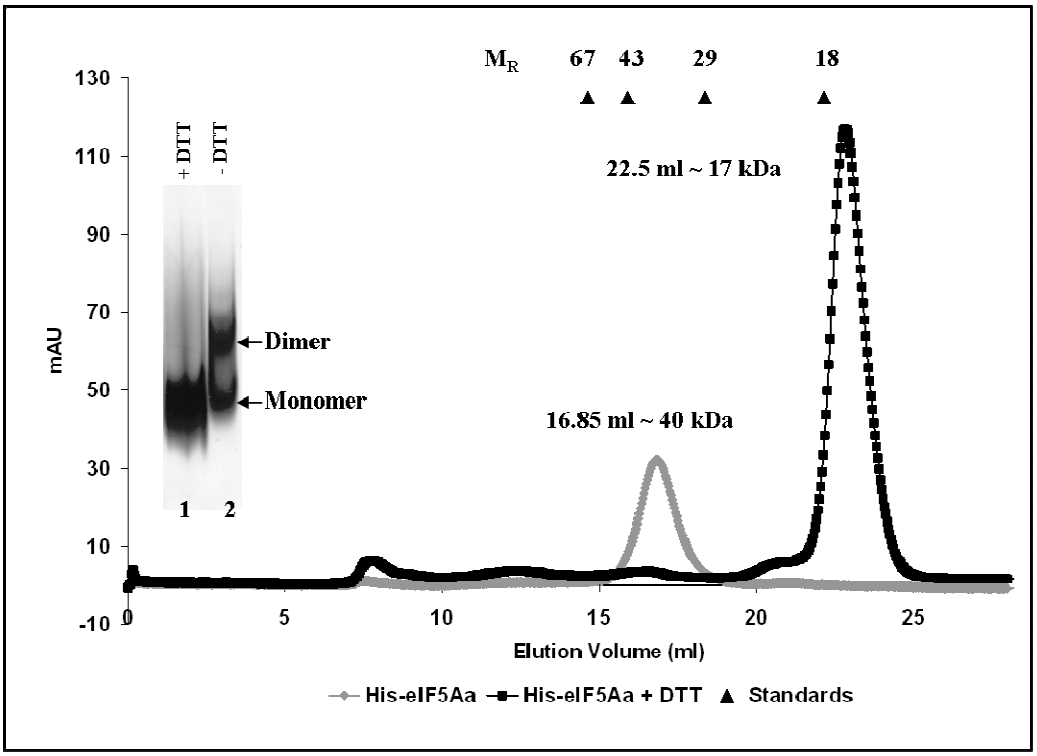

Figure 5.7: Effect of DTT on the oligomeric state of hypusinated His-eIF5A. Gel filtrations profiles of yeast His-eIF5A proteins in the presence and absence of DTT-treatment. Inset: Native PAGE analysis of His-eIF5A proteins in the absence (lane 2) and presence (lane 1) of DTT. Proteins Myoglobin (18 kDa), Carbonic anhydrase (29 kDa), Ovalbumin (43 kDa) and Bovine serum albumin (67 kDa) were used to calibrate the column (represented by triangles).

Since the yeast *TIF51A* protein contains two cysteine residues (present at positions Cys 23 and Cys 39, near the N-terminus of the eIF5A protein), it was logical to investigate whether these residues were important in stabilising dimerisation of hypusinated His-eIF5A. With this in mind, the coding sequence of His-eIF5A in plasmid pPG20 was mutated at Cys 23 and at Cys 39 to encode serine residues (C23S and C39S). The resulting complementation plasmids (pPG20-C23S and pPG20-C39S, respectively) were used in the transformation of PGY10 cells to determine whether the functionality of mutant proteins. Transformants were growth in YPGal broth and diluted before being plated onto medium containing either galactose or glucose to ascertain whether the C23S or the C39 mutations affected the ability to complement the lethal phenotype on glucose. Both the C23S and the C39S mutations were able to complement the lethal phenotype (Figure 5.8), suggesting that these cysteine residues were not essential for the biological function of His-eIF5A.

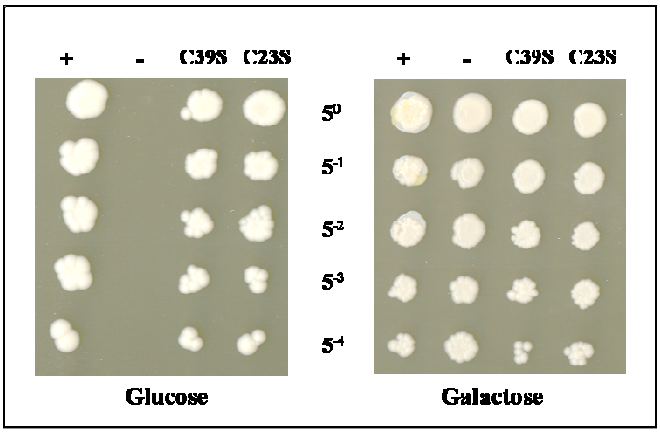

Figure 5.8: Functional analysis of His-eIF5A mutants C23S and C39S. Five-fold serial dilutions of PGY10 cells transformed with either pYES2 (-), pPG20 (+), pPG20-C23S or pPG20-C39S, plated onto medium containing either glucose (left) or galactose (right).

The results of the complementation assay suggested that that (1) Cys39 and Cys 23 were not required for dimerisation of hypusinated His-eIF5A, or (2) that dimerisation of the protein was not required for function in yeast cells. To investigate whether these mutant proteins were able to dimerise, the His-eIF5A-C39S and His-eIF5A-C23S proteins were over-expressed and purified using Ni affinity chromatography, from yeast cells. As observed in *E. coli*, expression levels of the His-eIF5A-C23S mutant were too low to continue with the biochemical analyses. Analysis of hypusinated His-eIF5A-C39S by gel filtration and native PAGE revealed that like the wild-type, the C39S mutant protein retained its dimeric state (Figure 5.9 and inset). This was in contrast to the result obtained in a similar experiment using His-eIF5A-C39S protein produced in *E. coli* which showed that this mutant protein was destabilised from its dimeric state and existed in a predominantly monomeric form (Section 4.3.6, Figure 4.7).

This result suggested that either the unhypusinated His-eIF5A purified from *E. coli* was using a different mechanism to dimerise. Alternatively, the apparent dimerisation of the protein may be as a result of misfolding of the recombinant protein, which does not necessarily result in an insoluble aggregate, since the protein was determined to be soluble in Section 3.3.1. Misfolding of heterologously-produced eukaryotic proteins is frequently observed, but does not necessarily involve the production of insoluble aggregates and inclusion bodies (Georgiou & Valax, 1996; Baneyx & Mujacic, 2004; González-Montalbán *et al*., 2007). The *E. coli* His-eIF5A dimer, consisting as it does of unhypusinated protein, could be self-associating via a mechanism involving Cys 39. Importantly, this data showed that in yeast cells, dimerisation of hypusinated His-eIF5A is utilising other critical residues.

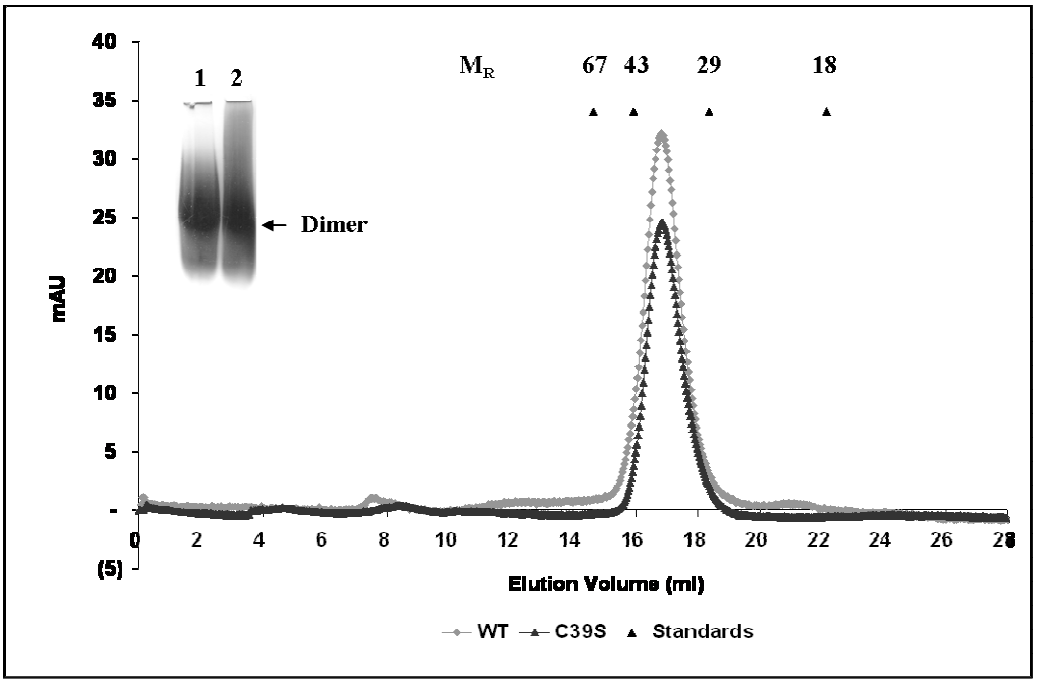

Figure 5.9: Effect of the C39S mutation on the oligomeric state of yeast His-eIF5A. Gel filtration and native PAGE analysis (inset) of His-eIF5A and His-eIF5A-C39S mutant protein produced yeast. The positions of the calibration proteins, Myoglobin (18 kDa), Carbonic anhydrase (29 kDa), Ovalbumin (43 kDa) and Bovine serum albumin (67 kDa) are indicated by triangles.

5.3.4 Role of hypusine in the dimerisation of His-eIF5A in yeast cells

The results in the previous section indicated that in yeast cells, dimerisation of His-eIF5A appeared to be mediated via a mechanism that was not dependent upon Cys39. The major difference between the two experimental systems is that heterologously-produced (*E. coli*) His-eIF5A lacks the post-translational hypusine modification while homologously-produced HiseIF5A (yeast) undergoes hypusination at the highly conserved lysine residue (Lys 51). This raised the question of whether hypusination was required for the dimerisation of His-eIF5A in yeast cells. Accordingly the effect of a K51R mutation was investigated. This lysine residue is critical in the function of the yeast eIF5A (Park *et al*., 1997), but it has not been ascertained what effect mutation of this lysine residue would have on the structural characteristics of the protein. To this end, a pPG20-K51R mutant was constructed and complementation assays conducted to confirm that this mutation abolished biological function of the protein. Serial dilutions of pPG20-K51R-transformed PGY10 cells were plated onto medium containing either glucose or galactose. As expected, complementation of the lethal phenotype on glucose was not obtained, confirming the importance of Lys 51 in the functioning of eIF5A (Figure 5.10A).

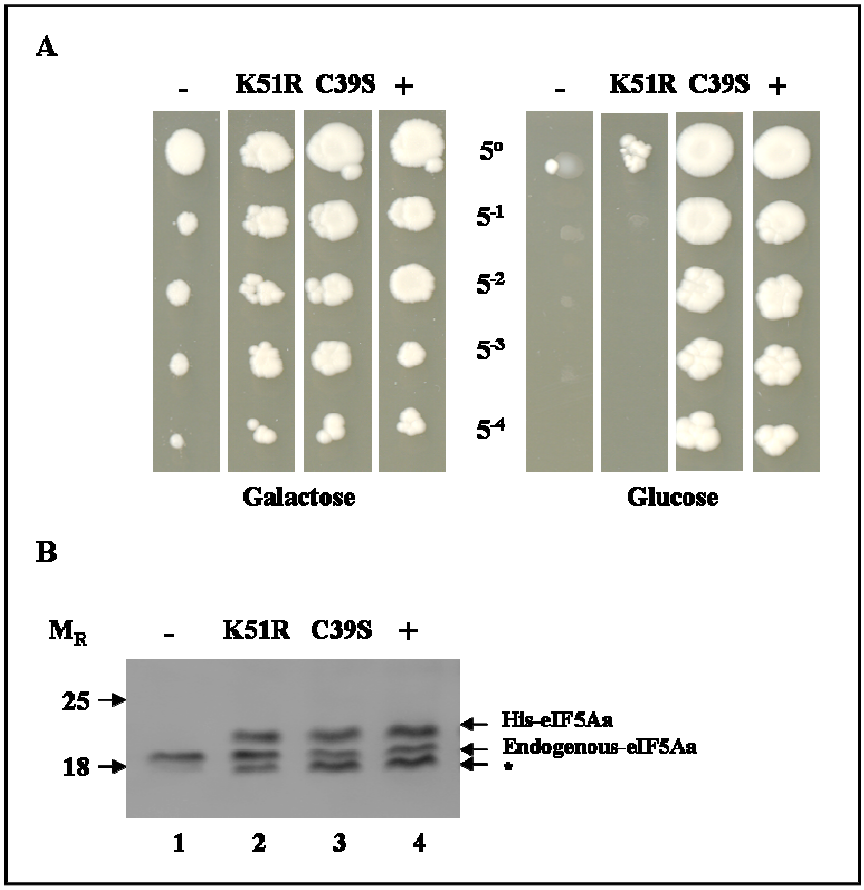

Figure 5.10: Functional analysis of His-eIF5A and its mutants K51R and C39S. (A) Five-fold serial dilutions of PGY10 cells transformed with pYES2 (-), pPG20-K51R (K51R), pPG20-C39S (C39S), pPG20 (+) on medium containing either galactose (left) or glucose (right). (B) Western analysis of His-eIF5A protein extracts obtained from PGY10 cells transformed with the plasmids in (A) using anti-eIF5A antibodies.

To rule out the possibility that the lack of complementation of the lethal phenotype in strain PGY10 with pPG20-K51R was as a result of the lack of protein expression, protein extracts were resolved by SDS-PAGE and subjected to Western analysis using anti-eIF5A antibodies. His-eIF5A-K51R, His-eIF5A-C39S and (wild-type) His-eIF5A were detected (Figure 5.10B lanes 2-4), confirming that they were all expressed in the cells and that the lack of complementation was due to the critical nature of Lys 51, rather than lack of protein expression. Also observed was residual "endogenous" eIF5A resulting from expression of eIF5A from *LEU2::*P_{GAL}*-TIF51A* (Section 3.2.8) in medium containing galactose, but was distinguishable from His-eIF5A, in that His-eIF5A resolved at a higher mobility (Figure 5.10B). This residual protein was clearly not sufficient to maintain viability of PGY10 cells. In addition, a degradation product of His-eIF5A was observed (Figure 5.10B, asterisk). In protein extracts obtained from cells expressing no eIF5A (Figure 5.10B, lane 1), only the endogenous eIF5A was detected.

Next, the effect of the Lys 51 mutation on the oligomeric state of the protein was investigated using gel filtration and native PAGE analysis. His-eIF5A-K51R mutant proteins were produced in yeast and *E coli*, using cells transformed with pPG39-K51R or pPG8-K51R. The final purified protein concentrations were 3 mg/ml (yeast) and 4 mg/ml (*E. coli*). The data revealed that the K51R mutant protein existed as a dimer in *E. coli* (Figure 5.11A) but as a monomer in yeast (Figure 5.11B). This result strongly suggested that Lys 51 is not only important in the function of His-eIF5A, but also plays a structural role in the dimerisation of the protein. Conversely, the Lys 51 residue plays no role in the dimerisation of unmodified His-eIF5A, and this further supports the argument that the dimer observed in heterologously-produced His-eIF5A is an artifact associated with a misfolded protein.

A loose connection between structure and function of His-eIF5A has thus been developed from this data: Mutation of Lys 51 that impairs dimer formation abolishes the eIF5A activity, whereas mutation of Cys 39 affects neither dimerisation nor the activity. From this it can be deduced that the function of eIF5A is dependent on the protein forming a dimeric structure.

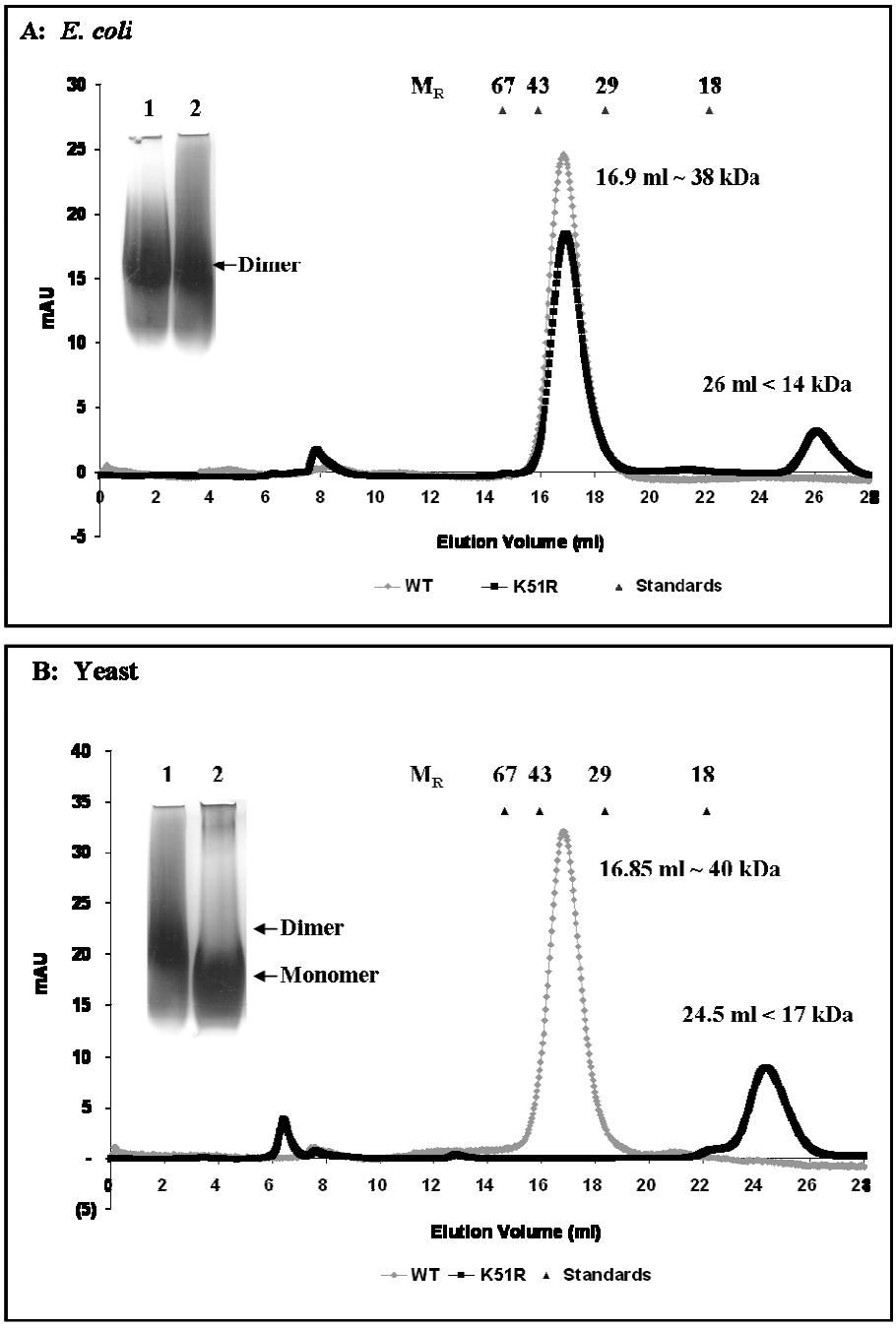

Figure 5.11: Effect of Lys 51 substitution on the oligomeric profiles of His-eIF5A. Gel filtration profiles obtained from His-eIF5A and His-eIF5A-K51R produced in *E. coli* (A) or in yeast (B). Insets: Native PAGE analysis of His-eIF5A (lane 1) and His-eIF5A-K51R) mutants (lane 2). The positions of the calibration proteins, Myoglobin (18 kDa), Carbonic anhydrase (29 kDa), Ovalbumin (43 kDa) and Bovine serum albumin (67 kDa) are indicated by triangles.

5.3.5 Role of RNA in the dimerisation of His-eIF5A

Since it is known that hypusine is required for the binding of RNA (Xu & Chen, 2001; Jao & Chen, 2006), and that it was demonstrated here that Lys 51 (hypusine) is required for the dimerisation of eIF5A (Section 5.3.4), it was next decided to determine the effect on the oligomeric state of eIF5A in the absence of RNA.

The His-eIF5A from *E. coli* and yeast were digested with RNase A for 10 to 20 minutes and the product analysed using gel filtration and native PAGE. No change in the dimeric state of *E. coli*-produced His-eIF5A was observed following RNase digestion (Figure 5.12A and inset). In contrast, there was a shift in the dimeric state to an intermediate state consisting of both monomers and dimers following RNase-treatment of hypusinated His-eIF5A purified from yeast (Figure 5.12B, "+RNase"). After 20 minutes of RNase-treatment, a complete shift to the monomeric form was observed (Figure 5.12B, "++RNase and inset). This result indicated that hypusinated His-eIF5A protein is directly involved with RNA and the His-eIF5A dimer is stabilised by the presence of both RNA and hypusine. Since hypusine is required for RNA binding (Xu & Chen, 2001; Jao & Chen, 2006) this explains why the K51R mutant existed as a monomer in solution, because it would be unable to interact with RNA. Thus unmodified His-eIF5A produced in yeast, which cannot bind RNA, is unable to dimerise. Furthermore, it been shown that eIF5A expressed in *E. coli* (unhypusinated) does not bind RNA, thus the presence of bound RNA may account for the observed difference in the integrated elution volumes of hypusinated His-eIF5A (yeast) (16.85 ml ~ 40 kDa) and unhypusinated His-eIF5A (*E. coli*) (16.9 ml ~ 38 kDa).

The data suggests that the dimeric state of protein produced in *E. coli* is dependent on a different dimerisation mechanism which possibly involves disulphide-bridging or may be an artifact associated with the heterologous production of eukaryotic proteins, particularly those requiring post-translational modifications such as hypusination (Park *et al*., 1993; Park, 2006) and phosphorylation (Kang *et al*., 1993).

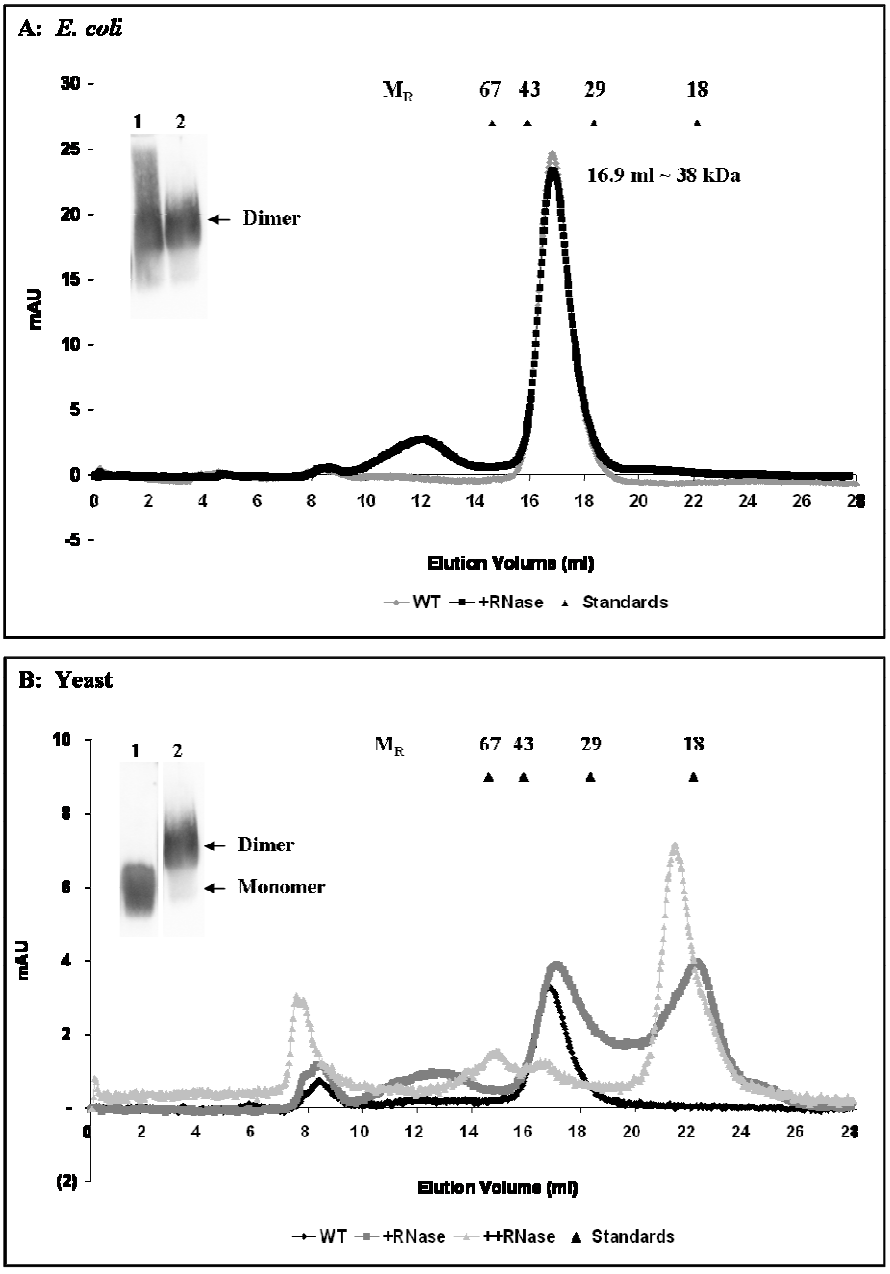

Figure 5.12: Effect of RNase on the dimeric state of His-eIF5A. (A) Elution profile obtained following the gel filtration or native PAGE analysis of His-eIF5A produced in *E. coli* before ("WT" and inset lane 2) and after ("+RNase" and inset lane 1) a 20 minute RNAse-treatment. (B) Gel filtration and native PAGE analysis obtained for His-eIF5A produced in yeast prior to ("WT" and inset lane 2) and following RNase-treatment for 10 minutes ("+RNase") or 20 minutes ("++RNase" and inset lane 1). The positions of the standard proteins Myoglobin (18 kDa), Carbonic anhydrase (29 kDa), Ovalbumin (43 kDa) and Bovine serum albumin (67 kDa) are represented on the chromatograms as triangles.

Unhypusinated His-eIF5A (*E. coli*) and hypusinated His-eIF5A (yeast) are both susceptible to monomerisation or destabilisation upon treatment with DTT. The data in Section 4.3.6 suggested that unhypusinated His-eIF5A (*E. coli*) relied on the presence of Cys 39 to form a

dimer, which was not the case for His-eIF5A (yeast) (Section 4.3.3). This can be explained by the observations that DTT, thought to be a specific reducing agent, can act as a general reducing agent, influencing the redox potential to effect changes in the global structure of the protein. This often involves residues other than cysteine, such as serine, threonine and methionine residues (Alliegro, 2000; Salvador & Klein, 1999). As a result, both hypusinated His-eIF5A (yeast) and unhypusinated His-eIF5A dimers are disrupted in the presence of DTT.

5.3.6 His-eIF5A exists as a homodimer

Finally, the question remained as to eliminate the possibility that the 37 kDa dimeric species was not due to His-eIF5A interacting with another cellular protein of similar size as opposed to existing as a homodimer. Purified hypusinated His-eIF5A was treated with RNase to produce the monomeric form and then subjected to nickel-affinity chromatography. The reasoning was that if His-eIF5A was interacting with another protein, then that protein would appear in the flow-through fraction during the purification, since it would not be His-tagged. The procedure was followed using SDS-PAGE analysis. Purified (dimeric) His-eIF5A treated with RNase (Figure 5.13, lane 1) was passed through a Ni-NTA spin column (Qiagen). The flow-through fraction (Figure 5.13, lane2) contained no visible unbound protein of similar size to His-eIF5A. This ruled out the possibility that His-eIF5A interacted with an untagged cellular protein of similar size, and confirmed that eIF5A exists as a homodimer.

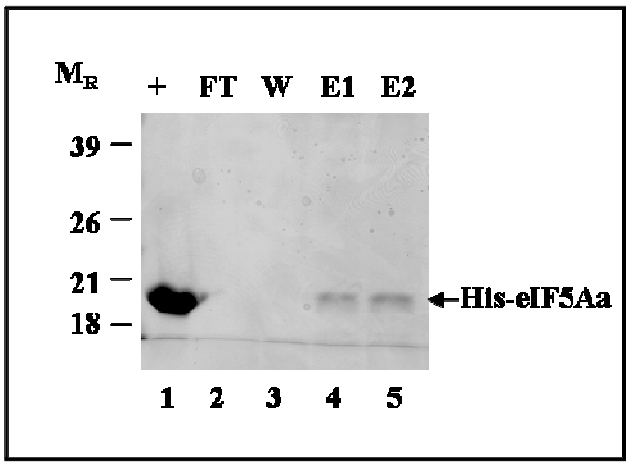

Figure 5.13: His-eIF5A exists as a homodimer. SDS-PAGE analysis of purified His-eIF5A fractions collected during nickel affinity purification following treatment with RNase. Lane1: RNase-treated purified His-eIF5A (+); Lane 2: Flow through (FT) fraction collected following binding to the column; Lane 3: Wash fraction (W); Lanes 4 and 5: Eluted His-eIF5A protein.

5.4 Conclusions

The demonstration that hypusinated eIF5A exists as a dimer in solution is in agreement with an early finding by Chung *et al*. (1991) that proposed that mammalian eIF5A exists as monomers, dimers and trimers. The data presented in this chapter also demonstrate that dimerisation is dependent upon RNA binding and not hypusination since treatment of the His-eIF5A dimer with RNase destabilised the dimer releasing monomeric hypusinated His-eIF5A.

While initial experiments with unhypusinated His-eIF5A indicated that the protein was dimeric (Section 4.3.2) several lines of evidence support the argument that the mechanism for dimerisation of protein produced in *E. coli* is different to that produced in yeast:

(1) While both dimers are disrupted under reducing conditions, Cys 39 was required for dimerisation in *E. coli* but not in yeast. This was attributed to the global reducing action of DTT acting on residues other than Cys 39 in hypusinated His-eIF5A (yeast), rather than specific action affecting Cys 39 in unhypusinated His-eIF5A (*E. coli*).

(2) A K51R mutation had no effect on the *E. coli* dimer, while it resulted in the disruption of the dimeric protein purified from yeast. This indicated that Lys 51, or hypusine, was aiding the dimerisation process in native His-eIF5A.

(3) In yeast, the formation of the dimer is dependent upon RNA binding while there is no RNA binding required for dimerisation in *E. coli*. This indicated too that the presence of hypusine allowed for RNA binding in His-eIF5A from yeast.

Thus one must conclude that the apparent solubility of His-eIF5A produced in *E. coli* does not necessarily equate to correctly folded and functional protein, which could be due to the cytosolic environment in the *E. coli* cell (slightly more reducing environment) as compared with yeast (slightly more oxidizing environment) (Carmel-Harel & Storz, 2000). An alternative explanation could be that hypusine and thus the presence of RNA, is important in ensuring the correct folding of the active protein.

This data raises concerns about the potential implications of misfolding of His-eIF5A expressed in *E. coli* which has been routinely used for crystallographic studies. The crystal structures of aIF5A from the archaea and eIF5A from the protozoans could thus represent alternatively-folded proteins. If this is so, then it is expected that the less ordered regions (such as the loop structure around the site of hypusination) are folded in a conformation different to that which was previously thought. The presence of hypusine and RNA, resulting in a dimer, may effect additional conformational changes in the protein, as is expected when a protein binds any ligand. The following chapter addresses the possibility of such conformational changes upon RNA binding.

Chapter 6: General discussion and conclusions

Chapter 6: General discussion and conclusions

While there is a wealth of information on the biological function of eIF5A and the process of hypusination, information on the structural aspects of eIF5A in the literature is confined to archaeal homologues. The structures of two *Leishmania* eIF5A were recently deposited on the database, but these, like the aIF5A structures shed no light on the structural role of hypusine since the crystals were derived from protein produced in *E. coli*. The principal aim of the research described in this thesis was to address this knowledge gap by using yeast eIF5A to develop insight into the structure of eIF5A, particularly with respect to the role of hypusine and how this relates to its biological function.

The approach was first to use available structural information derived from the *Leishmania* and archaeal homologues to derive a homology model of the yeast eIF5A. Structural data from the HEX-1 analogue of eIF5A was then used to produce dimeric structural models. Second, a biochemical and functional analysis was carried out which demonstrated that hypusinated eIF5A exists as a homodimer in solution and that dimerisation is dependent upon hypusination and RNA binding.

6.1 Homology modeling of eIF5A

6.1.1 Models based on *Leishmania* and archaeal eIF5A homologues

The possibility that an homology model of yeast eIF5A could be produced based on currently available structural data of the archaeal homologues was explored. A comparison of the homology models based on the archaeal vs. *Leishmania* structures showed clearly that the archaeal homologues were poor templates for eIF5A homology models, mainly because of the relatively low sequence identity between aIF5A and eIF5A. The model produced using the *Leishmania* eIF5A as a template was comparable with the human eIF5A model produced by Facchiano *et al*., (2001). These structural differences are consistent with recent evidence that as aIF5As are functionally different to their eukaryotic counterparts. In particular, aIF5As exhibit ribonucleolytic activity rather than RNA-binding activity and lack an N-terminal intracellular localisation signal that is functionally restricted to eIF5As (Wagner & Klug, 2007; Parreiras-e-Silva *et al*., 2007). Although recently, Cano *et al*. (2008) and Dias *et al*. (2008) demonstrated that truncated mutants of this N-terminal 10 amino acid extension in human and yeast eIF5A (not present in aIF5A) is able to complement the yeast *tif51A* knockout strain. This implies that the N-terminal region is not functionally required.

Moreover the C-terminal α-helix is proposed to be an essential structural element in yeast eIF5A (Dias *et al*., 2008).

Homology models of yeast eIF5A based on unpublished eIF5A homologues (*L. mexicana* and *L. brasiliensis* eIF5As) deposited on the Protein Data Bank not only produced models of greater confidence, but also revealed the presence of an α-helix in the C-terminal domain of eIF5A, unique to eukaryotes. This helix was also predicted in the homology modeling of the human eIF5A (Costa-Neto *et al*., 2006), based on the *L. brasiliensis* eIF5A. The presence of the α-helix was also predicted to occur on the C-terminal domain using the secondary structure prediction program JPred (Cuff & Barton, 1999). Forming part of an oligonucleotide binding fold (Murzin, 1993, this study), this helix is potentially involved in the binding of specific mRNAs identified by Xu and Chen (2001) by the hypusinated form of the protein. However, both domains of aIF5A, as well as the flexible linker region between the domains have been implicated by Kim *et al*., 1998; Peat *et al*., 1998 and Wagner & Klug, 2007 as potential RNA binding sites, and the minimal region for biological activity of eIF5A includes the N- and C-terminal β-sheet core structures (Cano *et al*., 2008). Whether this is the case for yeast eIF5A remains to be seen.

6.1.2 Dimeric models of eIF5A based on HEX-1

Since eIF5A and aIF5A were proposed to exist in a number of oligomeric states (Chung *et al*., 1991; Wagner & Klug, 2007), potential dimer configurations, based on the interactions observed in homologues and analogues of eIF5A (aIF5As and HEX-1, respectively), were predicted. The potential dimeric conformations (Types I, II and III) stabilised by salt bridging, extensive hydrogen bonding and possible intra-subunit disulphide bridging, provided a means to visualise potential yeast eIF5A dimers. Of the three types of predicted dimer configurations, the most likely configuration is the Type II model (Figure 6.1). This stable configuration potentially involves residues Lys 35, Ser 47, Gly 53, Thr 66 and Lys 69 as well as Lys 51 (hypusine), and could create a loose “interlocking finger” formation in the loop region of the N-terminal domain (Figure 6.1 marked in red). Cano *et al*., 2008 showed that mutations in residues Lys 47 and Gly 49 in human eIF5A (equivalent to Lys 48 and Gly 50 in yeast eIF5A) result in the abolishment of growth in a yeast eIF5A null strain. These critical residues are positioned in near proximity to those predicted here to be involved in dimerisation. This strongly supports the argument that the highly-conserved residues in the loop region, including Lys 51 may be involved in dimerisation. Given that hypusination extends the Lys 51 residue, it is possible that the reach is extended at the loop region, thus

allowing dimerisation. In the absence of Lys 51 (hypusine), the reach required to create the "interlocking finger" or loose dimer may not be achieved. Also, this configuration would create an aromatic groove in the centre of the dimer interfaces that could house an RNA molecule. The ssRNA molecule represented in Figure 6.1, is loosely based on the structure of the RNA molecules found to associate with eIF5A and identified by Xu *et al*., 2004. Namely the represented mRNA molecule consists of more than 40 nucleotides, contains secondary structures such as hairpins, bulges and stem-and-loops.

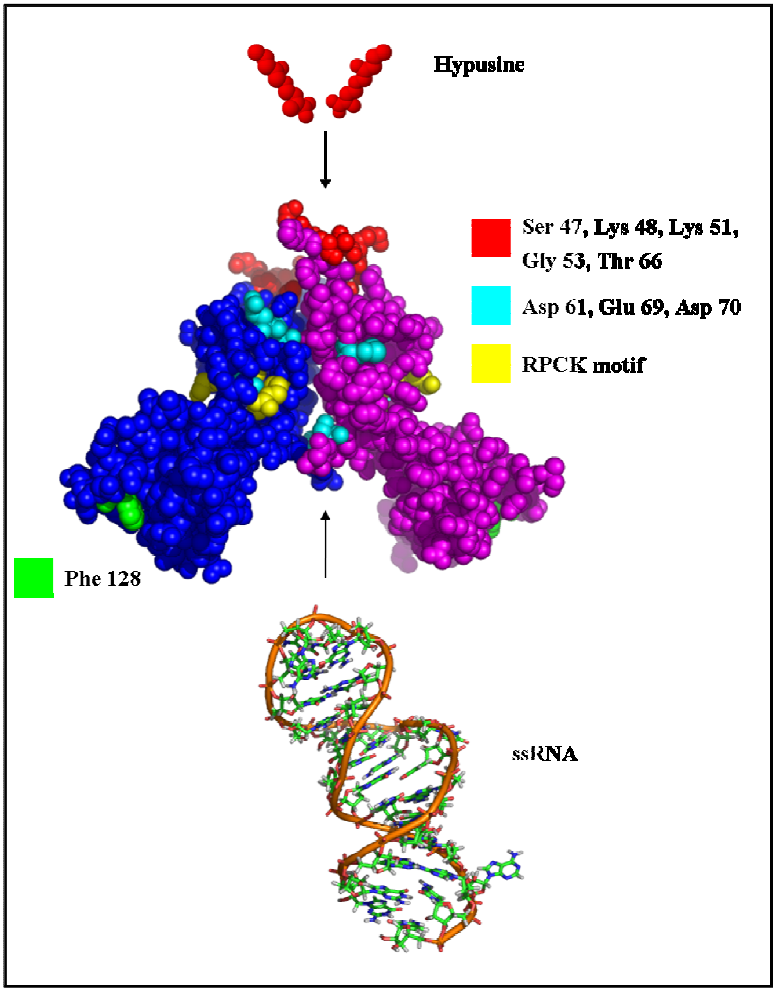

Figure 6.1: Type II dimer model incorporating the factors though to be involved for the dimerisation of yeast eIF5A. Space-fill representation of the predicted yeast eIF5A Type II dimer depicting the amino acid residues thought to be involved in dimerisation. The residues in red represent those in the loop structure thought to be involved in interlocking the N-terminal domain of each hypusinated monomer. The residues in cyan represent those thought to be involved at the dimer interface, creating the hydrophobic pocket where ssRNA can bind. The figure was generated using Pymol (DeLano, 2002) and the hypusine residue was modeled using ACD/ChemSketch Freeware V.8.17. The random RNA molecule was generated using the M-Fold program (Zuker, 2003).

6.1.3 Strengths and weaknesses of the dimeric models of eIF5A

The dimer models provide an opportunity to identify amino acid residues that might be involved in the correct folding of the protein. However, these models may not necessarily reflect the true contact sites of eIF5A, in that it is highly possible that several conformational changes can take place within the protein *in vivo*. In particular, the effect of hypusine on the folding of the protein is unknown because all structures used as templates to generate the eIF5A homology model were solved using protein produced in *E. coli* which would be unhypusinated. Structured regions of the protein (α-helices and β-sheets) are unlikely to be affected by conformational changes, while the variable loop regions, which are typified as being highly conserved throughout eIF5As, are unlikely to withstand positional variation during conformational change. Attempts at modelling the highly conserved, but structurally variable loop region bearing the site of hypusination (Costa-Neto *et al*., 2006), show that a more structured form of the loop can be achieved in a hydrophobic environment. Perhaps the extension of Lys 51 to hypusine results in a conformational change in the loop region such that it extends into the hydrophobic pocket created by the dimer, rather than the loop interacting with the hydrophobic core of DHS, as suggested by Costa-Neto *et al*., 2006.

There is substantial evidence from this work to suggest that protein produced in *E. coli* is misfolded despite being soluble (discussed below in Section 6.2.2). A further concern in extrapolating information from the models of the yeast eIF5A dimers is that the templates are based on monomeric homologues in the unhypusinated form, and do not incorporate the presence of RNA. Thus the difficulty with interpreting the homology models is three-fold: (1) The current structural data is produced from protein produced in *E. coli* and is thus not hypusinated; (2) Hypusine is required for the binding of RNA and thus would also not be reflected in the model and (3) Dimerisation of the protein would almost certainly produce conformational changes in the protein. Determination of these conformational changes can only be achieved by obtaining structural data of hypusinated eIF5A in the presence of RNA.

6.2 Factors affecting dimerisation of native, eIF5A

6.2.1 In yeast

To test the hypothesis that eIF5A existed as a dimer in solution, extensive biochemical and functional analyses were carried out on yeast eIF5A (hypusinated). It was shown that yeast eIF5A exists predominantly as a dimer in solution whether in its hypusinated form. Higher order oligomeric states could artificially be achieved upon cross-linking, but this was not observed in the native protein. This finding is supported by an early report that mammalian

eIF5A exists in a number of oligomeric states (Chung *et al*. 1991), and that the activity of aIF5A depends on its oligomeric state (Wagner & Klug, 2007). eIF5A dimers were destabilised by treatment with the reducing agent, DTT. DTT has been shown to act as a general reducing agent, influencing the redox potential to effect changes in the structure of the protein, often involving not only cysteine, but also serine, threonine and methionine residues (Alliegro, 2000; Salvador & Klein, 1999). Cys 23 and Cys 39 are not required for the biological function of eIF5A and mutation of Cys39 does not affect dimerisation. Thus it is likely that there are threonine, serine and/or methionine residues involved in stabilisation of the hypusinated dimer.

Mutation of Lys 51 to Arg 51 (K51R) resulted in monomerisation of eIF5A. It is known that Lys 51 is required for the function of eIF5A (Park *et al*., 1997, this study) and that hypusine is required for RNA binding, but there is no direct evidence for a function of hypusine in dimerisation. However, the presence of RNA was found to the critical in the dimerisation of hypusinated eIF5A. Xu & Chen (2001) showed that sequence-specific RNA binding is dependent on the presence of hypusine, but in the light of data presented in this thesis, it is now apparent that both RNA and the site of hypusination are required for dimerisation. This leads to the following question: Is the function (activity) of eIF5A dependent on its oligomeric state, as proposed for the *Halobacterium sp*.NRC-1 aIF5A (Wagner & Klug, 2007)? In other words, it could be that hypusine alone is not directly required for the function of eIF5A, but rather that hypusine plays a structural role to produce a loose dimer. This loose dimer allows RNA to bind, which results in stabilisation of the dimer and these two factors (hypusine and RNA) in concert ultimately produce a functional (dimeric) protein. Precisely which residues are involved in dimerisation and RNA binding cannot be determined without solving the crystal structure of the protein together with its hypusine modification and RNA counterpart. However, the dimer models and biochemical data from this study suggest that Asp 61, Glu 69 and Asp 70 are important at the dimer interface, and Phe 128 and Ser 16 are residues likely to be interacting with RNA.

6.2.2 In *E. coli*

As in yeast, the eIF5A dimer purified from *E. coli* was disrupted following the addition of reducing agents (DTT and β-mercaptoethanol). The integrity of these eIF5A dimers was dependent upon the presence of Cys 39, leading to the conclusion that here dimerisation was due to a folding mechanism making use of disulphide bridging as opposed to an alternate dimerisation mechanism in hypusinated eIF5A. In contrast to dimerisation in yeast the *E. coli*

dimer did not rely on the presence of Lys 51 (the site of hypusination), suggesting that the (unhypusinated) dimer might be self-associating as a result of protein misfolding, which is sufficiently ordered for the dimer to remain soluble. This data has important implications for the interpretation of available structural data derived from crystals generated from protein purified in *E. coli*. Firstly, these crystals were produced from recombinant protein using DTT (Kim *et al*., Peat *et al*., Yao *et al*., 2003; Sun *et al*., 2005) which, from data in this study, would have resulted in the monomeric form of the protein. Secondly, the structures did not accommodate the RNA molecule, because the protein was unhypusinated. This would have resulted in misfolded, but soluble protein, the structures of which would be affected in the highly conserved, but variable loop structures. The implication is that data derived from such models in these regions may not accurately reflect the structure of the protein *in vivo*.

6.3 Proposed mechanism of dimerisation for yeast eIF5A

As discussed above, the dimer models of yeast eIF5A produced in this study are limited for the following reasons: (1) The structural templates used to generate the monomeric models are derived from non-hypusinated protein in the absence of RNA; (2) The templates used to generate the monomeric models may represent soluble, but misfolded protein and (3) The template structures cannot account for conformational changes that may take place during protein-protein interactions (dimerisation) or protein-RNA binding.

If, as data presented in this study suggest, hypusination and RNA binding do result in conformational changes, these changes are likely to affect the apparently disordered, but highly conserved loop structures of eIF5A, particularly the loop presenting the site of hypusination. The reasoning is that highly structured (ordered) regions such as β-sheets and α-helices would not be altered, while the highly conserved, unstructured (loop) regions of the protein would be targets of conformational change. Since the site of hypusination is found in such an unstructured region, it is possible that an extension of the lysine to hypusine would result in a greater molecular reach, thus allowing for the possible interlocking of two N-terminal domains (in the Type II dimer configuration) or between the N-terminal domain of one molecule and the C-terminal domain of another molecule (in the Type I dimer configuration). Cano *et al.* (2008) have recently reported two residue changes in this loop region (other than the lysine that becomes hypusinated) that result in the loss of growth in a yeast eIF5A null strain. Since these two mutants (K47D and G49A) are still hypusinated, it could be that they may play a role in either dimerisation or in RNA-binding.

Other regions likely to be affected by conformational change would be putative RNA contact regions. These include the area preceding and following the highly ordered α-helix (amino acids Asp 129 - Leu 134 and Lys 110 - Glu 119), the flexible inter-domain linker region (amino acids Pro 83 - Lys 86) and the loop structures on the N-terminal domain preceding the anti-parallel β-sheet arrangement (amino acids Ser 45 - Lys 57). Although the precise eIF5A-RNA contact regions have yet to be determined, it may be possible to speculate on the nature of the RNA molecule bound to hypusinated eIF5A. The minimal consensus of the single-stranded RNA molecules required to bind eIF5A is AAAUGUCACAC (Xu & Chen, 2001). A number of the RNA molecules identified in a subsequent study (Xu *et al*., 2004) have the potential to form hairpins and internal loop structures which serve as potential recognition sites for eIF5A. Since it is not yet possible to precisely predict the RNA contact points unless a solution or crystal structure of the eIF5A-RNA molecule is solved, it is worth hypothesising how the specified length of sequence-specific RNA could be involved in the dimerisation mechanism of eIF5A.

The following model represents a potential mechanism for producing functional eIF5A using the Type II dimer based upon a dimer configuration of the structural analogue HEX-1 (Sections 2.3.5 and 2.3.6). Since RNA binding requires hypusine it is proposed that the protein undergoes the following dimerisation process. Following translation of eIF5A, the hypusination enzymes (DHS and DOHH) perform the post-translational modification of Lys51- to HYP-51-eIF5A (Figure 6.2A Step 1). This is the point where a conformational change in the monomer is predicted (denoted in Figure 6.2 as Δ). The hypusinated eIF5A monomers then loosely associate to produce an interlocking finger (Type II) dimer configuration in the N-terminal domain which may involve hypusine (Figure 6.2A Step 2). This loose dimer configuration creates a groove at the dimer interface that allows specific RNA (represented by a 30-mer in Figure 6.2B) to bind, resulting in a further conformational change (Δ) that locks the dimer in place and enables it to perform its functions *in vivo* (Figure 6.2 Step 3). The RNA molecule is represented here such that the loop regions interact at the dimer interface, and each of the RNA termini interact with one of the α-helices. In the absence of hypusine, the loose dimer configuration cannot be achieved, and in the absence of RNA, the loose dimer is disassociated (unstable). Whether the hypusination-dimerisation-RNA-binding mechanism is achieved in a step-wise approach (as represented in Figure 6.2A and B) or whether hypusination and RNA-binding occur simultaneously to result in dimerisation (Figure 6.2A and B Steps 2 and 3 combined), is yet to be determined. This could be tested by monomerising the hypusinated protein using DTT and then adding back an

RNA transcript (based on the SELEX transcripts identified by Xu *et al*., 2004) to observe whether dimerisation reoccurs. Alternatively, the hypusinated protein could be monomerised using RNAse, re-purified and cross-linked using glutaraldehyde. Should dimerisation of hypusinated eIF5A re-occur, it would be plausible that the step-wise mechanism of dimerisation is employed.

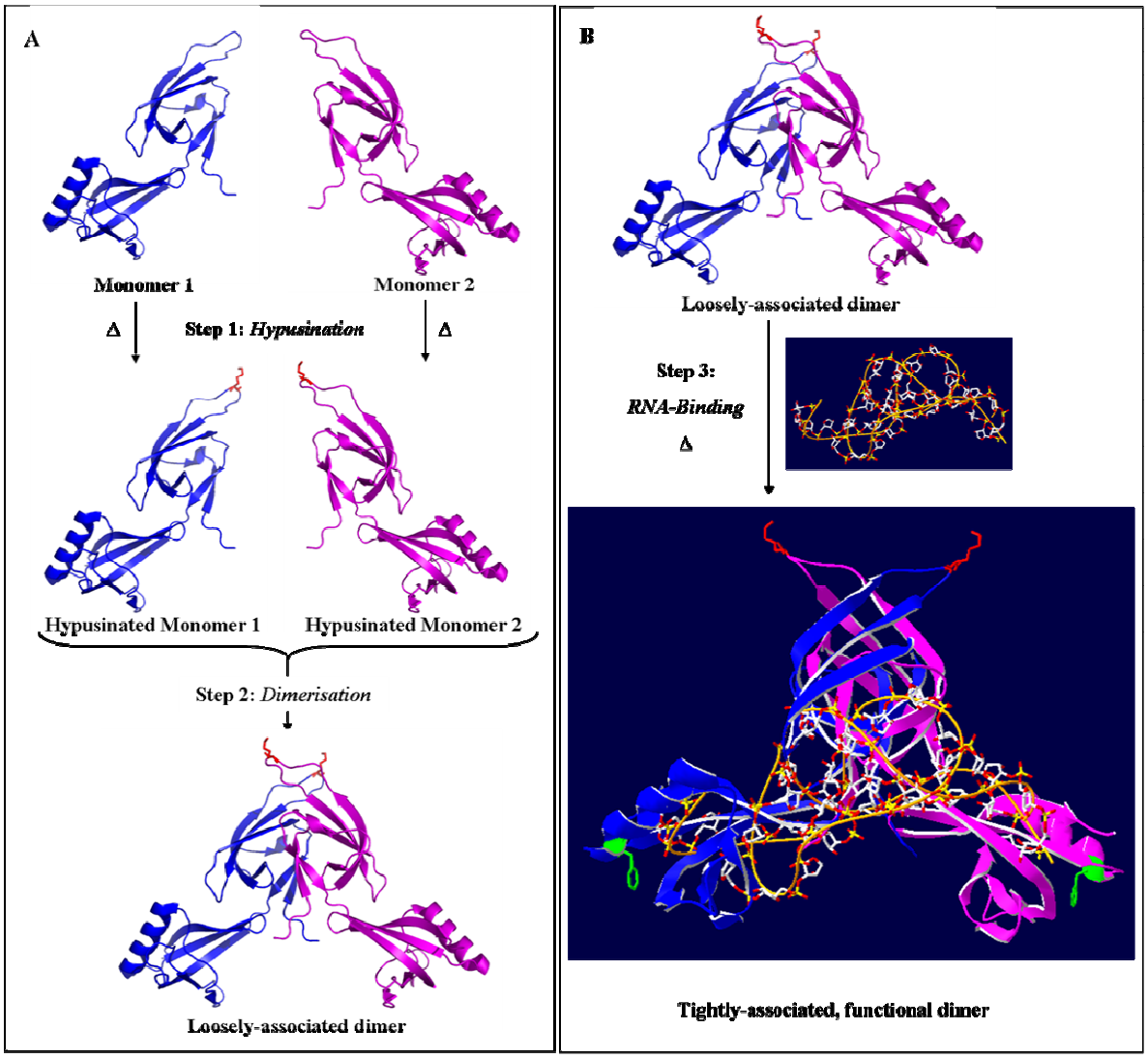

Figure 6.2: Proposed dimerisation mechanism of yeast eIF5A. Schematic representation of the dimerisation mechanism proposed for yeast eIF5A. (A) Step 1 involves hypusination of the monomeric eIF5A effecting a conformational change in the protein (represented by Δ). The hypusinated monomers associate to form a loose dimer configuration (Step 2). (B) ssRNA (represented as a 30-mer) binds to the loose dimer which effects another conformational change (Step 3) to produce the tightly-associated functional dimer. The 30-mer RNA molecule (orange strand) was randomly introduced in the tightly-associated dimer to give some idea of scale. The possibility that Steps 2 and 3 occur simultaneously cannot be ruled out. The figure was generated in part using Pymol (DeLano 2002) and DeepView/Swiss PDB Viewer (Guex & Peitsch, 1997).

6.4 Concluding remarks and opportunities for further research

While the mechanism of dimerisation is yet to be elucidated, this study has contributed to the understanding of which factors may be important for the dimerisation and hence function of yeast eIF5A. The limited information that can be derived from the homology models produced during the course of this investigation have highlighted the need for an eIF5A crystal or solution structure in its hypusinated form and in the presence of RNA, which involves crystallising the native protein in the absence of DTT. The apparent need for the addition of a reducing agent during crystallisation of eIF5A (Kim *et al*., 1998; Peat *et al*., 1998; Yao *et al*., 2003; Sun *et al*., 2005) could be overcome by stabilisation of the dimer in the presence of RNA. Should it not be possible to produce crystals of hypusinated eIF5A, an alternative approach could be to use or Nuclear Magnetic Resonance (NMR) solution studies. The eIF5A monomer is potentially still within the size limitation for solving solution structures of protein structures using NMR. Comparison of the structures of K51R-eIF5A with hypusinated eIF5A as well as the presence or absence of RNA could result in a structure for the loop including hypusine.

In the absence of further structural data, the dimerisation model would need to be tested using site directed mutagenesis amino acid residues predicted to interact at the dimer interface or potentially contacting RNA. The generation of the yeast experimental system, anti-eIF5A antibodies, vectors for heterologous and homologous expression of eIF5A or eIF5A mutants and biochemical tools used to detect dimerisation and RNA binding can be used to identify further residues and/or regions of eIF5A critical for dimerisation and RNA binding. Functional characterisation of these mutants *in vivo* together with their dimerisation characteristics and RNA binding properties would be useful in identifying important domains. Potentially important regions could include the unique α-helical region on the C-terminus of the protein, the loop structure housing the site of hypusination and internal N-terminal domain loop regions preceding this loop.

REFERENCES

Abbruzzese, A., Park, M. H. & Folk, J. E. (1986) Deoxyhypusine hydroxylase from rat testis. Partial purification and characterization. *J Biol Chem* **261**, 3085-3089.

Abbruzzese, A. (1988) Developmental pattern for deoxyhypusine hydroxylase in rat brain. *J Neurochem* **50**, 695-699.

Abbruzzese, A., Park, M-H., Beninati, S. & Folk, J. E. (1989) Inhibition of deoxyhypusine hydroxylase by polyamines and by a deoxyhypusine peptide. *Biochim Biophys Acta* **997**, 248-255.

Abbruzzese, A., Hanauske-Abel, H. M., Park, M.H., Henke, S. & Folk, J. E. (1991) The active site of deoxyhypusyl hydroxylase: use of catecholpeptides and their component chelator and peptide moieties as molecular probes. *Biochim Biophys Acta* **1077**, 159-166.

Alani, E., Cao, L. & Klier, H. (1987) A method for gene disruption that allows repeated use of *URA3* selection in the construction of multiply disrupted yeast strains. *Genetics* **118**, 541-543.

Alberts, B., Johnson, A., Lewis, J., Raff, M., Roberts, K. & Walter, P. (2002). *Mol Biol Cell*, pp. 985-991, Garland Science, USA.

Alliegro, M. C. (2000) Effects of dithiothreitol on protein activity unrelated to thiol-disulfide exchange: for consideration in the analysis of protein function with Cleland's Reagent. *Anal Biochem* **282**, 102-106.

Altschul, S. F., Madden, T. L., Schaffer, A. A., Zhang, J., Zhang, Z., Miller, W. & Lipman, D. J. (1997) Gapped BLAST and PSI-BLAST: a new generation of protein database search programs. *Nucleic acids Res* **25**, 3389-3402.

Andrade, M. A., Petosa, C., O'Donoghue, S. I., Muller, C. W. & Bork, P. (2001) Comparison of ARM and HEAT protein repeats. *J Mol Biol* **309**, 1-18.

Andrus, L., Szabo, P., Grady, R. W., Hanauske, A-R., Huima-Byron, T., Slowinska, B., Zagulska, S. & Hanauske-Abel, H. M. (1998) Antiretroviral effects of Deoxyhypusyl Hydroxylase Inhibitors. *Biochem Pharmacol* **55**, 1807-1818.

Aoki, H., Adams, S. L., Turner, M. A. & Ganoza, M. C. (1997a) Molecular characterization of the prokaryotic efp gene product involved in a peptidyltransferase reaction. *Biochimie* **79**, 7-11.

Aoki, H., Dekaney, K., Adams, S-L. & Ganoza, M. C. (1997b) The gene encoding the Elongation Factor P protein is essential for viability and is required for protein synthesis. *J Biol Chem* **272**, 32254-32259.

Arrigo, S. J. & Chen, I. S. (1991) Rev is necessary for translation but not cytoplasmic accumulation of HIV-1 vif, vpr, and env/vpu 2 RNAs. *Genes Dev* **5**, 808-819.

Ausubel, F., Kingston, R., Moore, D., Seidman, J., Smith, J. & Struhl, K. (1983) In *Curr Prot Molec Biol*, Wiley Interscience, New York

Balabanov, S., Gontarewicz, A., Ziegler, P., Hartmann, U., Kammer, W., Copland, M., Brassat, U., Priemer, M., Hauber, I., Wilhelm, T., Schwarz, G., Kanz, L., Bokemeyer, C., Hauber, J., Holyoake, T. L., Nordheim, A., & Brummendorf, T. H. (2007) Hypusination of eukaryotic initiation factor 5A (eIF5A): a novel therapeutic target in BCR-ABL-positive leukemias identified by a proteomics approach. *Blood* **109**, 1701-1711.

Baneyx, F. & Mujacic, M. (2004) Recombinant protein folding and misfolding in *Escherichia coli*. *Nat Biotechnol* **22**, 1399-1408.

Bartig, D., Lemkemeier, K., Frank, J., Lottspeich, F., & Klink F. (1992) The archaebacterial hypusine-containing protein. Structural features suggest common ancestry with eukaryotic translation initiation factor 5A. *Eur J Biochem* **204**, 751-758.

Beninati, S., Abbruzzese, A. & Folk, J. E. (1990) High-performance liquid chromatographic method for determination of hypusine and deoxyhypusine. *Anal Biochem* **184**, 16-20.

Beninati, S., Nicolini, L., Jakus, J., Passeggio, A. & Abbruzzese, A. (1995) Identification of a substrate site for transglutaminases on the human protein synthesis initiation factor 5A. *Biochem J* **305**, 725-728.

Beninati, S., Gentile, V., Caraglia, M., Lentini, A., Tagliaferri, P. & Abbruzzese, A. (1998) Tissue transglutaminase expression affects hypusine metabolism in BALB/c 3T3 cells. *FEBS Lett* **437**, 34-38.

Benne, R., Brown-Luedi, M. L. & Hershey, J. W. (1978) Purification and characterization of protein synthesis initiation factors eIF-1, eIF-4C, eIF-4D, and eIF-5 from rabbit reticulocytes. *J Biol Chem* **253**, 3070-3077.

Benne, R. & Hershey, J. W. (1978) The mechanism of action of protein synthesis initiation factors from rabbit reticulocytes. *J Biol Chem.* **253**, 3078-3087.

Berghammer, H. & Auer, B. (1993) "Easypreps": fast and easy plasmid minipreparation for analysis of recombinant clones in *E. coli*. *Biotechniques* **14**, 524-528.

Botstein, D. & Fink, G. R. (1988) Yeast: an experimental organism for modern biology. *Science* **240**, 1439-1443.

Bourdon, J. C. (2007) *Curr Pharm Biotechnol* **8**, 332-336.

Bradford, M. M. (1976) A rapid and sensitive method for the quantitation of microgram quantities of protein utilizing the principle of protein-dye binding. *Anal Biochem* **72**, 248-254.

Brochier, C., López-García, P. & Moreira, D. (2004) Horizontal gene transfer and archael origin of deoxyhypusine synthase homologous genes in bacteria. *Gene* **330**, 169-176.

Brunton, V. G., Grant, M. H. & Wallace, H. M. (1991) Mechanisms of spermine toxicity in baby-hamster kidney (BHK) cells. The role of amine oxidases and oxidative stress. *Biochem J* **280**, 192-198.

Cano, V. S., Jeon, G. A., Johansson, H. E., Henderson, C. A., Park, J. H., Valentini, S. R., Hershey, J. W. & Park, M. H. (2008) Mutational analyses of human eIF5A-1 - identification of amino acid residues critical for eIF5A activity and hypusine modification. *FEBS J* **275**, 44-58.

Caraglia, M., Passeggio, A., Beninati, S., Leardi, A., Nicolini, L., Improta, S., Pinto, A., Bianco, R., Tagliaferri, P. & Abbruzzese, A. (1997) Interferon α2 recombinant and epidermal growth factor modulate proliferation and hypusine synthesis in human epidermoid cancer KB cells. *Biochem J* **324**, 737-741.

Caraglia, M., Tagliaferri, P., Budillon, A. & Abbruzzese, A. (1999) Post-translational modifications of eukaryotic initiation factor-5A (eIF-5A) as a new target for anti-cancer therapy. *Adv Exp Med Biol* **472**, 187-198.

Caraglia, M., Marra, M., Giuberti, G., D'Alessandro, A. M., Budillon, A., del Prete, S. , Lentini, A., Beninati, S., & Abbruzzese, A. (2001) The role of eukaryotic initiation factor 5A in the control of cell proliferation and apoptosis. *Amino Acids* **20**, 91-104.

Carmel-Harel, O. & Storz, G. (2000) roles of the glutathione- and thioredoxin-dependent reduction systems in the *Escherichia coli* and *Saccharomyces cerevisiae* responses to oxidative stress. *Annu Rev Microbiol* **54**, 439-461.

Chattopadhyay, M. K., Tabor, C. W., & Tabor, H. (2003) Spermidine but not spermine is essential for hypusine biosynthesis and growth in *Saccharomyces cerevisiae*: Spermine is converted to spermidine *in vivo* by the FMS1-amine oxidase. *Proc Natl Acad Sci USA* **100**, 13869-13874.

Chen, K. Y. & Liu, A. Y. (1997) Biochemistry and function of hypusine formation on eukaryotic initiation factor 5A. *Biol Signals* **6**, 105-109.

Chenna R., Sugawara, H., Koike, T., Lopez, R., Gibson, T. J., Higgins T.G. & Thompson, J. D. (2003) Multiple sequence alignment with the CLUSTAL series of programs. *Nucleic acids Res* **31**, 3597-3599.

Cherry, J. M., Ball, C., Weng, S., Juvik, G., Schnidt, R., Adler, C., Dunn, B., Dwight, S., Riles, L., Mortimer, R. K. & Botstein, D. (1997) Genetic and physical maps of *Saccharomyces cerevisiae*. *Nature* **387**, 67-73.

Cheung, D. T. & Nimni, M. E. (1982) Mechanism of crosslinking of proteins by glutaraldehyde II. Reaction with monomeric and polymeric collagen. *Connect Tissue Res* **10**, 201-216.

Chung, S. I., Park, M. H., Folk, J. E. & Lewis, M. S. (1991) Eukaryotic initiation factor 5A: the molecular form of the hypusine-containing protein from human erythrocytes. *Biochim Biophys Acta* **1976**, 448-451.

Clague, M. J. (1998) Molecular aspects of the endocytic pathway. *Biochem J* **336**, 271-282.

Cochrane, A. W., Perkins, A. & Rosen, C. A. (1990) Identification of sequences important in the nucleolar localization of human immunodeficiency virus Rev: relevance of nucleolar localization to function. *J Virol* **64**, 881-885.

Cooper, H. L., Park, M. H., Folk, J. E., Safer, B. & Braverman, R. (1983) Identification of the hypusine-containing protein Hy^+ as translation initiation factor eIF-4D. *Proc Natl Acad Sci USA* **80**, 1854-1857.

Costa-Neto, C.M., Parreiras-e-Silva, L., Ruller, R., Oliveira, E. B., Miranda, A., Oliveira, L. & Ward, R. J. (2006) Molecular modeling of the human eukaryotic translation initiation factor 5A (eIF5A) based on spectroscopic and computational analyses. *Biochem Biophys Res Commun* **347**, 634-640.

Cousens, L. S. Shuster J. R., Gallegos, C., Ku, L. L., Stempien, M. M., Urdea, M. S., Sanchez-Pescador, R., Taylor, A., & Tekamp-Olson, P. (1987) High level expression of proinsulin in the yeast, *Saccharomyces cerevisiae*. *Gene* **61**, 265-267.

Csonga, R., Ettmayer, P., Auer, M., Eckerskorn, C., Eder, J. & Klier, H. (1996) Evaluation of the metal ion requirement of the human deoxyhypusine hydroxylase from HeLa cells using a novel enzyme assay. *FEBS Lett* **380**, 209-214.

Cuff, J. A. & Barton, G. J. (1999) A consensus method for protein secondary structure prediction: Evaluation and improvement of multiple sequence methods for protein secondary structure prediction. *Proteins* **34**, 508-519.

De Jaeger, G., Fiers, E., Eeckhout, D. & Depicker, A. (2000) Analysis of the interaction between single-chain variable fragments and their antigen in a reducing intracellular environment using the two-hybrid system. *FEBS Lett* **467**, 316-320.

DeLano, W. L. (2002). The Pymol Molecular Graphics System. Delano Scientific, San Carlos, CA, USA.

Dias, C.A.O., Cano V.S.P., Rangel, S.M., Apponi, L.H., Frigieri, M.C., Muniz, J.R.C., Garcia, W., Park, M.H., Garratt, R.C., Zanelli, C.F. & Valentini, S.R. (2008) Structural modeling and mutational analysis of yeast eIF5A reveal new critical residues and reinforce its involvement in protein synthesis. *FEBS J* (In press)

Dou, Q-P. & Chen, K. Y. (1990) Characterization and reconstruction of a cell free system for NAD^+ dependent deoxyhypusine formation on the 18kDa eIF-4D precursor. *Biochim Biophys Acta* **1036**, 128-137.

Eijkelenboom, A.P., Lutzke, R.A., Boelens, R., Plasterk, R.H., Kaptein, R. & Hård, K. (1995) The DNA-binding domain of HIV-1 integrase has an SH3-like fold. *Nat Struct Biol* **2**, 807-810.

Facchiano, A. M., Stiuso, P., Chiusano, M. L., Caraglia, M., Giuberti, G., Abbruzzese, A. & Colonna, G. (2001) Homology modelling of the human eukaryotic initiation factor 5A (eIF-5A). *Protein Eng* **14**, 881-890.

Feinberg, M. B., Jarrett, R. F., Aldovini, A., Gallo, R. C. & Wong-Staal, F. (1986) HTLV-III expression and production involve complex regulation at the levels of splicing and translation of viral RNA. *Cell* **46**, 807-817.

Feng, W., Tejero, R., Zimmerman, D. E., Inouye, M. & Montelione, G. T. (1998) Solution NMR Structure and Backbone Dynamics of the Major Cold-Shock Protein (CspA) from *Escherichia coli*: Evidence for Conformational Dynamics in the Single-Stranded RNA-Binding Site. *Biochemistry* **37**, 10881-10896.

Fesus, L. (1998) Transglutaminase-Catalyzed Protein Cross-Linking in the Molecular Program of Apoptosis and Its Relationship to Neuronal Processes. *Cell Molec Neurobiol* **18**, 683-694.

Frigieri, M. C., Thompson, G. M., Pandolfi, J. R., Zanelli, C. F. & Valentini, S. R. (2007) Use of a synthetic lethal screen to identify genes related to *TIF51A* in *Saccharomyces cerevisiae*. *Genet Mol Res* **6**, 152-165.

Ganoza, M. C., Kiel, M. C. & Aoki, H. (2002) Evolutionary Conservation of Reactions in Translation. *Microbiol. Mol Biol Rev* **66**, 460-485.

Georgiou, G. & Valax, P. (1996) Expression of correctly folded proteins in *Escherichia coli*. *Curr Opin Biotechnol* **7**, 190-197.

Gerner, E. W., Vejda, S., Gelbmann, D., Bayer, E., Gotzmann, J., Schulte-Hermann, R. & Mikulits, W. (2002) Concomitant Determination of Absolute Values of Cellular Protein Amounts, Synthesis Rates and Turnover Rates by Quantitative Proteome Profiling. *Molec Cell Proteomics* **1**, 528-537.

Gietz, R. D. & Sugino, A. (1988) New yeast *Escherichia coli* shuttle vectors constructed with in vitro mutagenized yeast genes lacking six-base pair restriction sites. *Gene* **74**, 527-534.

Glick, B. R. & Ganoza, M. C. (1975) Identification of a soluble protein that stimulates peptide bond synthesis. *Proc Natl Acad Sci USA* **72**, 4257-4260.

Goffeau, A., Barrell, B. G., Bussey, H., Davis, R. W., Dujon, B., Feldmann, H., Galibert, F., Hoheisel, J. D., Jacq, C., Johnston, M., Louis, E. J., Mewes, H. W., Murakami, Y., Philippsen, P., Tettelin, H. & Oliver, S. G. (1996) Life with 6000 genes. *Science* **275**, 1051-1052.

González-Monalbán, N., García-Fruitós, E., & Villaverde, A. (2008) Recombinant protein solubility - does more mean better? *Nat Biotechnol* **25**, 718-720.

Gordon, E. D., Mora, R., Meredith, S. C., Lee, C. & Lindquist, S. (1987) Eukaryotic Initiation Factor 4D, the Hypusine-containing Protein, Is Conserved among Eukaryotes. *J Biol Chem* **262**, 16585-16589.

Grootjans, J. J., Zimmermann, P., Reekmans, G., Smets, A., Degeest, G., Durr, J. & David, G. (1997) Syntenin, a PDZ protein that binds syndecan cytoplasmic domains. *Proc Natl Acad Sci USA* **94**, 13683-13688.

Guex, N. & Pietsch, M. C. (1997) SWISS-MODEL and the Swiss-PdbViewer: An environment for comparative protein modelling. *Electrophoresis* **18**, 2714-2723.

Hanahan, D. (1983) Studies on transformation of *Escherichia coli* with plasmids. *J Mol Biol* **166**, 557-580.

Hanahan, D. (1985) In: *DNA Cloning*, Vol. 1, Glover, D., ed., IRL Press, Ltd., pp.109.

Hanauske-Abel, H. M, Park, M-H., Hanauske, A. R. Popowicz A. M., Lalande, M. & Folk, J. E. (1994) Inhibition of the G1-S transition of the cell cycle by inhibitors of deoxyhypusine hydroxylation. *Biochim Biophys Acta* **1221**, 115-124.

Hanauske-Abel, H. M., Slowinska, B., Zagulska, S., Wilson, R. C., Staiano-Coico, L., Hanauske, A-R., McCaffrey, T. & Szabo, P. (1995) Detection of a sub-set of polysomal mRNAs associated with modulation of hypusine formation at the G1-S boundary (Proposal of a role for eIF5A in onset of DNA replication). *FEBS Lett* **366** , 92-98.

Hanawa-Suetsugu, K., Sekine, S., Sakai, H., Hori-Takemoto, C., Terada, T., Unzai, S., Tame, J. R. H., Kuramitsu, S., Shirouzu, M. & Yokoyama, S. (2004) Crystal structure of elongation factor P from *Thermus thermophilus* HB8. *Proc Natl Acad Sci USA* **101**, 9595-9600.

Hauber, I., Bevec, D., Heukeshoven, J., Kratzer, F., Horn, F., Choidas, A., Harrer, T. & Hauber, J. (2005) Identification of cellular deoxyhypusine synthase as a novel target for antiretroviral therapy. *J Clin Invest* **115**, 76-85.

Harlowe, E. & Lane, D. (1988) In: Antibodies, A laboratory manual, Cold Spring Harbor Laboratory Press, Cold Spring Harbor, New York pp. 462-465

Heinisch, J. J., Lorberg, A., Schmitz, H. P. & Jacoby, J. J. (1999) The protein kinase C-mediated MAP kinase pathway involved in the maintenance of cellular integrity in *Saccharomyces cerevisiae*. *Mol Microbiol* **32**, 671-680.

Hofmann, W., Reichart, B., Ewald, A., Muller, E., Schmitt, I., Stauber, R. H., Lottspeich, F., Jockusch, B. M., Scheer, U., Hauber, J. & Dabauvalle, M.C. (2001) Cofactor Requirements for Nuclear Export of Rev Response Element (RRE)- and Constitutive Transport Element (CTE)-containing Retroviral RNAs: An Unexpected Role for Actin. *J Cell Biol* **152**, 895-910.

Holm, L. & Sander, C. (1999) Protein folds and families: sequence and structure alignments. *Nucleic acids Res* **27**, 244-247.

Hooft, R. W., Vriend, G., Sander, C. & Abola, E. E. (1990) Errors in protein structures. *Nature* **381**, 272.

Jakus, J., Wolff, E. C., Park, M. H. & Folk, J. E. (1993) Features of the spermidine-binding site of deoxyhypusine synthase as derived from inhibition studies. Effective inhibition by bis- and mono-guanylated diamines and polyamines. *J Biol Chem* **268**, 13151-13159.

Jao, D. L-E. & Chen, K. Y. (2006) Tandem affinity purification revealed the hypusine-dependent binding of eukaryotic initiation factor 5A to the translating 80S ribosomal complex. *J Cell Biochem* **97**, 583-598.

Jasiulionis, M. G., Luchessi, A. D., Moreira, A. G., Souza, P. P., Suenaga, A. P., Correa, M., Costa, C. A., Curi, R. & Costa-Neto, C. M. (2007) Inhibition of eukaryotic translation initiation factor 5A (eIF5A) hypusination impairs melanoma growth. *Cell Biochem Funct* **25**, 109-114.

Jedd, G. & Chua, N. H. (2000) A new self-assembled peroxisomal vesicle required for efficient resealing of the plasma membrane. *Nat Cell Biol* **2**, 226-231.

Jiang, W., Hou, Y. & Inouye, M. (1997) CspA, the Major Cold-shock Protein of *Eschericia coli*, is an RNA Chaperone. *J Biol Chem* **272**, 196-202.

Jin, B. F, He, K., Hu, M., Shen, B. F. & Zhang, X. M. (2003) The effect of eIF-5A on the G1-S in cell cycle regulation. *Zhongguo Shi Yan Xue Ye Xue Za Zhi.* **11**, 325-328.

Joe, Y. A., Wolff, E. C. & Park, M. H. (1995) Cloning and Expression of Human Deoxyhypusine Synthase cDNA. *J Biol Chem* **270**, 22386-22392.

Johnson, T. C. (1994) Negative regulators of cell proliferation. *Pharmacol Ther* **62**, 247-265.

Kaiser, C., Michaelis, S. & Mitchell, A. (1994). In *Methods in Yeast Genetics*. pp. 208-209, Cold Spring Harbor Laboratory, Cold Spring Harbor, NY.

Kang, H. A. & Hershey, J. W. B. (1994) Effect of Initiation Factor eIF-5A Depletion on Protein Synthesis and Proliferation of *Saccharomyces cerevisiae*. *J Biol Chem* **269**, 3934-3940.

Kang, K. R., Schwelberger, H. G. & Hershey, J. W. B. (1993) Translation Initiation Factor eIF-5A, the Hypusine-containing Protein, Is Phosphorylated on Serine in *Saccharomyces cerevisiae*. *J Biol Chem* **268**, 14750-14756.

Kang, K. R., Wolff, E. C., Park, M. H., Folk, J. E. & Chung, S. I. (1995) Identification of *YHRO68*w in *Saccharomyces cerevisiae* Chromosome VIII as a Gene for Deoxyhypusine Synthase. *J Biol Chem* **270**, 18408-18412.

Kang, K. R. & Chung, S. I. (1999) Characterization of yeast deoxyhypusine synthase: PKC-dependent phosphorylation *in vitro* and functional domain identification. *Exp Mol Med* **31**, 210-216.

Kang, K. R., Kim, J-S., Chung, S. I., Park, M. H., Kim, Y. W., Lim, D. & Lee, S-Y. (2002) Deoxyhypusine synthase is phosphorylated by protein kinase C *in vivo* as well as *in vitro*. *Exp Mol Med* **34**, 489-495.

Kang, K. R., Kim, Y. S., Wolff, E. C. & Park, M. H. (2007) Specificity of the Deoxyhypusine Hydroxylase-Eukaryotic Translation Initiation Factor (eIF5A) Interaction: identification of amino acid residues of the enzyme required for binding of its substrate, deoxyhypusine-containing eIF5A. *J Biol Chem* **282**, 8300-8308.

Katahiri, J., Ishizaki, T., Sakai, H., Adachi, A., Yamamoto, K. & Shida, H. (1995) Effects of translation initiation factor eIF-5A on the functioning of human T-cell leukemia virus type I Rex and human immunodeficiency virus Rev inhibited trans dominantly by a Rex mutant deficient in RNA binding. *J Virol* **69**, 3125-3133.

Kim, K. K., Hung, L-W., Yokota, H., Kim, R. & Kim, S-H. (1998) Crystal structures of eukaryotic translation initiation factor 5A from *Methanococcus jannaschii* at 1.8Å resolution. *Proc Natl Acad Sci USA* **95**, 10419-10424.

Kim, Y. S., Kang, K. R., Wolff, E. C., Bell, J. K., McPhie, P. & Park, M. H. (2006) Deoxyhypusine Hydroxylase Is an Fe(II)-dependent, HEAT-repeat Enzyme: identification of amino acid residues critical for Fe(II) binding and catalysis. *J Biol Chem* **281**, 13217-13225.

Kyrpides, N. C. & Woese, C. R. (1998) Universally conserved translation initiation factors. *Proc Natl Acad Sci USA* **95**, 224-228.

Lalande, M. & Hanauske-Abel, H. M. (1990) A new compound which reversibly arrests T lymphocyte cell cycle near the G1/S boundary. *Exp Cell Res* **188**, 117-121.

Lane, D. P. (1992) p53, guardian of the genome. *Nature* **358**, 15-16.

Laskowski, R. A., Moss, D. S. & Thornton, J. M. (1993) Main-chain Bond Lengths and Bond Angles in Protein Structures. *J Molec Biol* **231**, 1049-1067.

Leardi, A., Caraglia, M., Selleri, C., Pepe, S., Pizzi, C., Notaro, R., Fabbrocini, A., De Lorenzo, S., MusicO, M., Abbruzzese, A., Bianco, A. R. & Tagliaferri, P. (1998) Desferioxamine increases iron depletion and apoptosis induced by ara-C of human myeloid leukaemic cells. *Br J Haematol* **102**, 746-752.

Lee, C. H. & Park, M. H. (2000) Human deoxyhypusine synthase: interrelationship between binding of NAD and substrates. *Biochem J* **352**, 851-857.

Lee, C. H., Um, P. Y., and Park, M. H. (2001) Structure-function studies of human deoxyhypusine synthase: identification of amino acid residues critical for the binding of spermidine and NAD. *Biochem J* **355**, 841-849.

Lee, Y. B., Joe, Y. A., Wolff, E. C., Dimitriadis, E. K. & Park, M. H. (1999) Complex formation between deoxyhypusine synthase and its protein substrate, the eukaryotic translation factor 5A (eIF5A) precursor. *Biochem J* **340**, 273-281.

Li, A-L., Li, H-Y., Jin, B-F., Ye, Q-N., Zhout, T., Yu, X-D., Pan, X., Man, J-H., He, K., Yu, M., Hu, M-R., Wang, J., Yang, S-C., Shen, B-F. & Zhang, X-M. (2004) A Novel eIF-5A Complex Functions as a Regulator of p53 and p53-dependent Apoptosis. *J Biol Chem* **279**, 49251-49258.

Liao, D-I, Wolff, E. C, Park, M. H, & Davies, D. R. (1998) Crystal structure of the NAD complex of human deoxyhypusine synthase: an enzyme with a ball-and-chain mechanism for blocking the active site. *Structure* **6**, 23-32.

Liu, Y. P., Nemeroff, M., Yan, Y. P. & Chen, K. Y. (1997) Interaction of eukaryotic initiation factor 5A with the human immunodeficiency virus type 1 Rev response element RNA and U6 snRNA requires deoxyhypusine or hypusine modification. *Biol Signals* **6**, 166-174.

Lodi, P. J., Ernst, J. A., Kuszewski, J., Hickman, A. B., Engelman, A., Craigie, R., Clore, G. M. & Gronenborn, A. M. (1995) Solution structure of the DNA binding domain of HIV-1 integrase. *Biochemistry* **34**, 9826-9833.

Magdolen, V, Klier, H , Woehl, T, Klink, F., Hauber, J, & Lottspeich, F (1994) The function of the hypusine-containing proteins of yeast and other eukaryotes is well conserved. *Molecular Gen Genetics* **244**, 646-652.

Malim, M.H., Bohnlein, S., Hauber, J. & Cullen, B. R. (1989) Functional dissection of the HIV-1 Rev trans-activator-Derivation of a trans-dominant repressor of Rev function. *Cell* **58**, 205-214.

Marra, M., Agostinelli, E., Tempera, G., Lombardi, A., Meo, G., Budillon, A., Abbruzzese, A., Giuberti, G., & Caraglia, M. (2007) Anticancer drugs and hyperthermia enhance cytotoxicity induced by polyamine enzymatic oxidation products. *Amino Acids* **33**, 273-281.

Martinez, O. & Goud, B. (1998) Rab proteins. *Biochim Biophys Acta* **1404**, 101-112.

McCann, P. P. & Pegg, A. E. (1992) Ornithine decarboxylase as an enzyme target for therapy. *Pharmacol Ther* **54**, 195-215.

McCloskey, D. E., Casero, R. A., Woster, P. M. & Davidson, N. E. (1995) Induction of Programmed Cell Death in Human Breast Cancer Cells by an Unsymmetrically Alkylated Polyamine Analogue. *Cancer Res* **55**, 3233-3236.

Mehta, K. D., Leung, D., Lefebvre, L. & Smith, M. (1990) The *ANB1* Locus of *Saccharomyces cerevisiae* Encodes the Protein Synthesis Initiation Factor eIF-4D. *J Biol Chem* **265**, 8802-8807.

Melnick, L. & Sherman, F. (1993) The Gene Clusters ARC and COR on Chromosomes 5 and 10, Respectively, of *Saccharomyces cerevisiae* Share a Common Ancestry. *J Mol Biol* **233**, 372-388.

Mitchell, J. L. A., Diveley, R. R., Bareyal-Leyser, A. & Mitchell, J. L. (1992) Abnormal accumulation and toxicity of polyamines in a difluoromethylornithine-resistant HTC cell variant. *Biochim Biophys Acta (BBA) - Molec Cell Res* **1136**, 136-142.

Murphey, R. J. & Gerner, E. W. (1987) Hypusine Formation in Protein by a Two-step Process in Cell Lysates. *J Biol Chem* **262**, 15033-15036.

Murzin, A. G. (1993) OB (oligonucleotide/oligosaccharide binding)-fold: common structural and functional solution for non-homologous sequences. *EMBO J* **12**, 861-867.

Nakaoka, H., Perez, D. M., Baek, K. J., Das, T., Husain, A., Misono, K., Im, M. J. & Graham, R. M. (1994) Gh: a GTP-binding protein with transglutaminase activity and receptor signaling function. *Science* **264**, 1593-1596.

Nishimura, K., Murozumi, K., Shirahata, A., Park, M. H., Kashiwagi, K. & Igarashi, K. (2005) Independent roles of eIF5A and polyamines in cell proliferation. *Biochem J* **385**, 779-785.

O'Dwyer, M. E. & Druker, B. J. (2001) The role of the tyrosine kinase inhibitor STI571 in the treatment of cancer. *Curr Cancer Drug Targets* **1**, 49-57.

Packham, G. & Cleveland, J. L. (1994) Ornithine decarboxylase is a mediator of c-Myc-induced apoptosis. *Mol Cell Biol* **14**, 5741-5747.

Park, J-H., Wolff, E. C., Folk, J. E. & Park, M. H. (2003) Reversal of the Deoxyhypusine Synthase Reaction. *J Biol Chem* **278**, 32683-32691.

Park, J.H., Aravind, L., Wolff, E. C., Kaevel, J., Kim, Y. S. & Park, M. H. (2006) Molecular cloning, expression, and structural prediction of deoxyhypusine hydroxylase: A HEAT-repeat-containing metalloenzyme. *Proc Natl Acad Sci USA* **103**, 51-56.

Park, M. H., Cooper, H. L. & Folk, J. E. (1981) Identification of hypusine, an unusual amino acid, in a protein from human lymphocytes and of spermidine as its biosynthetic precursor. *Proc Natl Acad Sci* **78**, 2869-2873.

Park, M. H., Cooper, H. L. & Folk, J. E. (1982) The biosynthesis of protein-bound hypusine (N epsilon -(4-amino-2- hydroxybutyl)lysine). Lysine as the amino acid precursor and the intermediate role of deoxyhypusine (N epsilon -(4-aminobutyl)lysine). *J Biol Chem* **257**, 7217-7222.

Park, M. H., Chung, S. I., Cooper, H. L. & Folk, J. E. (1984) The Mammalian Hypusine-containing Protein, Eukaryotic Initiation Factor 4D. *J Biol Chem* **259**, 4563-4565.

Park, M. H., Liu, T-Y., Neece, S. H. & Swiggard, W. J. (1986) Eukaryotic Initiation Factor 4D. *J Biol Chem* **261**, 14515-14519.

Park, M. H. (1987) Regulation of Biosynthesis of Hypusine in Chinese Hamster Ovary Cells. *J Biol Chem* **262**, 12730-12734.

Park, M. H. (1989) The Essential Role of Hypusine in Eukaryotic Translation Initiaion Factor 4D (eIF-4D). *J Biol Chem* **264**, 18531-18535.

Park, M. H., Wolff, E. C. & Folk, J. E. (1993) Hypusine: its post-translational formation in eukaryotic initiation factor 5A and its potential role in cellular regulation. *Biofactors* **4**, 95-104.

Park, M. H., Lee, Y. B. & Joe, Y. A. (1997) Hypusine is essential for Eukaryotic Cell Proliferation. *Biol Signals* **6**, 115-123.

Park, M. H., Joe, Y. A. & Kang, K. R. (1998) Deoxyhypusine Synthase Activity is Essential for Cell Viability in the Yeast *Saccharomyces cerevisiae*. *J Biol Chem* **273**, 1677-1683.

Park, M. H. (2006) The Post-Translational Synthesis of a Polyamine-Derived Amino Acid, Hypusine, in the Eukaryotic Translation Initiation Factor 5A (eIF5A). *J Biochem.* **139**, 161-169.

Parker, M. T. & Gerner, E. W. (2002) Polyamine-mediated post-transcriptional regulation of COX-2. *Biochimie* **84**, 815-819.

Parreiras-e-Silva, L., Gomes, M. D., Oliveira, E. B. & Costa-Neto, C. M. (2007) The N-terminal region of eukaryotic translation initiation factor 5A signals to nuclear localization of the protein. *Biochem Biophys Res Commun* **362**, 393-398.

Peat, T. S., Newman, J., Waldo, G. S., Berendzen, J. & Terwilliger, T. C. (1998) Structure of translation initation factor 5A from *Pyrobaculum aerophilum* at 1.75Å resolution. *Structure* **6**, 1207-1214.

Pegg, A. E., Secrist, J. A., III, & Madhubala, R. (1988) Properties of L1210 Cells Resistant to {alpha}-Difluoromethylornithine. *Cancer Res* **48**, 2678-2682.

Pegg, A. E. & McCann, P. P. (1992) S-adenosylmenthionine decarboxylase as an enzyme target for therapy. *Pharmacol Ther* **56**, 359-377.

Rahman-Roblick, R., Johannes Roblick, U., Hellman, U., Conrotto, P., Liu, T., Becker, S., Hirschberg, D., Jornvall, H., Auer, G. & Wiman, K. G. (2007) p53 targets identified by protein expression profiling. *Proc Natl Acad Sci USA* **104**, 5401-5406.

Regenass, U., Mett, H., Stanek, J., Mueller, M., Kramer, D. & Porter, C.W. (1994) CGP 48664, a New S-Adenosylmethionine Decarboxylase Inhibitor with Broad Spectrum Antiproliferative and Antitumor Activity. *Cancer Res* **54** , 3210-3217.

Rimsky, L., Dodon, M.D., Eric, P. & Greene, W. C. (1989) Trans-dominant inactivation of HTLV-I and HIV-1 gene expression by mutation of the HTLV-I Rex transactivator . *Nature* **341**, 453-456.

Rosorius, O., Reichart, B., Krätzer, F., Heger, P., Dabauvalle, M-C. & Hauber, J. (1999) Nuclear pore localisation and nucleocytoplasmic transport of eIF-5A: evidence for direct interaction with the export receptor CRM1. *J Cell Sci* **112**, 2369-2380.

Ruhl, M., Himmelspach, M., Bahr, G. M., Hammershmid, F., Jaksche, H., Wolff, B., Aschauer, H., Farrington, G. K., Hans, P., Bevec, D. & Hauber, J. (1993) Eukaryotic Initiation Factor 5A Is a Cellular Target of the Human Immunodeficiency Virus Type 1 Rev Activation Domain Mediating *Trans*-Activation. *J Cell Biol* **123**, 1309-1320.

Sadaie, M. R., Benter, T. & Wong-Staal, F. (1988) Site-directed mutagenesis of two trans-regulatory genes (tat-III,trs) of HIV-1. *Science* **239**, 910-913.

Sakai, H., Siomi, H., Shida, H., Shibata, R., Kiyomasu, T. & Adachi, A. (1990) Functional comparison of transactivation by human retrovirus rev and rex genes. *J Virol* **64**, 5833-5839.

Sali, A., Potterton, L., Yuan, F., van Vlijmen, H., & Karplus, M. (1995) Evaluation of comparative protein modeling by MODELLER. *Proteins* **23**, 318-326.

Salvador, M. L. & Klein, U. (1999) The Redox State Regulates RNA Degradation in the Chloroplast of *Chlamydomonas reinhardtii*. *Plant Physiol* **121**, 1367-1374.

Sambrook, J., Fritsch, E. F. & Maniatis, T. (1989). *Molecular Cloning: A Laboratory Manual*. Cold Spring Harbor Laboratory, Cold Spring Harbor, NY.

Sasaki, K., Abid, R. & Miyazaki, M. (1996) Deoxyhypusine synthase gene is essential for cell viability in the yeast *Saccharomyces cerevisiae*. *FEBS Lett* **384**, 151-154.

Schafer, B., Hauber, I., Bunk, A., Heukeshoven, J., Dusedau, A., Bevec, D., & Hauber, J. (2006) Inhibition of Multidrug-Resistant HIV-1 by Interference with Cellular S-adenosylmethionine Decarboxylase Activity. *J Infect Dis* **194**, 740-750.

Schindelin, H., Jiang, W., Inouye, M. & Heinemann, U. (1994) Crystal Structure of CspA, the Major Cold Shock Protein of *Escherichia coli*. *Proc Natl Acad Sci USA* **91**, 5119-5123.

Schnier, J., Schwelberger, H. G., Smit-McBride, Z., Kang, H. A. & Hershey, J. W. B. (1991) Translation Initiation Factor 5A and its Hypusine Modification are Essential for Cell Viability in the Yeast *Saccharomyces cerevisiae*. *Mol Cell Biol* **11**, 3105-3114.

Schrader, R., Young, C., Kozian, D., Hoffmann, R. & Lottspeich, F. (2006) Temperature-sensitive eIF5A Mutant Accumulates Transcripts Targeted to the Nonsense-mediated Decay Pathway. *J Biol Chem* **281**, 35336-35346.

Schwede, T., Kopp, J. , Guex, N. & Peitsch, M. C. (2003) SWISS-MODEL: an automated protein homology-modelling server. *Nucleic acids Res* **31**, 3381-3385.

Schwelberger, H. G., Kang, K. R. & Hershey, J. W. B. (1993) Translation Initiation Factor eIF-5A Expressed from Either of Two Yeast Genes or from Human cDNA. *J Biol Chem* **268**, 14018-14025.

Shiba, T., Mizote, H., Kaneto, T., Nakajima, T. & Kakimoto, Y. (1971) Hypusine, a new amino acid occurring in bovine brain. Isolation and structural determination. *Biochim Biophys Acta* **244**, 523-531.

Singh, U. S., Li, Q. & Cerione, R. (1998) Identification of the Eukaryotic Initiation Factor 5A as a Retinoic Acid-stimulated Cellular Binding Partner for Tissue Transglutaminase II. *J Biol Chem* **273**, 1946-1950.

Smit-McBride, Z., Dever, T. E., Hershey, J. W. B. & Merrick, W. C. (1989) Sequence Determination and cDNA Cloning of Eukaryotic Initiation Factor 4D, the Hypusine-containing Protein. *J Biol Chem* **264**, 1578-1583.

Sodroski, J., Goh, W. C., Rosen, C., Dayton, A., Terwilliger, E. & Haseltine, W. (1986) A second post-transcriptional trans-activator gene required for HTLV-III replication. *Nature* **321**, 412-417.

Studier, F. W. & Moffat, B. A. (1986) Use of bacteriophage T7 RNA polymerase to direct selective high-level expression of cloned genes. *J Mol Biol* **189**, 113-130.

Sun, Y., Li, X., Wu, B., Sun, P. & Rao, Z. (2005) Crystallization and Preliminary Crystallographic Analysis of Human Eukaryotic Translation Initiation Factor 5 A (eIF-5A). *Prot Pept Lett* **12**, 713-715.

Tabor, C. W. & Tabor, H. (1984) Methionine adenosyltransferase (S-adenosylmethionine synthetase) and S-adenosylmethionine decarboxylase. *Adv Enzymol Relat Areas Mol Biol.* **56**, 251-282.

Tabor, C. W. & Tabor, H. (1985) Polyamines in microorganisms. *Microbiol Mol Biol Rev* **49**, 81-99.

Tao, Y. & Chen, K. Y. (1994) PCR-based cloning of the full-length *Neurospora* eukaryotic initiation factor 5A cDNA: polyhistidine-tagging and overexpression for protein affinity binding. *Biochem J* **302**, 517-525.

Tao, Y. & Chen, K. Y. (1995) Molecular Cloning and Functional Expression of *Neurospora* Deoxyhypusine Synthase cDNA and Identification of Yeast Deoxyhypusine Synthase cDNA. *J Biol Chem* **270**, 23984-23987.

Taylor, A., Schuster, K., McKenzie, P. & Harris, L. (2006) Differential cooperation of oncogenes with p53 and Bax to induce apoptosis in rhabdomyosarcoma. *Mol Cancer* **5**, 53.

Taylor, Catherine A., Sun, Zhong, Cliche, Dominic O., Ming, Hong, Eshaque, Bithi, Jin, Songmu, Hopkins, Marianne T., Thai, Boun, & Thompson, John E. (2007) Eukaryotic translation initiation factor 5A induces apoptosis in colon cancer cells and associates with the nucleus in response to tumour necrosis factor [alpha] signalling. *Exp Cell Res* **313**, 437-449.

Terwilliger, E., Burghoff, R., Sia, R., Sodroski, J., Haseltine, W. & Rosen, C. (1988) The art gene product of human immunodeficiency virus is required for replication. *J Virol* **62**, 655-658.

Thompson, G. M., Cano, V. S. P. & Valentini, S. R. (2003) Mapping eIF5A binding sites for Dys1 and Lia1: *In vivo* evidence for regulation of eIF5A hypusination. *FEBS Lett* **555**, 464-468.

Tobias, K. E. & Kahana, C. (1995) Exposure to ornithine results in excessive accumulation of putrescine and apoptotic cell death in ornithine decarboxylase overproducing mouse myeloma cells. *Cell Growth Differ* **6**, 1279-1285.

Tomasicchio, M., Venter, P. A., H.J.Gordon, K., N.Hanzlik, T. & Dorrington, R. A. (2007) Induction of apoptosis in *Saccharomyces cerevisiae* results in the spontaneous maturation of tetravirus procapsids *in vivo*. *J Gen Virol* **88**, 1576-1582.

Tome, M. E. & Gerner, E. W. (1997) Cellular eukaryotic initiation factor 5A content as a mediator of polyamine effects on growth and apoptosis. *Biol Signals* **6**, 150-156.

Tome, M. E., Fiser, S. M., Payne, C. M. & Gerner, E. W. (1997) Excess putrescine accumulation inhibits the formation of modified eukaryotic initiation factor 5A (eIF-5A) and induces apoptosis. *Biochem J* **328**, 847-854.

Umland, T. C., Wolff, E. C., Park, M. H., & Davies, D.R. (2004) A New Crystal Structure of Deoxyhypusine Synthase Reveals the Configuration of the Active Enzyme and of an Enzyme NAD Inhibitor Ternary Complex. *J Biol Chem* **279**, 28697-28705.

Unbehaun, A., Borukhov, S. I., Hellen, C. U. T. & Pestova, T. V. (2004) Release of initiation factors from 48S complexes during ribosomal subunit joining and the link between establishment of codon-anticodon base-pairing and hydrolysis of eIF2-bound GTP. *Genes Dev* **18**, 3078-3093.

Valentini, S. R., Casolari, J. M., Oliveira, C. C., Silver, P. A. & McBride, A. E. (2002) Genetic Interactions of Yeast Eukaryotic Translation Initiation Factor 5A (eIF-5A) Reveal Connections to Poly(A)-Binding Protein and Protein kinase C Signaling. *Genetics* **160**, 393-405.

van der Spuy, J., Cheetham, M. E., Dirr, H. W. & Blatch, G. L. (2001) The Cochaperone Murine Stress-Inducible Protein 1: Overexpression, Purification, and Characterization. *Prot Expr Purif* **21**, 462-469.

Venter, P.A. 2001. Non-host production of the *Helicoverpa armigera stunt virus* in *Saccharomyces cerevisiae*. Rhodes University PhD Thesis.

Veress, I., Haghighi, S., Pulkka, A. & Pajunen, A. (2000) Changes in gene expression in response to polyamine depletion indicates selective stabilization of mRNAs. *Biochem J* **346**, 185-191.

Vriend, G. (1990) WHAT IF: a molecular modeling and drug design program. *J Mol Graph* **8**, 52-56.

Wagner, S. & Klug, G. (2007) An Archaeal Protein with Homology to the Eukaryotic Translation Initiation Factor 5A Shows Ribonucleolytic Activity. *J Biol Chem* **282**, 13966-13976.

Wang, T-W., Lu, L., Wang, D. & Thompson, J. E. (2001) Isolation and Characterisation of Senescence-induced cDNAs Encoding Deoxyhypusine Synthase and Eukaryotic Translation Initiation Factor 5A from Tomato. *J Biol Chem* **276**, 17541-17549.

Watson, P. A., Hanausket-Abel, H. H., Flint, A. & Lalande, M. (1991) Mimosine reversibly arrests cell cycle progression at the G1-S phase border. *Cytometry* **12**, 242-246.

Wolff, E. C., Folk, J. E. & Park, M. H. (1997) Enzyme-Substrate Intermediate Formation at Lysine 329 of Human Deoxyhypusine Synthase. *J Biol Chem* **272**, 15865-15871.

Wolff, E. C. & Park, M. H. (1999) Identification of Lysine^{350} of Yeast Deoxyhypusine Synthase as the site of enzyme intermediate formation. *Yeast* **15**, 43-50.

Wöhl, T., Baur, M., Friedl, A. A. & Lottspeich, F. (1992) Chromosomal localization of the HYP2-gene in *Saccharomyces cerevisiae* and use of pulsed-field gel electrophoresis for detection of irregular recombination events in gene disruption experiments. *Electrophoresis* **13**, 651-653.

Wöhl, T., Klier, H., Ammer, H., Lottspeich, F. & Magdolen, V. (1993) The *HYP2* gene of *Saccharomyces cerevisiae* is essential for aerobic growth: characterization of different isoforms of the hypusine-containing protein Hyp2p and analysis of gene disruption mutants. *Molecular Gen Genetics* **241**, 305-311.

Xu, A. & Chen, Z. P. (2001) Hypusine is required for a Sequence-specific Interaction of Eukaryotic Initiation Factor 5A with Postsystematic Evolution of Ligands by Exponential Enrichment RNA. *J Biol Chem* **276**, 2555-2561.

Xu, A., Jao, D. L-E. & Chen, K. Y. (2004) Identification of Messenger RNA that Binds to Eukaryotic Initiation Factor 5A by affinity co-purifiation and differential display. *Biochem J* **15**, 585-590.

Yao, M., Ohsawa, A., Kikukawa, S., Tanaka, I. & Kimura, M. (2003) Crystal Structure of Hyperthermophilic Archael Initiation Factor 5A: A Homologue of Eukaryotic Initiation Factor 5A (eIF-5A). *J Biochem (Tokyo)* **133**, 75-81.

Yuan, P., Jedd, G., Kumaran, D., Swamramanyam, S., Shio, H., Hewitt, D., Chua, N-H. & Swaminathan, K. (2003) A HEX-1 crystal lattice is required for Woronin body function in *Neurospora crassa*. *Nat Struc Biol* **10**, 264-270.

Zanelli, C. F. & Valentini, S. R. (2005) Pkc1 Acts Through Zds1 and Gic1 to Suppress Growth and Cell Polarity Defects of a Yeast eIF5A Mutant. *Genetics* **171**, 1571-1581.

Zanelli, C. F., Maragno, A. L. C., Gregio, A. P. B., Komilli, S., Pandolfi, J. R., Mestriner, C. A., Lustri, W. R. & Valentini, S. R. (2006) eIF5A binds to translational machinery components and affects translation in yeast. *Biochem Biophys Res Commun* **348**, 1358-1366.

Zanelli, C. F. & Valentini, S. R. (2007) Is there a role for eIF5A in translation? *Amino Acids* **33**, 351-358.

Zuk, D. & Jacobson, A. (1998) A single amino acid substitution in yeast eIF-5A results in mRNA stabilization. *EMBO J* **17**, 2914-2925.

Zuker, M. (2003) MFold web server for nucleic acid folding and hybridization prediction. *Nucleic Acids Res* **31**, 3406-3415.

Appendices

Appendices

Appendix A: Growth Media

Yeast Extract, Peptone, Dextrose Medium (YPD)

Per liter: 2 % yeast extract (w/v)
1 % peptone (w/v)
2 % glucose (v/v)
* 17 g Agar

.

* Omit for liquid medium

Yeast Extract, Peptone,Galactose Medium (YP-Gal)

Per liter: 2 % yeast extract (w/v)
1 % peptone (w/v)
2 % galactose (v/v)
.* 17 g Agar

.

* Omit for liquid medium

Synthetic Minimal Medium (SMM) (Kaiser *et al*., 1994)

Per liter: 1.7 g yeast nitrogen base (YNB) without amino acids and ammonium sulphate (Difco).
5 g Ammonium sulphate
20 g glucose or 20 g galactose as required
* 15 g Agar
* omit for liquid medium.

Supplements (Sigma) as required for each yeast strain, were added subsequent to autoclaving at the following final concentrations

Uracil	20 mg/L
L - Tryptophan	20 mg/L
L - Histidine	20 mg/L
L - Leucine	100 mg/L

Luria-Bertani agar/broth (Sambrook *et al*., 1989)

Per litre: 10 g peptone
5 g yeast extract
5 g NaCl
* 15 g Agar
* omit for liquid medium.

Appendix B: *E. coli* competent cells

Based on a method by Hanahan, (1985)

E. coli DH5 α or BL21 (DE3) cells were grown in Luria broth to an $OD_{600\ nm}$ of between 0.6 and 0.8, before harvesting cells at 5000 rpm (JA 14 rotor, 10 minutes, 4 ^{o}C). Pellets were resuspended in 50 ml RF1 solution and incubated on ice for 20 minutes before harvesting again. The pellet was resuspended in 4 ml of RF2 solution before aliquoting and freezing at -80 ^{o}C.

RF1 Solution (pH 5.8, 1 L)

100 mM KCl

50 mM $MnCl_2$

30 mM CH_3COOK

10 mM $CaCl_2$

15 % v/v Glycerol

RF2 Solution (pH 6.8, 500 ml)

10 mM MOPS

10 mM KCl

75 mM $CaCl_2$

15 % v/v Glycerol

Appendix C: Primers used in the course of this study

C1: Primers used in DNA sequencing *

Table A1: List of the primers used for PCR extension during Cycle Sequencing

Primer name	Sequence	Sense/ Antisense	Binds
T7F	GGGAGCTGCATGTGTCAGAGG	Sense	T7-RNA polymerase
T7R	CGCTGAGATAGGTGCCTCAC	Antisense	SP6 RNA polymerase
pUCF	CGCCGAGGTTTTCCCAGTCACGAC	Sense	Lac operon
pUCR	TCACACAGGCAGCTATGAC	Antisense	Lac operon
AI2F	GGCGAGCTCTAGAAGCCGCCGAGCGGGTGAC	Sense	P_{GAL1}
AI1R	CCGGCCGCGGATTAAAGCCTTCGAGCGTC	Antisense	T_{CYC1}
HISG	GTGGTGCARGAACGCARGAGAAAGCCCCC	Sense	*HisG*
URA1	GGAACGTGCTGCTACTCATCCTAGTCC	Sense	*URA3*

*For each of the tables in this section: Note: (S) = Sense Primer; (A) = Antisense Primer; Sites introduced are marked either in **bold** or underlined, corresponding to the site in the sequence.

C2: Primers used in site-directed mutagenesis *

Table A2: List of the primers used in site-directed mutagenesis

Primer Name	Sequence	(S)/ (A)	Binds; Introduces, Mutation
PG10a	TCTAAGACTGGTAGACACGGTCACGCT	S	*TIF51A*; Arg 51
PG10b	AGCGTGACCGTGTCTACCAGTCTTAGA	A	*TIF51A*; Arg 51
PG15F	GGAAGATTTGTCTGGATCCACTCACAACTTGGAAG	S	*TIF51B*; *Bam* HI
PG16R	CTTCCAAGTTGTGAGTGGATCCAGACAAATCTTCC	A	*TIF51B*; *Bam* HI
PG17F	GGTTGCCATTAGATCTATCTTCACTGG	S	*TIF51A*; *Bgl* II
PG18R	CCAGTGAAGATAGATCTAATGGCAACC	A	*TIF51A*; *Bgl* II
PG34F	ACCTACCCAATGCAATCTTCTGCCTTGAGAAAG	S	*TIF51A*; Ser 23
PG35R	CTTTCTCAAGGCAGAAGATTGCATTGGGTAGGT	A	*TIF51A*; Ser 23
PG36F	GAGTAGACCATCTAAGATT**GTTGAC**ATGTCCAGTTCCACTTCT	S	*TIF51A*; ***Hinc* II,** Ser 39
PG37R	AGAAGTGGAACTGGACAT**GTCAAC**AATCTTAGATGGTCTACTC	S	*TIF51A*; ***Hinc* II,** Ser 39

C3: PCR Amplification Primers *

Table A3: List of the primers used for PCR amplification (cloning)

Primer Name	Sequence	(S)/ (A)	Binds; Introduces
PG1F	AAGCTTACAATGTCTGACGAAGAACATACC	S	5'-*TIF51A*; *Hind* III
PG2R	**CCCGGG**ATCCGTTCTAGCAGCTTCCTTGAA	A	3'-*TIF51A*; ***Sma* I**, *Bam* HI
PG3F	GATCCCGGGCATCATCATCATCATCAT**TAG**	S	3'-*TIF51A*; 6 x His tag, **Stop**
PG4R	CCGGGCATCATCATCATCATCAT**TAG**AATT	A	3'-*TIF51A*; 6 x His tag, **Stop**
PG5F	CATATGTCTGACGAAGAACATACCTTTGAAACT	S	5'-*TIF51A*; *Nde* I
PG6R	GGGATCCTT**AAT**CGGTTCTAGCAG	A	3'-*TIF51A*; Bam HI, **Stop**
PG8F	ACCGGTGTTTCGAAGGTGAAGGAAC	S	5'-P_{TIF51A}; *Age* I
PG13F	GGGCGTTCAAAGTTTCCTATTCC	S	5'-*TIF51B*; (none)
PG14R	CATCGCGTATTTTGTAAGCTATAG	A	3'-*TIF51B*; (none)
PG30F	ATA**CAGCTG**ATGCATCACCATCACCATCACTCTGACGA AGAACATACC	S	*TIF51A*; ***Pvu* II** N-terminal His tag
PG31R	CAT**CAGCTG**TATATATGAGTTGGTATTTGTGTGTG	A	*TIF51A*; ***Pvu* II**, N-terminal His tag
PG32F	GGGGACCGGTGGGCCCTTCAATATGCGCAC	S	5'-$P_{ADH2/GAPDH}$; *Age* I
PG33R	CCCCAAGCTT**CAGCTG**TGTTTATGTGTGTTTATTCG	S	3'- $P_{ADH2/GAPDH}$; ***Pvu* II**, *Hind* III

Appendix D: Yeast genomic DNA extraction procedure

Adapted from Kaiser *et al*., (1994)

10 ml yeast culture was grown to saturation in YPD at 30 ^{o}C before collecting by centrifugation at 2000xg. The pelleted cells were washed in 500 µl sterile water. Following centrifugation, the pellet was resuspended in 200 µl of chromosomal extraction buffer (2 % Triton X-100, 1 % SDS; 100 mM NaCl, 10 mM Tris-HCl (pH 8), 1 mM Na_2EDTA) and 200 µl Phenol: Chloroform: Isoamyl alcohol (25:24:1). Next, 0.3 g of nitric-acid washed glass beads were added before vortexing for 3 minutes (intervals of 30 second on ice, 30 seconds vortexing). Then 200 µl TE buffer (10 mM Tris-HCl, pH 8, 1 mM Na_2EDTA) was added before microfuging for 5 minutes (13 000 rpm). The top layer was transferred to a fresh tube with 1 ml of ice-cold 100 % ethanol. The pellet achieved after microfuging again was resuspended in 400 µl of TE buffer and 10 µl of RNAse A (10 mg/ml) and incubated at 37 ^{o}C for 15 minutes. 10 µl ammonium acetate (4M) was used to stop the reaction. Finally, 1 ml of 100 % ethanol was added before the final microfuging step. The pellet obtained was air-dried and resuspended in 50 µl of TE buffer. 2-4 µl (equivalent to approximately 10 µg of DNA) was used for further experiments.

Appendix E: SDS- and Native PAGE

The usual procedure was used for SDS-PAGE (12 % SDS-polyacrylamide resolving and 4.5% stacking gels) and for native PAGE (10 % polyacrylamide SDS-resolving and 4.5 % stacking gels). The variation was the buffer in which the protein was suspended prior to electrophoresis.

Dissociation buffer for SDS-PAGE (2 X)

1.25 ml 1 M Tris-HCl, pH 6.8
4 ml 10 % SDS
1 ml β-Mercaptoethanol
1 ml Glycerol
0.001 g Bromophenol Blue
Made up to 10 ml

Non-reducing tracking buffer for native PAGE (2X)

1.25 ml 1 M Tris-HCl, pH 8.8
1 ml Glycerol
0.001 g Bromophenol Blue
Made up to 10 ml

Appendix F: Western Analysis

Transfer Buffer	**TBS-Tween**	**1 % BSA**
3.03 g Tris	100 ml 1 M Tris pH7.5	1 g BSA (Fraction V) in 100 ml of TBS-Tween
14.4 g Glycine	30 ml 5 M NaCl	
200 ml methanol in 1L	1 ml Tween-20	
Made fresh and chilled	Made up to 1 L with dH_2O	

5 % Milk Powder (Blocking Agent)	**Dilution of Secondary Antibody**
5 g of Fat Free milk powder in 100 ml of TBS-Tween	1:12 500 dilution of the Roche BM Chemiluminescence Western Blotting Kit anti-mouse IgG-POD/anti-rabbit IgG-POD secondary antibody was made in 1 % BSA

Appendix G: Antibody Pre-adsorption protocol

Adapted from Harlow & Lane, (1988)

BL21 (DE3) cells were transformed with pT7-7. The cells were harvested and lysed by sonication. This lysate was incubated in a ratio of 1:3 at 4^oC for 12 hours at 50 rpm, with the antibody ("Day 39" serum) followed by a clearing spin at 2000xg for 20 minutes. The supernatant (pre-adsorbed antiserum) was analysed using lysates of cells harbouring either pPG6 (eIF5A-His) or pT7-7 to determine the specificity to eIF5A.

Appendix H: Extraction of yeast protein

Adapted from Kaiser *et al*., (1994)

Cell pellets were resuspended in either 20 µl of EB buffer (2 % SDS, 80 mM Tris-HCl, pH 6.8, 10 % Glycerol, 1.5 % DTT, 0.01 mg/ml Bromophenol Blue) or in lysis buffer (in Appendix K) and 0.3 g of nitric acid washed glass beads per 2 $OD_{600\ nm}$ units of cells before vortexing for a total of 4 minutes (30 seconds on ice, 30 seconds vortexing) before a 1 minute low-speed (4000 rpm) microfuging. The supernatant was used for SDS-PAGE analysis.

Appendix I: Southern Blotting Procedure

Procedure as outlined in Sambrook *et al*., (1989) and Ausubel *et al*., (1983)

I1: General notes

Following transfer the membrane was washed in 2 x SSPE buffer. The blot was then subjected to pre-hybridization, hybridization with the "hot" probe and washing steps, followed by exposure to X-Ray film (Agfa CP-BU Medical X-Ray film, 180 x 240 mm) for a period of 2 weeks in a Kodak BioMax intensifying screen and cassette at -80^{o}C.

The "hot" probe was prepared using 50 µCi of $_{\alpha\text{-}32}$P CTP [10 mCi/ml] (Amersham Biosciences) at the same time as a "cold" probe. The transcribed RNA from both the "hot" and "cold" reactions was precipitated using 70% ice-cold ethanol and the pellet resuspended in 100 µl of DEPC-treated water. Binding of the radioactively-labelled probe was detected by incubation of the membrane under film (AGFA CP-BU Medical X-Ray film, 180 x 240 mm) at -70^{o}C with an intensifying screen (Kodak Biomax) for a period of two weeks. Visualisation of radioactive exposure was performed using standard photographic techniques and solutions (Kodak or AGFA).

I2: Hybridisation and wash conditions

All hybridisation and wash steps were carried out in a Hybaid Omnigene Hybridisation Oven.

1. The nitrocellulose membrane was incubated at 42 °C in 25 ml pre-hybridisation solution containing denatured salmon sperm DNA to block non-specific binding sites for 8 hours.
2. The radioactively labelled DNA probe was denatured at 100 °C for 5 minutes on a heating block, and then added to the membrane in the pre-hybridisation solution. The membrane was incubated with the probe at 42 °C for at least 12 hours.
3. Highly stringent washes were carried out as follows:
    - i) 2 x SSPE with 0.1 % SDS for 10 minutes at room temperature. Repeat.
    - ii) 0.5 x SSPE with 0.1 % SDS for 15 minutes at room temperature
    - iii) 0.5 x SSPE with 0.1 % SDS for 30 minutes at 42°C
    - iv) 0.5 x SSPE with 0.1 % SDS for 10 minutes at 65°C

20 x SSC

3 M NaCl

0.3 M Sodium Citrate

20 x SSPE

3.6 M NaCl

0.2 M Sodium Phosphate

0.2 M EDTA pH7.7

Pre-Hybridisation Solution

5 x SSPE

5 x Denhardt's Solution

0.5 % (w/v) SDS

50 % formamide

To 25 ml, add 0.5 ml of a 1 mg solution of denatured salmon sperm DNA per ml

Neutralising Solution

1.5 M NaCl

0.5 M Tris pH 7.2

0.001 M EDTA

Denaturing Solution

1.5 M NaCl

0.5 M NaOH

Denhardt's Solution (5x))

2 % (w/v) BSA

2 % (w/v) Ficoll

2 % (w/v) polyvinylpyrrolidone

Appendix J: Additional plasmids

J1: Plasmid pPG30

Plasmid pPG30 was used in making the RNA-transcript for Southern analysis of the various yeast strains produced in this study (Figure J1).

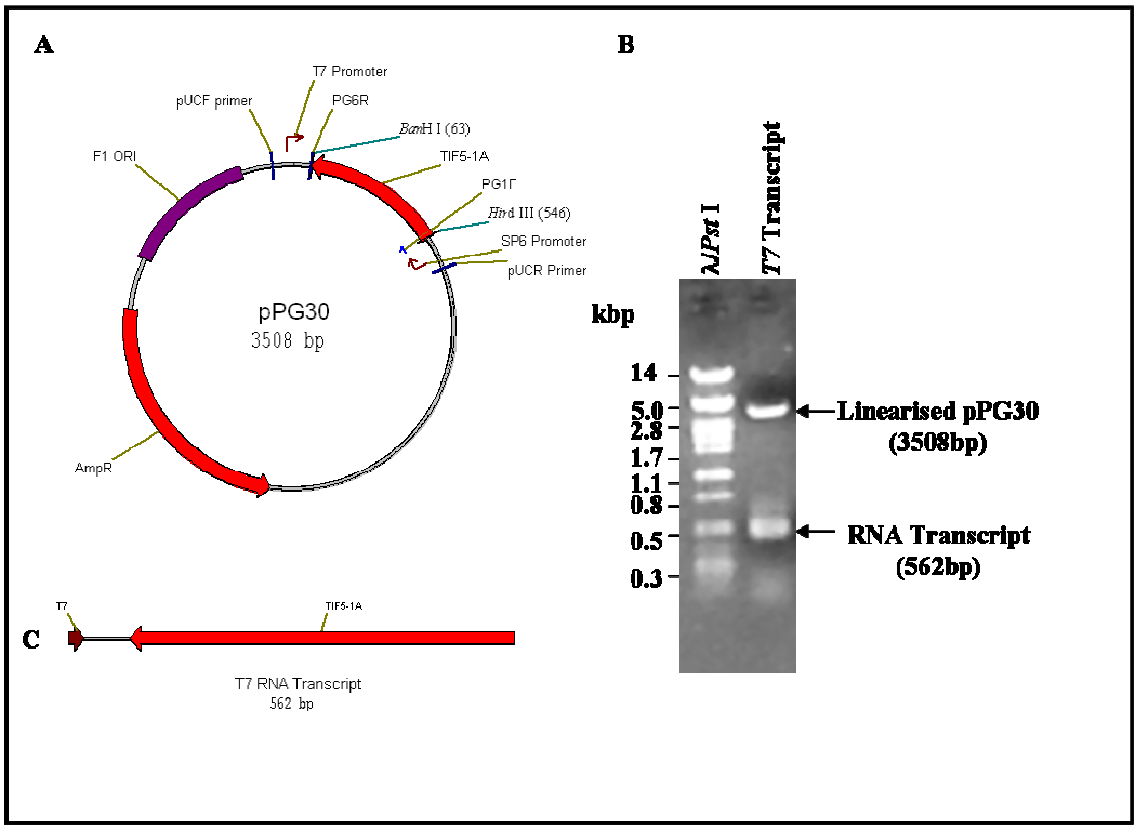

Figure A1: Plasmid pPG30, used for making the RNA-transcript in the Southern Analysis of the yeast strains. (A) pPG30, a pGEM-T-Easy-derived plasmid housing the *TIF51A* gene used in making the T7-RNA transcript. (B) The T7-RNA transcript "cold" resolved on a 1% agarose gel. (C) Diagrammatic representation of the T7-RNA transcript.

J2: Plasmid pPG10-His

Depicted in Figure J2, is plasmid pPG10-His. This plasmid was derived from pPG10, which was used in the complementation of the *TIF51A/TIF51B* disrupted strain. pPG10-His houses *TIF51A* ORF followed by a 6 x His Tag. The plasmid was used to complement PGY10 to show that the tagged eIF5A protein was functional.

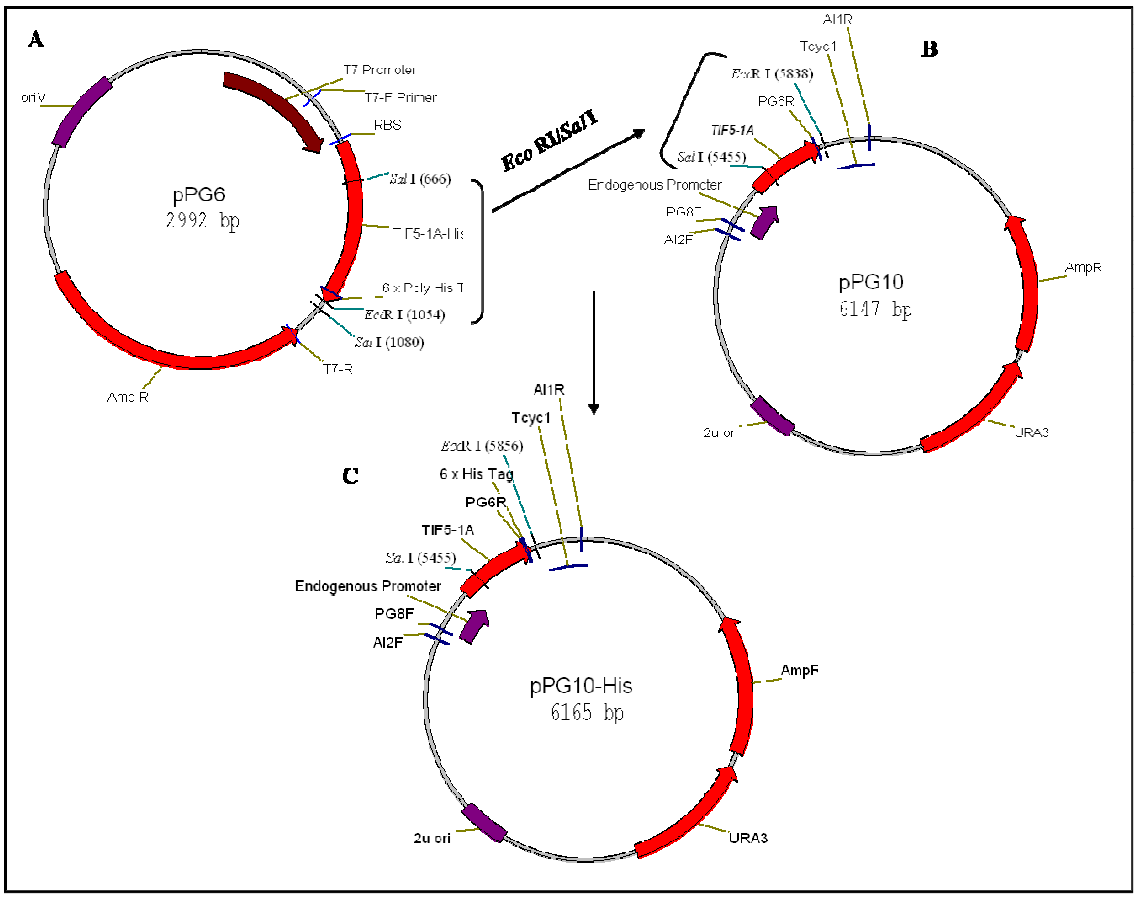

Figure A2: Schematic representation of plasmid pPG10-His. Plasmid pPG10-His, derived by digesting, pPG6 (A), the eIF5A-His expression vector with *Sal* I and *Eco* RI and ligating it to the wild-type complementation plasmid pPG10 (B) digested using the same enzymes. The resulting plasmid, pPG10-His (C) was used in complementation assays of strain PGY10 to demonstrate that a 6 x His tag, placed on the C-terminus did not affect the function of eIF5A.